COST EFFECTIVE MANUFACTURING AND OPTIMAL DESIGN OF X-STREAM TRIMS FOR SEVERE SERVICE CONTROL VALVES

Matthew Charlton

Master of Science by Research

2014

University of Huddersfield

School of Computing and Engineering

ABSTRACT

Control valves are used under severe service conditions for a wide range of applications. These valves are installed with X-Stream cage trims in order to control the flow rate and the pressure drop within the valve. The X-Stream cage trims have a specific capacity rating, commonly known as Flow Coefficient (or Cv). These values of the X-Stream are important as far as customer's requirements are concerned as are other features of the trim like reduction in erosion via velocity control and the prevention of cavitation via controlled pressure let-down.

The X-Stream is a complex geometry part and is traditionally manufactured using a process called electric discharge machining. This is considered a relatively expensive and time consuming process and as a result control valves industry has been extensively reviewing other methods of manufacture. A process known as selective laser melting has been identified as a high potential for cost reduction and competiveness for the business, however early tests have seen issues during the manufacturing process and significant reductions in the Cv of the X-Stream.

This study reviews the SLM method of manufacture and evaluates improvements in performance of the X-Stream when reviewing the process of manufacture and the design of the X-Stream component. Extensive flow loop testing of X-Streams have been carried out to calculate Cv of the trims. Then, Computational Fluid Dynamics based techniques have been incorporated to find out the same. The results have been compared and validated. Further tests at higher pressures of water have been conducted to evaluate Cv at severe service conditions

This report includes details of the test procedures, CFD modelling and full set of results for each flow condition and the effect of manufacturing constraints like surface roughness on the final Flow Coefficient (Cv) and other performance characteristics to improve the potential for SLM specifically for application with X-Stream.

DECLARATION

- The author of this thesis (including any appendices and/or schedules to this thesis) owns any copyright in it (the "Copyright") and he has given The University of Huddersfield the right to use such Copyright for any administrative, promotional, educational and/or teaching purposes.

- Copies of this thesis, either in full or in extracts, may be made only in accordance with the regulations of the University Library. Details of these regulations may be obtained from the Librarian. This page must form part of any such copies made.

- The ownership of any patents, designs, trademarks and any and all other intellectual property rights except for the Copyright (the "Intellectual Property Rights") and any reproductions of copyright works, for example graphs and tables ("Reproductions"), which may be described in this thesis, may not be owned by the author and may be owned by third parties. Such Intellectual Property Rights and Reproductions cannot and must not be made available for use without the prior written permission of the owner(s) of the relevant Intellectual Property Rights and/or Reproductions.

ACKNOWLEDGEMENTS

I am using this opportunity to express my gratitude to everyone who supported me throughout the course of this MSc by research project. I am thankful for their inspiring guidance, invaluably constructive criticism and friendly advice during the project work. I am sincerely grateful to them for sharing their truthful and illuminating views on a number of issues related to the project.

I express my warm thanks to Professor Mishra and Dr. Asim for their support and guidance, in the field of fluid dynamics, with the expertise on CFD packages and on surface metrology. Their support has been greatly appreciated and influential for the completion of this project

I also thank my colleagues at Weir Valves and Controls, Mr. K Gibson for his assistance on Solid Modelling and Dr S Tsopanos from The Welding Institute for the support in the field of SLM and with manufacturing samples he provided.

I would also like to thank my wife Rebecca and my family for their support during the late nights and weekend working over the past 6 months, without you I would never have made it.

Matthew Charlton

CONTENTS

LIST OF FIGURES

LIST OF TABLES

NOMENCLATURE AND SYMBOLS

A	Area (ins2, unless stated)
C	(As Cv)
C_i	Cavitation Index [6]
Cp	Static Pressure at the surface of the cylinder (Dimensionless)
Cv	Flow Coefficient (non SI control valve coefficient)
D	Diameter (m)
F_L	Pressure Recovery Value
F_P	Piping Geometry Factor
F_R	Reynolds Number Factor (1 for turbulent flows)
g	Acceleration due to Gravity (m/sec^2)
K	Constant Representing Losses in a Control Valve
K_{IC}	Cavitation Co-efficient, determined through testing
KE	Kinetic Energy (J)
m	mass (kg)
n	number of stages of pressure let down
N_1	Numerical Constant (0.865)
P_1	Inlet Pressure (lb/ins^2)
P_2	Outlet Pressure (lb/ins^2)
P_v	Vapour Pressure of the fluid (lb/ins^2)
P_{Min}	Minimum Static Pressure (lb/ins^2)
pm	Gas and Liquid mixture density at pressure and temperature (lb/ft^3)
P_θ	Gauge static pressure at angle theta (Pascal's)
Q	Volumetric Flow rate (US Gallons/min)
r	Outer radius of the cylinder (m)
r_1	Radial distance from axis of cylinder to where the velocity is taken (m)
T_1	Inlet Temperature (°C)
U_0	Free stream velocity (m/s)
U_x	Velocity distribution, tangential to a cylinder surface (m/s)
V	Velocity (m/s)
Ve	Fluid Erosion Velocity (ft/sec)
X_{FZ}	A Cavitation Co-efficient
ρ	Density (Kg/m^3)
ρ_1	Density of the working fluid (kg/m^3)
ρ_0	Relative Density of Water at 15°C (kg/m^3)
σ	Cavitation Index
σ_{MP}	Manufacturer's Recommended Limit for Cavitation index
θ	Angle from the stagnation point (degrees)

CHAPTER # 1
INTRODUCTION

This chapter introduces the control valves and their variations, as well as an explanation of severe service. There is also an introduction to severe service control valves and their components. The problem statement has been defined, and the aims and objectives of this study have been drawn in this chapter.

1.1 Control Valves

Control valves are one of the most complex flow components used in most production processes(eg Oil & Gas). They are designed to provide accurate control of one or all of the following;

- Fluid flow to or from a process
- Fluid level in a tank or column
- Fluid pressure up or downstream (of the valve)
- Fluid temperature up or downstream (of the valve)

Valves achieve this by constantly varying the position of a plug, against a seat, whereby further away the plug is from the seating face, the more flow can pass through the valve. Control valves come in many shapes and sizes; the style of valve depends on the process conditions that they are required to operate against. Control valves differ significantly from standard on/off isolating valves because their inherent function is to provide control over the process variables as opposed to isolation.

Control valves act as a variable resistance within the pipeline, and it is this function that differentiates them from shut off valves, which are normally in either the closed or full open positions. On the basis of this function, control valves are a mechanism for dissipating energy; when the pressure is dropped across the system and the excess fluid energy is dissipated through noise, heat and vibration. A standard modulating control valve consists of 2 main components:

- The valve body envelope
- The actuation device (Actuator)

Table 1.1 shows some of the standard control valve body styles and provides a brief explanation of the services for which they might be used.

Table 1.1 Typical valves and their uses

Valve Body Style	Typical Use
Globe – Single Port	All Service types – The most flexible body shape
Globe – Double Port	Low pressure, high volume services
Globe – Three Way	Used for either mixing or diverting fluids
Angle (Choke Valves)	Similar to globe, requiring specific piping design
Rotary Butterfly	High volume, low pressure drop services
Rotary Ball	High Volume, low pressure drop services
V-Notch Ball types	Medium pressure drop medium volume services

There are other types of valves not listed in table 1, that may be used on control services, however they are also typically of the lower pressure drop type services. Severe service type control valves, often simplified as a valve with a high pressure drop, would almost always warrant the use of either a globe or angle type control valve.

1.2 Introduction to Severe Service

Severe services are the most interesting and lucrative services to control valve manufacturers. They are generally defined by one or a number of the following;

- High pressure drop
- Erosive services – Flashing liquids, multi-phase applications (wet gases or fluids with entrained solids)
- A cavitating fluid – when the pressure drops below the vapour pressure of the fluid, vapour bubbles are formed which collapse and reduces valve's remaining useful life.
- Noisy services – Typically gases, or cavitating fluids

The determination of what constitutes high pressure drop can be somewhat subjective. The valve type, operational mode and materials of construction can all come into play. Just as important are the customer's expectations of service life and performance. For example: A 10bar pressure drop may be considered high for a swing-through butterfly valve, but may not be considered high for a cage guided valve. A 1000bar drop would be considered high for just about any control valve application. While most control valve applications involve an aspect termed high pressure drop, clearly this is insufficient information to determine the severity of the application.

Erosion can be a problem even when pressure drops would not ordinarily be considered high. Wet gases and flashing liquids can be erosive and require skilled selection of valve and trim design and materials. Entrained solids are by far the most potentially damaging, and present the most difficult problems for design and material selection. In some applications, particularly in the Oil and Gas industry, entrained solids can be coincident with wet gas and or flashing liquids. The amount of entrained solids in any fluid stream can increase pressure drop significantly even at relatively small concentrations. Not all cavitation is damaging. Cavitation occurs in normal municipal water systems without damaging valves and piping components. Some liquids, such as diesel fuel can cavitate at even elevated pressure drops without causing damage to the system. Cavitation can almost always be eliminated in control valves by using some form of multi-stage trim.

Noisy services; noise in excess of 85dBA, almost always involve compressible fluids. Pressure drops that may be moderate for smaller liquid service valves can be high enough to cause noise problems in larger gas control valves. Applications with low outlet pressures,

such as many vent applications, are often the most difficult to achieve low enough noise levels. Often, pipe schedule is thicker to reduce the noise than to meet pressure requirements. Vent applications commonly have higher allowable noise than other gas letdown applications. However, it is important to be mindful of the subjective definitions of severe service. What may be considered a severe service control valve in a municipal water system might be thought of as mild service in a power station. More important is the definition of severe service as it applies to the type of valve. For example, severe service ball valves will not be used by engineer in an application requiring a severe service reciprocating valve. Hence this definition is subjective and selection of valves for appropriate application is made based on specific service requirements. It is clear from the above that specific applications will need special considerations in valve design and valve selection and this is the main reason why this topic has been selected for investigation in the present work.

1.3 Typical Control Valves

Control valves industry offers a wide variety of valves, such as:

1. Globe Control Valves
2. Top and Bottom Guided Valves
3. Double Seated Globe Valves (Double Ported Valves)
4. Three Way Globe Valves
5. Angle Control Valves
6. Choke Valves
7. De-Superheating Equipment

This research study reviews, in particular, the internal equipment of the Globe, Angle and Choke valve product ranges. These are all known as cage guided valves, which have various features to aid in their control duty, such as:

- Low pressure recovery
- Can be fitted with multiple cages or a disc stack style trim.
- Stable cage guiding, reducing pressure fluctuations and vibration
- Balanceable – reducing actuator load requirements
- Simple low cost in-line maintenance available – via clamped seats
- No special tooling requiring
- Contains erosive effects of the process fluids within the valve trim

Figure 1.1 Globe Control Valve [31]

Figure 1.1 shows a typical 4inch globe type control valve with a diaphragm actuator.

1.4 Components of Control Valves

A control valve, be it an angle type or globe type, is made up of a number of components. Although these components may change in design or size, their basic concept is applied to each control valve. The major components are discussed below.

1.4.1 Body and Bonnet / Pressure Envelope

The body, bonnet and the method of connecting the two together to form the pressure envelope are the most standard components with a valve. Their design will change based on size, manufacturing standard, temperature and material. A typical control valve is shown in figure 1.1. Typically control valves industry manufacture predominantly globe and angle style bodies, which would traditionally be supplied with bolted bonnets; a bonnet design connected to the valve through drilled and tapped holes in the body and connected by standard studs and nuts or bi-hexagonal bolts.

The bonnet design will also alter slightly when dealing with temperature extremes; standard bonnets are offered between temperature ranges of -46°C and 315°C. Above and below this range, the valve will be supplied with extended bonnets or normalising bonnets, to keep the valve packing away from the pressure envelope to increase its life span, and to enable the valve to be lagged. Valve packing is located at the top of the valve in the bonnet (an area

called the packing box) and is a softer sealing element around the valve stem. The packing prevents leakage through the stem area which is required to operate the valve. Packing, Studs and Nuts, body/bonnet and other gaskets/seals are all considered parts of the pressure envelope.

1.4.2 Valve Trim

The valve trim is made up of a seat, the plug/stem and the cage/stack. The plug and seat are standard components; the plug moves up and down in a vertical motion away from the seat to allow the fluid to flow through the valve. When fully closed i.e. the plug is in contact with the seat, the valve is considered to be closed preventing flow of fluid. The plug is connected to the stem, allowing for its motion. The plugs can come in a variety of designs and in different valve types are called discs, needles or balls, but the basic principle remains the same.

The cage or stack is the main controlling element of a control valve. The cage controls the amount of flow passing through the control valve based on the valve opening position. The most common type of cage in a control valve is a multiple drilled hole cage. In this design, the fluid is forced to change its direction, and is passed through orifices to reduce its pressure. Multiple cages installed in series distribute the pressure drop based on the area of each cage, and are called multiple stage cages or trims.

1.4.3 Actuator

The actuator is an important controlling device for the valve. It is mounted on the top of the valve body via means of a yoke. A stem from the actuator is connected to the stem from the valve via a stem connector. The actuator's motion moves the stem up and down, controlling the percent or degree of opening of the valve (termed in this study as valve opening position). The actuator style varies; the most common types are pneumatically operated actuators, where the air is used to move a piston or a diaphragm up or down a cylinder or against a spring. Other types of actuator include, Hydraulic (either from a ring main hydraulic supply or a fixed source local to the actuator), electric or manual; which would be a direct handwheel attachment.

The actuator type is generally determined by the customer depending on the nature of supply they have on the plant. An actuator type (piston, diaphragm, multi-spring, stepper) would then be selected by the manufacturer, depending on the thrust requirements and the requirements of the valve for operation i.e. operating loads. The user will then control the motion of the actuator by controlling the supply to the unit.

1.4.4 Control System

The final part of the control valve is the control system. Not all valves have an independent control system. If the valve is fitted with an electric actuator, then it is an internal system supplied with the actuator, and obviously manually operated valves don't have one. Pneumatically operated valves, however, will always have some sort of control system attached to the actuator for the end user to control the unit remotely (usually from the control room).

The most common method of control is via a valve positioner. Positioners convert an electrical input signal from the control room (4-20mA) into a pneumatic signal, deciphering this milliamp signal into a required valve opening percentage, and then applying air to the actuator in order to move the actuator to the required position. Most modern positioners are supplied with either an analogue HART signal or a digital control system (like Foundation Fieldbus), whereby they will then be able to communicate back the position of the valve to the control room

Positioners are the preferred method of control when dealing with modulating service control valves; however, for some on/off duty valves, the position of the valve will be controlled via a simple solenoid valve. Solenoids either apply air pressure or vent air, and are not suitable for controlling to specific positions. They only move the valve to the extremities of its motion. Instrumentation can become quite complex on control valves, depending on the requirements of operation and the end users requirements for how they wish to control the valve. There are a variety of additional instruments, some of which are listed below:

- Limit Switches – Report back certain position limits to the controller
- Volume Boosters – Increase the speed of air being sent to the actuator
- Filter Regulators – Regulate the air supply to the positioner and filter it
- Volume Tanks – Used as a back-up air supply to the actuator in case of air failure
- Spool valves – Used to change to another means of supply like a volume tank
- Airlocks – Lock the valve in position, used to make the valve fail in its last position

Valves that would be considered by the manufacturers as very simple and basic valves (with a simple trim) may have some complex control systems, as the user is reliant on the valve for certain functions within their process.

1.5 Disc Stack Technology

Cage guided trims are the most common trim design installed within globe and angle control valves. Other designs, like seat guided trims or plug guided trims, are used in either small (25-50mm) valves, or very low pressure services. Other manufactures use axial (plug guided)

trim designs in place of multiple cage trim designs, when dealing with higher pressure drops (example in Figure 1.2).

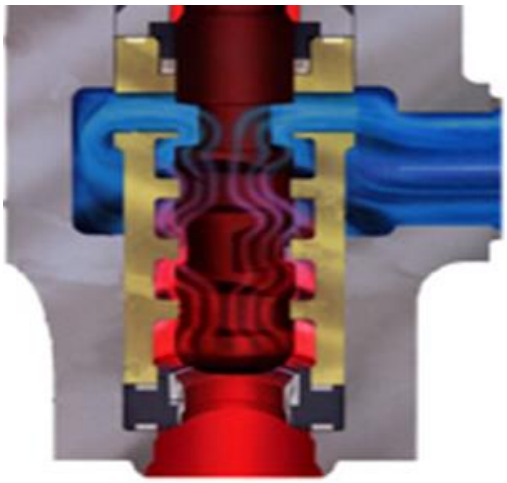

Figure 1.2 Axial Trim Design [6]

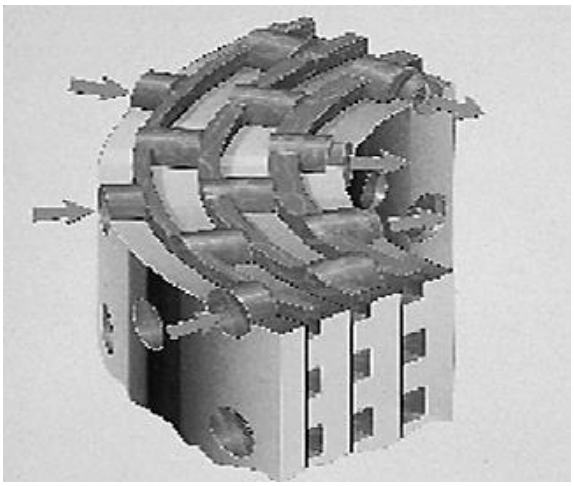

Figure 1.3 Multiple Cage Trim Design [6]

Multiple Cages (see figure 1.3) use a series of multiple hole drilled cages to provide a torturous path to the process fluid. They use the change of direction as a means to reduce pressure by forcing the fluid to do work. They are a relatively low cost trim design, providing lower pressure recovery values, and are of the anti-cavitation and low noise configuration for a control valve.

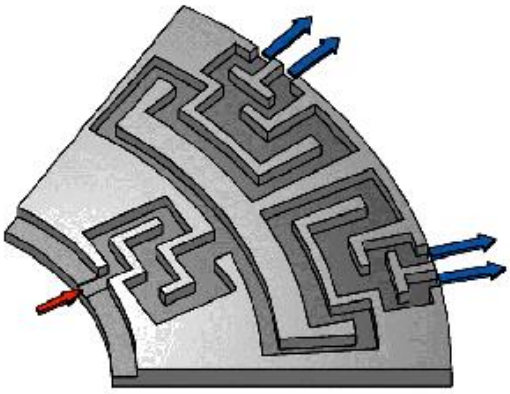

Figure 1.4 Typical Disc Stack Design [6]

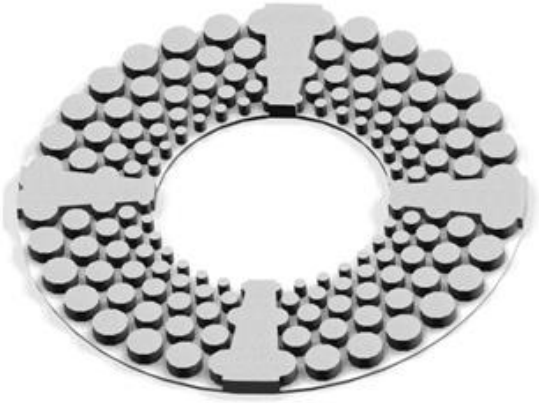

Figure 1.5 X-Stream Disc Design [6]

They however are limited in the number of cages that can be installed within a single valve. A standard valve will be able to accommodate up to five cages in series (five stages of pressure drop) where control valve manufacturers recommend a maximum differential pressure across a single cage as 50bar. They also have no consideration for flow velocity control, as the cages assume an equal area for the process fluid. They use small holes and turn the fluid through sharp 90 degree bends, which often leads to issues when used on services with solid contamination. Many of the same features and problems exist with the axial trim

designs, whereby the higher the number of stages of pressure drop, the larger the valve; thus higher the cost.

Some control valve manufacturers have another trim design that they offer when the required control cannot be accommodated within a standard cage or axial trim design. Often referred to as disc stack trims, these designs are also of the cage guided design type. However, they use a series of stacked discs, each with a complex flow path, typically turning the fluid through a labyrinth of right angle turns, expanding the area after each stage of pressure drop, in order to reduce the velocity of the fluid across the length of the disc, and reducing the overall trim exit velocity. Figure 1.4 shows a typical design of disc stack. An equivalent disc stack trim is called X-Stream, and was developed to predict areas within the standard right angle disc stacks that may be a cause of cavitation, high velocity (erosion) and noise. The standard disc stack designs were identified to have limited capacities due to the resistance to the flow inherent with this style of torturous path. The X-Stream design also uses a series of stacked discs, however achieves pressure reduction via 3 methods.

- Change of direction
- Contraction of the fluid
- Jet impingement

Figure 1.5 shows the latest design of X-Stream. This design has changed significantly since its original conception to further improve its performance. As can be seen in Figure 1.5, the design uses columns/cylinders as obstructions to the process fluid, with the columns installed in a series of circularly arranged rows. These restrictions force the fluid to change its direction around the cylinders (a stage of pressure reduction) and allowing the fluid to take a streamlined flow path, rather than passing through torturous perpendicular bends. The fluid flow is restricted as it passes between the cylinders, is then allowed to expand (increase of area) prior to the next row of columns, and is also subject to jet impingement from another stream of fluid passing from the other direction round the column. There are many variables to the design of the disc that control the capacity and the number of stages of pressure drop, some of which are:

1. The number of rows of columns – which links to the number of stages of pressure drop by the expression 2n - 2, where n is the number of rows
2. Number of cylinders per row
3. The size of the cylinders – Minimum and maximum

The latter 2 points control the size of the gaps for the fluid to flow between the cylinders, and as such are related to the pressure drop. All of these properties must also consider the manufacturing constraints, whereby the minimum gap must be sufficient enough to be manufactured cost effectively.

1.6 Performance Characteristics of Control Valves

After a long era of research regarding fluid flow through control valves, a breakthrough in valve sizing came with the development of a design parameter, experimentally derived by Ralph Rockwell in the late 1930's. In 1950, Chairman Al Hanssen of the standardization committee of the control valve section of the Fluid Controls Institute (FCI) began an effort to standardize the procedure for determining valve flow capacity, or Cv.

Test facilities were in place at Fisher (a major Control valve manufacturer) by 1952. The FCI standard Recommended Voluntary standard for Determining Control Valve Capacity was issued in 1958. The FCI standard was the basis for control valve testing, and was adapted and revised for incorporation into a later ISA standard, and subsequently a harmonised European standard, IEC BS EN standard 60534-2-1 [1]. Cv is now the fundamental parameter used in sizing control valves. The mathematical formulation for Cv varies, depending on whether the fluid flowing through the valve is an incompressible fluid or a compressible fluid. Cv formula for an Incompressible fluid is calculated as follows:

$$Cv = Q \times \sqrt{\frac{\rho_1/\rho_0}{P_1 - P_2}} \tag{1.1}$$

where;

Q = Volumetric flow rate through the valve in US Gallons per minute
ρ_1 = Density of the working fluid in kg/m^3
ρ_0 = Relative density of Water at 15°C in kg/m^3
P_1 = Inlet pressure to the valve in psi
P_2 = Outlet pressure from the valve in psi

This expression was derived from the principles of Daniel Bernoulli, who, in his Hydrodynamica publication [2], stated that for an inviscid flow, an increase in the fluid velocity results in a decrease in its pressure. This is known as Bernoulli's principle and can be written as follows, when referring to control valves:

$$\frac{P_1}{\rho g} + \frac{v^2}{2g} = \frac{P_2}{\rho g} + \frac{v^2}{2g} + k\frac{v^2}{2g} \tag{1.2}$$

where;

P_1 = Pressure at inlet of the valve in Pa
P_2 = Pressure at outlet of the valve in Pa

ρ = Density of the working fluid in kg/m^3
g = Acceleration due to gravity in m/sec^2
k = A constant representing losses within the control valve

Assuming that:

- The inlet and outlet sections of the valve have the same geometrical dimensions
- The inlet and outlet of the valve are at the same elevation

Eq. (1.2) can be re-arranged to obtain the sizing equation for Cv for a control valve:

$$\frac{P_1}{\rho g} - \frac{P_2}{\rho g} = \frac{v^2}{2g} - \frac{v^2}{2g} + k\frac{v^2}{2g} \tag{1.3}$$

$$\frac{P_1 - P_2}{\rho g} = k\frac{v^2}{2g} \tag{1.4}$$

Since v (Velocity) = Q (Flow rate) / A (Area):

$$\frac{P_1 - P_2}{\rho g} = \frac{k}{2g}\frac{Q^2}{A^2} \tag{1.5}$$

$$Q = \sqrt{\frac{2A^2(P_1 - P_2)}{k\rho}} \tag{1.6}$$

or,

$$Q = \text{constant}\sqrt{\frac{P_1 - P_2}{\rho}} \tag{1.7}$$

Now,

$$Q = \text{constant}\sqrt{\frac{\frac{P_1 - P_2}{\rho_o}}{\frac{\rho}{\rho_o}}} \tag{1.8}$$

Hence,

$$Q = \text{constant}\sqrt{\frac{P_1 - P_2}{\frac{\rho}{\rho_o}}} \tag{1.9}$$

The constant in equation (1.9) could be re-written as Cv, and this constant is related to the area. After understanding the Cv of the process conditions, the valve manufacturers need to supply a valve that is capable of achieving the Cv requirements of the process. The valve itself is a restriction to the flow. There is a pressure drop across the valve, even when is at 100% open position. So, the valve also has its own Cv, which is a summation of the Cv's for each of the three restricting elements of the valve, i.e.:

- Valve Body
- Valve Trim (Cage / Disc Stack / Plug)
- Valve Seat

These restrictions add up to give the total Cv of the valve system, which is defined as:

$$\frac{1}{Cv_{Valve}^{\ 2}} = \frac{1}{Cv_{Body}^{\ 2}} + \frac{1}{Cv_{Trim}^{\ 2}} + \frac{1}{Cv_{Seat}^{\ 2}} \tag{1.10}$$

which becomes,

$$Cv_{Valve} = \frac{1}{\sqrt{\frac{1}{Cv_{Body}^{\ 2}} + \frac{1}{Cv_{Trim}^{\ 2}} + \frac{1}{Cv_{Seat}^{\ 2}}}} \tag{1.11}$$

Furthermore, as shown above (eq.1.6), Area A and the loss constant K were replaced with a single value constant; Cv, thus Cv can be shown to be related to Area as:

$$Cv = A \times K \tag{1.12}$$

so,

$$A \times K = Q \times \sqrt{\frac{\rho_1/\rho_0}{P_1 - P_2}} \tag{1.13}$$

Thus, when area is known, and with a given set of process conditions, K can be determined for each element of the valve. These values for Cv for each element can then be substituted into equation 1.11 to determine the overall valve Cv. Determining K from empirical testing is required as part of this study, for each of the proposed modified designs.

1.7 Cavitation and Erosion

In the following sections, cavitation and erosion phenomena in severe service control valves are discussed.

1.7.1 Cavitation

Cavitation is a process whereby a fluid undergoes changes in its state. As liquid passes through the control valve trim there is an increase in its velocity due to area reduction, which as shown in Figure 1.6, results in the decrease of its static pressure. If this pressure falls below the vapour pressure of the liquid, vapour bubbles are formed. After the Vena Contracta; the point of minimum static pressure, the pressure recovers back above the vapour pressure of the liquid (P_v) and the vapour bubbles collapse, resulting in the phenomena known as cavitation.

The onset of cavitation can affect the valve in a number of ways:

1. The flow within the valve trim element becomes choked. Choked flow is a condition whereby there will be no further increase in mass flow rate with a reduction in downstream pressure (P_2)

2. Valve generated noise will increase, which is a major concern for plant operators. Cavitation noise is very distinctive, similar to ball bearings rattling around a metal container. Fully developed cavitation can cause a high pitched scream, resulting in mechanical vibrations of the trim and the other elements of the valve or pipework

3. Potential for premature trim erosion. The impact damage of the bubbles collapsing is incredibly erosive and can erode contact areas

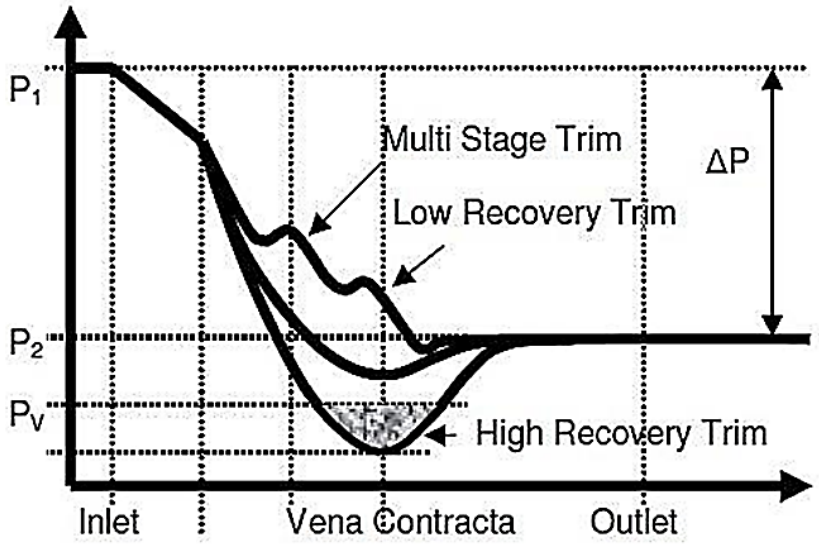

Figure 1.6 Typical pressure drop curve within a control valve [6]

Ideally, cavitation needs to be eliminated, which is achieved with the use of low pressure recovery trims, as shown in Figure 1.6. Typically low pressure recovery trims are of the

multi-stage type. In order to avoid cavitation the static pressure of the fluid needs to be prevented from falling below the vapour pressure. In multi-stage trims, this is achieved by distributing the pressure drop across a number of stages, each with their own pressure recovery value, preventing the static pressure from falling below P_v at any point within the trim. The number of stages of pressure drop required to prevent cavitation is dependent on three main factors:

1. The differential pressure across the system
2. The vapour pressure of the fluid
3. The pressure recovery value of the trim (F_L)

The ISA specification RP75.23-1995 – Considerations for Evaluating Cavitation, defines the various states of cavitation, Incipient (cavitation or damage), Choking or Constant. There is also a recognised formula for determining the cavitation index of the fluid (σ).

$$\sigma = \frac{P_1 - P_v}{P_1 - P_2} \tag{1.14}$$

RP75.23-1995 [3] identifies that σ quantifies only the service conditions and that by itself does not provide any information relating to the performance of any particular valve with these conditions. RP75.23-1995 [3] further identifies that factors such as valve style, opening, duty cycle, location, desired life and past experience should be considered, and that the valve manufacturer should always be consulted. RP75.23-1995 [3] advises that a manufacturer may recommend a limit for cavitation based on these factors which are defined as σ_{MR}. Manufacturers generally publish values for σ_{MR} for their various trims and valve designs, and often publish within their various technical manuals the criteria for the determination for this value. Control valves industry use the following formula within their technical literature for σ_{MR}:

$$\sigma_{MR} = \frac{1}{K_{IC} - FL^2} \tag{1.15}$$

where;
K_{IC} is a cavitation co-efficient, determined through testing

This study does not intend to determine values for K_{IC} , as this type of testing must be carried out with physical models, however, it is intended that this research can predict the areas of minimum static pressure (and their values), which when compared against the vapour pressure of the fluid, would identify potential areas for cavitation. Cavitation is a major consideration when defining trim designs within control valves. The use of the manufacturers recommended limits does not necessarily determine whether cavitation will be prevented. RP75.23-1995 [3] concludes that σ_{MR} may or may not coincide with other cavitation coefficients, such as incipient damage or constant cavitation, meaning that cavitation may still occur, however, the manufacturer has deemed that other properties, like material, size

etc., mean that they do not anticipate the cavitation to cause significant damage. Samson et al in their technical paper "Predicting Cavitation damage in Control Valves" [4] identify that the strength value of the bubble formed, which can be theoretically calculated based on the fluid, has a significant impact on the erosive force of the cavitation. This paper discusses a value X_{FZ} as another cavitation coefficient, which appears similar to σ, rather than assuming the vapour pressure of the fluid. The value of P_{min} is used, however, they also identify that P_{min} would be in the unstable vortex region and cannot be determined by direct measurement. (shown in Equation 1.16)

$$x_{FZ} = \frac{p_1 - p_2}{p_1 - p_{min}} \tag{1.16}$$

There is another parameter used by some control valve manufacturers to determine the potential for the fluid to cavitate. This is called the cavitation index. This works in much the same way as the standardised method for σ and σ_{MR}, however, rather than separating these two values apart, they are joined together into one formula. Introl 'Technical Sizing and Selection manual [5] and WEIR 'Technical Sizing Manual' [6] use Equation 1.17, which shows the formula they use. Please note that some manufacturers denote different letters for certain fields, however, for the sake of this thesis, these letters have been kept in line with those above for the same subject.

$$C_i = \Delta P - F_{L^2} \times K_I \times (P_1 - P_v) \tag{1.17}$$

which alters slightly, while using multiple stages, to:

$$C_i = \frac{\Delta P}{n} - F_{L^2} \times K_I \times (P_2 + \frac{\Delta P}{n} - P_v) \tag{1.18}$$

They then define allowable levels for each trim design and material of manufacture, as shown in Figure 1.7. If the value is negative, then this is an indication that the selected trim design is sufficient for this duty, and if the value is positive, they advise to either change material or increase the number of stages. Cavitation is one of the major issues affecting valves in liquid applications. The pressure recovery values for trim designs, and areas of re-circulating flow are important in the performance of the product, for preventing or reducing cavitation.

Material	Cavitation Index (C_i)			
	Single stage		Multi-stage	
	psi	bar	psi	bar
316L	5	0.3	3	0.2
17.4 PH	8	0.5	5	0.3
Full stellite grade 6	20	1.4	10	0.7
Full stellite grade 12	26	1.8	12	0.8
Monel	8	0.5	5	0.3
Ferralium	10	0.7	8	0.5

Figure 1.7 Advised Cavitation values for various materials [6]

1.7.2 Erosion

Erosion in control valves occurs as a result of general wear between two objects, whether this is a fluid and a solid, or a solid and another solid. This is no different in control valves. However, a control valve is designed to either control the flow rate or pressure drop, and as a result, there is a change in velocity and pressure through the trim; as pressure is reduced, velocity increases. The instrument engineers handbook discusses that erosion can occur as a result of high velocity impingement, erosive particles or a combination of erosion – corrosion. They also state that erosion damage will increase with the square of velocity, which fits with the definition of kinetic energy, i.e.:

$$KE = \frac{1}{2}\, m \times v^2 \tag{1.19}$$

Controls can be used on a variety of applications, sometimes defined as simply modulating or on/off, or with more detailed application information, like the service boiler feed water regulator. Each of these services can require full open or close motion, or simple minor adjustments with varied frequencies of operation. Hence, design around wear against another mating component is generally not considered. Instead, they design around the principle of velocity control within the valve body, and within the trim. Control valve manufacturers will assign maximum recommended velocity limits through the valve body (for either incompressible or compressible services) depending on the shape/style of the valve, and the material it is made from. Figure 1.8 depicts such limits advised by Weir Valves and Controls [6]. There is further consideration of velocity, by control valve manufacturers when selecting/proposing the trim design for the valve.

Miller [7] suggests restricting the exit velocity from the trim to approximately 30m/s (100ft/sec) for liquids and is more specifically defined by Miller and Stratton [8] for compressible fluids. Miller explains the theory behind this further in his publication "Control Valve Trim Fluid Exit Kinetic Energy and Velocity" [9], where he states that the trim exit kinetic energy criteria was chosen to expand the methodology, that is used for liquids to other fluids, specifically gases. It is frequently referred to as Velocity Head, but that is also the dynamic pressure of the fluid at velocity V and the volumetric kinetic energy of the fluid. The paper advises that as such this formula/method is a strong representative expression of the force driven by the pressure difference causing the expansion of the fluid through the valve. There are likewise 'recommendations' for the maximum velocity head through a control valve of 4.8bar for standard duty. This value can change when dealing with other more severe services, however the article by Miller [9] does explain how this value has come about. Miller advises;

> "The 4.8bar (70psi) criterion is based on water traveling at 30m/s (100ft/s), which was the criterion for trim exit used in many valves and for many years by Control

Components Inc.(CCI). Thus; $\rho V^2/2g$, is nearly equal to 4.8bar (70 psi) when the velocity is 30m/s and the density (water) is 1000kg/m^3 (62.4lb/ft3)."

Material	Rating
Aluminium Bronze	Low
Carbon Steels WCB, LCB, LCC	Medium
Monel 400	
Hastelloy B2 & C276	
Chrome Moly WC6, WC9, C5, C12A	High
Stainless Steel CF8M, CF3M	
Duplex Stainless Steel A890 Gr 4A & Gr 6A	
Inconel 625	

Valve Size (mm)	Guiding Type	Maximum Velocity m/s		
		Low	Medium	High
15 -25	Cage	12	18.3	20
40 - 200		9	13.5	15
250 - 500		8	11.5	13.5
600 - 900		5.5	8	9.5
15-50	Top, or Top & Bottom	8	12	13
80-150		7	11	12
200-350		7	10.5	12
400-450		5	7.5	8
500		4	6	7
600		3	4	4
15 - 50	Seat	8	12	13

Figure 1.8 Recommended Velocity Limits [6]

$$KE = \frac{\rho \times v^2}{2g} \tag{1.20}$$

The American Petroleum Institute Recommended Practice 14E, Offshore Production Platform Piping Systems, [10], uses the Kinetic Energy methodology as a design criterion for piping systems.

The equation they use is:

$$V_e = \frac{C}{\sqrt{pm}} \tag{1.21}$$

where;
V_e = Fluid Erosion Velocity (ft/sec)
C = Empirical Constant – which differs depending on the duty
pm= Gas/liquid mixture density at flowing pressure temperature (lb/ft^3)

In this formula 'C' is equal to Velocity squared multiplied by the density. The values of 'C' are quite conservative values when compared to the values allowed by another valve manufacturer. Miller [9] argues that this again reflects the more rugged construction associated with the valve versus the piping system. A lot of valve companies used to have

their own recommendations for velocity limits, most of which were deemed proprietary information and were not disclosed. However with the introduction of the "Trim Exit Velocity" and "Velocity Head" theory by Miller [7] and Miller/Stratton [8], these values have been adopted by the ISA (Instrument Society of America) and published as 'guideline values' within their publication "practical guides for measurement and control" [11].

Weir Valves and Controls [6], as part of their sizing and design recommendations apply these 'guidelines', however they also consider the velocity at all stages within the trim rather than just at the exit. They have defined this approach as "Total Velocity Control" and impose further recommendations on the velocity of the fluid through the trim. They argue in one of their technical product catalogues (X-Stream) that at the trim inlet there is a higher potential for erosion, as most conventional disk stack designs use a constant expansion theory within their trims, reducing the velocity from a peak at the inlet to the lowest point at the exit; which is in line with the ISA recommendations [11].

However Weir argues that this approach has led to the premature failure of a number of trims, as too much emphasis is placed on exit velocity, rather than inlet. They advise that historical failure analysis and CFD studies performed on the typical 90° bend stacks indicate that they suffer from erosion as inlet velocities to the trim can reach values exceeding 100m/s. With liquids, as can be expected when approaching velocities of these values, the erosion potential is very high;, further on gas applications, the fluid expands and reduces in density as the pressure reduces through the valve. With that in mind it can also be argued that as density is at its highest at the inlet of the trim, the potential for erosion on gas discs is also high on the inlet.

The analysis of local velocity within this study is thus of great importance to the performance of the trim and thus the design. Areas within the trim that can result in high velocities are to be avoided as these areas have the potential to lead to premature failure.

1.8 Manufacturing Issues in the Valve Industry

1.8.1 Electric Discharge Machining

The most common method of manufacturing discs is a process called Electric Discharge Machining (EDM). This process is often called Spark Eroding, Wire Erosion or Spark Machining. The process is a thermal erosion process where metal is removed by a series of electric discharges between 2 electrodes, usually a cutting tool electrode and a conductive piece of material that needs to be machined (e.g. Steel), all in the presence of a dielectric liquid. The discharge results due to a voltage gap between the 2 electrodes. Heat from the spark erodes small particles of the piece of material, which are then removed by flushing the liquid.

The two main types of EDM are Probe/Ram (also called Die-Sink) and Wire Cut. In Ram EDM, the tool is connected to a positive pole of a power supply, and the work piece is connected to the negative pole. A gap is left between the two electrodes, and is filled with the fluid. When turned on, the power supply passes thousands of DC impulses across the gap, starting the erosion process. As the erosion occurs, the ram moves down to maintain a constant gap between the two pieces. The cutting electrode is fabricated with the negative side of the piece that needs to be machined using the RAM process, and will be larger than the cutting piece. The difference in size is called the overcut.

Wire EDM works slightly differently in the respect that electrode is actually a fine wire, which is constantly replaced on a feed system when it has worn away. This system operates much in the same way as RAM, requiring the fluid, the constant gap between the two pieces and the DC power supply. However, the wire, rather than a negative electrode, means that this system makes much smaller cuts that can be more accurately controlled for overcut. This method uses less power as the wire is thin, and thus the removal rates for material are reduced.

In general, the EDM process is considered as a relatively expensive process, however, the rates for manufacturing smaller components (outer diameters less than 150mm) are comparable with some milling machines (when dealing with more complex shapes/structures). However, when going to larger sizes, EDM processes are restricted. The cost to manufacture the electrode increases with size, with additional issues that are related to the amount of heat being transferred to the material, often resulting in deformation of the end shape. EDM was originally developed as a method of removing taps that had broken in their holes, however, through other technological advances, the process has expanded to its current use today.

1.8.2 Selective Laser Melting / Additive Manufacturing

Selective Laser Melting is a member of a group of manufacturing methods often called Solid Free Form Fabrication (SFF) technologies, using layer based direct fabrication of metal. Historically SFF technologies have been used with rapid prototyping for visual models, whereby free form means that no specific tooling is required for the manufacture process. Parts are built up in an additive layered manner by bonding two dimensional profiles to form a 3D profile. When used for something other than visual models, these processes are generally called Rapid Manufacturing (RM).

Burns [12] refers to Solid Freeform Fabrication as an automated fabrication process that meets five criteria, which were considered to be defining an RM/SFF process. The five criteria are:

- The process should take in raw material in some shapeless form, such as blocks, sheets or a fluid, and produce solid objects with a definite shape

- The process must do this without any significant human intervention

- The process must produce shapes with some degree of three-dimensional geometrical complexity. This criterion eliminates the forming of simple tubes or rods by extrusion, or the drilling of holes in sheet material

- The process must not involve the manufacture of new tools for each different shape that is generated (part-specific tooling). This criterion eliminates all type of moulding and casting, EDM sinking and copy milling

- Each item produced must be a single object, not an assembly of component parts, thus eliminating joining operations such as gluing, welding and riveting

Additive or Rapid Manufacturing offers greater potential than most other methods for producing objects with not just unique geometrical combinations, but also material combinations, and has led to the use of RM more and more in many industries as a method of manufacture for certain components. For all RM technologies, the starting point is the geometry of the part to be created, held within a computer model. From this, a set of instructions are generated that describe the geometry, and then further define these instructions to control the machine.

With SLM machines, there are a number of parameters that affect the build quality and that are responsible for the build itself. Laser spot size is the size of the laser beam at the application point, laser power is simply the power of the laser itself (this can be altered during the process), exposure time is the amount of the time that the metal is exposed to the laser, point distance is the distance between each laser spot and hatch distance is the distance between the lines of spots.

All of these features are important to determine the build quality of the part, their effects on the features of importance to manufacturing disc stacks requires further investigation. Some valve manufacturers have been investigating this method of manufacture for use with their disc stack products, with little overall success [6 &31]. Parts manufactured to date appear to suffer from deformities during the manufacturing process and do not deliver the dimensional and other requirements of the current designs, however the potential of the process, mainly with the significant reduction in lead times (hours rather than weeks), keeps this process as one showing potential for these complex geometry style products.

1.9 Motivation for Work

Severe Service valves have undergone significant development over the past few years from their original concept designs. This development program has been fully supported by the industries requiring the specific control these products provide, however as more and more services are requiring these products and the changes to the economic climate, there is a significant drive to reduce costs for these products.

Currently, 90% of the X-Streams that have been manufactured to-date, have been manufactured using the Electron Discharge Machining (EDM) method, often known as spark eroding, the other 10% are made using traditional machining operations (i.e. milling). This manufacturing method can be quite costly, especially when increasing the number of stages or the capacity of the disc. Furthermore, EDM has relatively long lead times (of up to 10 weeks per disc), limiting the delivery times for original equipment, and also spares replacements. Preliminary investigation of the SLM method of manufacture has shown that costs could be reduced by up to 50% on a like for like disc design, combined with a significant reduction in manufacturing lead times. The primary focus of this study is to customise the X-Stream design for the ALM/SLM manufacturing method, whilst critically evaluating the performance of the product following these new design proposals.

1.10 Research Aims

The overarching aim of this research study is to develop a novel manufacturing method and establish its effects on the performance characteristics on the X-Stream trims explicitly. The manufacturing technique should show cost and lead time reductions. It is important to determine at the outset, whether existing research has been undertaken for specific modifications to existing designs specifically due to the limitations of the ALM/SLM manufacturing technology's and to review of performance characteristics of X-Stream and other similar disc stacks with a view to highlighting the effect of the geometry.

The research will investigate current manufacturing limitations when using SLM specifically for the X-Stream product identifying limiting parameters within the X-Stream geometry and assembly process that restrict the performance without design modifications.

1.11 Overview of Thesis

An overview of the thesis is described as below:

Chapter 1- This chapter introduces valves and their performance characteristics, further introducing the reader to the X-Stream product and to some methods of manufacture of this product.

Chapter 2 – This is a critical appraisal of the literature relating to the SLM/ALM method of manufacture, performance of X-Stream trims and valves and the effect of surface roughness on fluid flow within valves.

Chapter 3 – This chapter will provide an explanation of the experimental and numerical formulation, including working of the CFD codes, geometry creation, methods to find Cv for the trims and the scope of the experimental and numerical works.

Chapter 4 – This chapter performs a critical comparison of process optimisation of the SLM process against design optimisation. Designs of an XLO8-040 X-Stream are reviewed; these designs are reviewed for manufacture and samples created. Samples are flow tested and compared against the original design, manufactured using an optimised process.

Chapter 5 – This chapter looks at the second research aim of completing numerical testing of new designs. The testing focuses on the changes to the performance characteristics for trims with hydro-dynamically smooth surfaces against trims with applied uniform surface roughness and also non uniform roughness. Contours of static pressure and velocity are reviewed to ascertain the effects of geometric features on the performance of the trims.

Chapter 6 – Concludes the findings of the research performed and details recommendations for future work.

CHAPTER # 2
LITERATURE REVIEW

This is a critical appraisal of the literature relating to Selective Laser Melting, the importance of geometry on performance of the product and the effect of surface finish on fluid flow. This chapter also defines the objectives for this thesis following the review of research in the above areas.

2.1 Literature Review Introduction

This chapter has been subdivided into four main sections to appropriately review the literature existing for the areas of research of this study. The chapter begins with an in-depth review of ALM/SLM manufacturing methods and research completed on this field that may provide valuable insight into current issues with manufacturing disc stacks using this process. It will also review the performance characteristics of the X-Stream trim and other severe service disc stacks to understand the principles of their design. A review of surface roughness effects on fluid flow within these severe service disc stack products will be completed. The chapter will conclude with the setting of specific research objectives following the literature review.

2.2 Selective Laser Melting / Additive Layer Manufacturing

In simplified terms, SLM uses a laser beam to fuse very small particles of powdered material, together which are held in a powder bed. Figure 2.1 shows a basic understanding of the principle components to form a typical powder bed SLM machine [13].

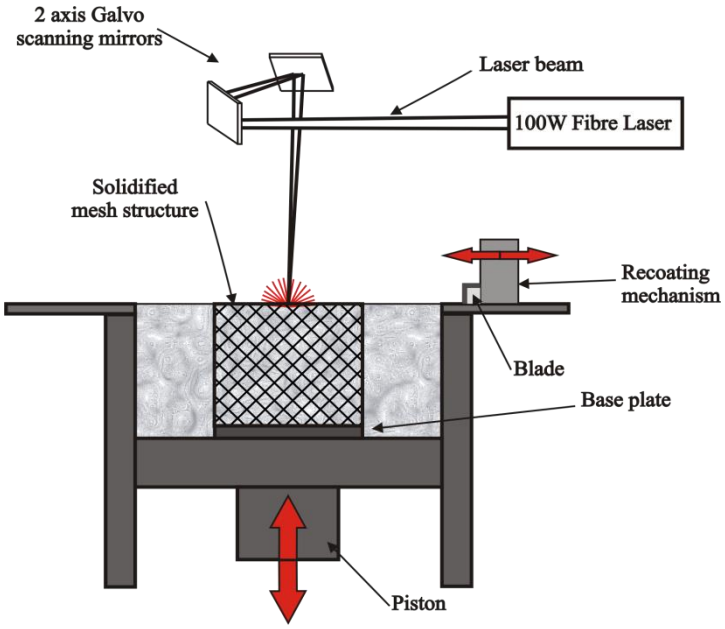

Figure 2.1 Example of an SLM Machine

The laser selectively fuses the particles together from a cross section, provided directly from a 3D model of the part on the surface of the powder bed. After each pass, a wiper arm comes back across the powder bed and deposits the next layer of powder on to the powder bed. This process is repeated until the part has been fully defined. Tsopanos [13] details a number of features that further define the minimum features in the RM process. He describes the slicing process and issues that can occur during the manufacturing phase. He also provides details of

a number of RM technologies, focusing on Selective Laser Melting. He gives an in depth analysis on various features important during the manufacturing phase, for example hatch distance, and how this affects thermal conductivity and the energy density, which formulates the length of exposure of the laser and the laser power. Tsopanos concludes that the process lends itself to be used for general manufacturing of complex parts, but that surface finish is a major concern and that dedicated control systems need to be considered for the optimisation of the this process.

The SLM process can be further optimised to work with more complex Nickel grades by using argon chambers for the lasers, and pre-heating for crack susceptible alloys. General systems use lasers around 200W in power, and can be focused to small spot sizes of around 40microns, with very fine layers of powder deposited (e.g. 20microns). Early work on SLM links the layer thickness, power and spot size to the overall surface finish, and build rate of the products, whereby the lower these values, the slower the process, but not necessarily more accurate. The Welding Institute (TWI) [14] is heavily involved in manufacturing and research, in the field of SLM, and has written and submitted a number of papers related to the process. Principally, SLM was used for Rapid prototyping, however, in recent years, development of newer higher powered lasers have meant that the process can, and is, being used for more generalised production purposes.

In an article submitted to the Association of Industrial Laser Users [15], the author summarises that SLM was typically used for product development, where parts made using this process are used for fitness and functional testing. Parts in these phases of development often require multiple changes, and SLM can perform a number of iterations of a design for performance evaluation. SLM is also used more frequently in low volume fabrication, often with bespoke, highly customised parts, where tooling costs for other methods of manufacture would not be cost effective. An uncredited article in high performance composites [16] discusses how the selective laser sintering (SLM) process has been changed from simple rapid prototyping to rapid manufacturing. They have developed composite sinterable powders that are able to meet the strength requirements for the harsh operation of the reed valve in a motorbike engine. The SLM process opens new possibilities for the manufacture of many products, by allowing the manufacture of components from materials that may not have been available from other forms.

Additive Spy [17], an organisation that monitors the applications for additive manufacture, is witnessing an increased use of SLM for the manufacture of complex geometric components, including another valve company, and a company using SLM for the manufacture of a complex geometry impeller for quieter cooling. The design of the impeller follows a very similar geometric profile to that of the X-Stream disc stack, turning the fluid around a number of cylinders (see figure 2.2)

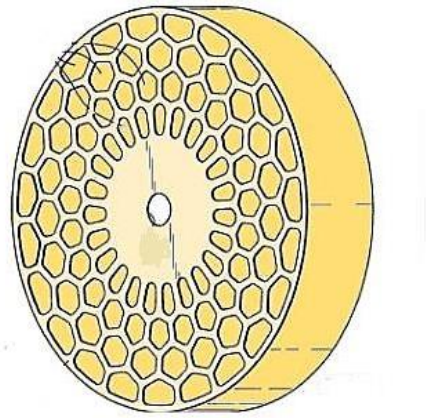

Figure 2.2 Impeller Design Example [17]

Development work on the laser sintering process also includes the effect of certain operating parameters on the overall surface finish, and other factors like the porosity of the samples. An article by Jobin et al [18] discusses the variance in the peak to valley corrugation, which ranged from 10µm to 20µm. They analysed a variety of samples manufactured, primarily from Inconel 718, and then performed a variety of finishing techniques on these samples, to properly characterise the topography of the samples. Their analysis measured the height of the peaks over an 8000 point analysis spectrum. This analysis shows how the SLM process can result in high peaks (200µm), but also how the various finishing techniques have improved the results. Figure 2.3 depicts these results in graphical form, showing that the finishing process, called MMP (Micro Machining Process) provides the optimal results.

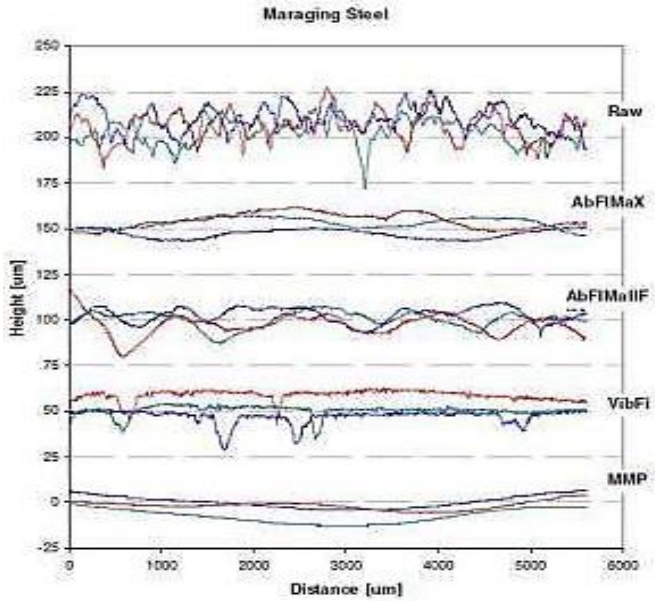

Figure 2.3 Finishing Processes [18]

The research by Jobin et al [18] was unfortunately restricted to a number of open ended samples or rather none complex shapes that had not had another layer built up on top of them.

This does not suggest that this finishing method would be able to produce reduced surface finish on the SLM parts. The effect of surface finish is of particular importance, as previous work on SLM by Weir Valves [31] has already identified that this can have significant impact on the performance characteristics of the parts. Details on surface finish related to fluid flow are provided in section 2.3. Regardless of the research by Jobin [18], there is still a significant requirement for the development of SLM, for use with a variety of applications. A paper by Yadroitsev et al [19] discusses the use of Direct Laser Manufacturing (or SLM) to apply various grades of materials, to fabricate a single part particularly to be used in the nuclear industry. The research discusses the accuracy of applying different material combinations in layers to achieve an overall improvement for radiation resistance. Although not directly appropriate for the current study, it does show some very complex parts being assembled using SLM, with coating systems included.

An article by Osakada and Shiomi [20] discusses the SLM process in detail, and explains the potential for the process. The article, however, does discuss some of the issues that have been observed previously by Weir Valves including the distortion of components during the manufacturing phase. Osakada and Shiomi [20] explain that the deformation is due to non-linear solidification of the part, and this leads to an overhang between various layers, in-turn often causing the layers to fracture and crack due to thermal stresses, when forming rapidly. The paper discusses the distributions of stresses across components and how these may cause cracking. They advise that the residual stress is determined by measuring the change of the strain of the base plate, during milling of the model, in a layer-by-layer manner, and that for successful manufacturing of components, it is imperative that residual stresses are removed.

Osakada and Shiomi [20] noticed that large tensile stresses occur in the top layers of the model, and that the residual stresses decreases rapidly with the distance from the top surface of the model showing the variations in graphical form (see figure 2.4). They advise that this large tensile stress can be reduced by heat treatment, but this is a post-manufacturing process, and will not prevent a failed build if the stresses are too high during manufacture. They advise that the stresses can be reduced by re-scanning during each layer, which will provide more optimised control of the heat being applied to the component, thus reducing the speed of manufacture and prevent rapid heating. They conclude that the material is a very important parameter in the process, and that materials like Titanium (with their high Ultimate Tensile Strength) are preferred, or rather lend themselves to the process.

The research by Osakada and Shiomi [20] however did not produce any quantitative data regarding the variation of residual stress, with relation to build speed, or even with relation to laser power. Further research needs to be carried out in order to determine the optimal build speed and laser power, to produce samples of suitable shape (i.e. parts without deformities caused by high residual stresses).

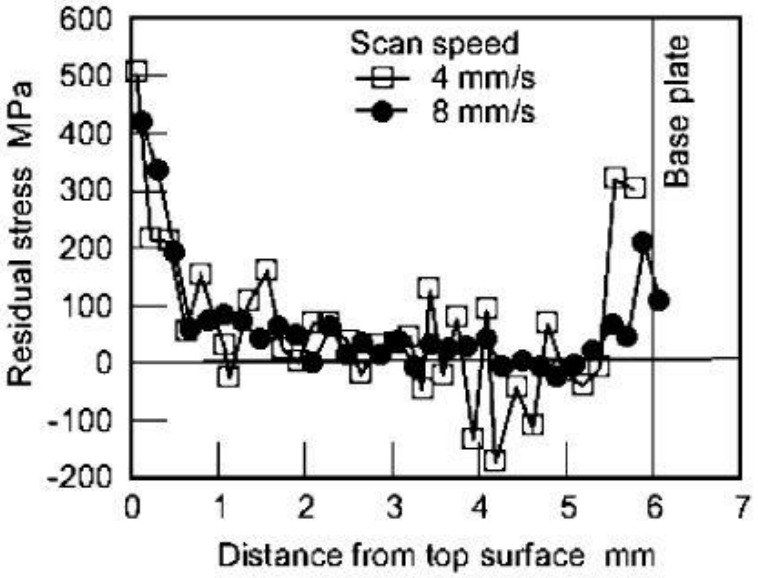

Figure 2.4 Residual Stress against distance from the top surface

Figure 2.5 shows an X-Stream sample produced by SLM that has suffered from such a deformity as a result of high residual stress, whereby the product is not flat on its top surface, nor is it round. As can be seen from the Figure, there is further material slippage on the side of the stack.

Figure 2.5 X-Stream C/w Material Slippage

A paper by Rossi et al [21] discusses improvements to surface finish of parts manufactured by Direct Laser Metal sintering. They have quantified the improvements to average surface finish (values in Ra) (Describer by B46.1 [22] as "the arithmetic average of the absolute values of the profile height deviations from the mean line, recorded within the evaluation length") of an untreated sample, using a number of finishing practices. The research is restricted to reasonably simple components that are of accessible geometry. One of the main considerations with the use of SLM technology is the porosity/density of the components. Weir Valves had noticed issues previously with porous components (see figure 2.5). An article by Thivillon et al [23] discusses the control of certain parameters to control density or

porosity of the samples. The paper specifically reviews the effect of hatch distance, which is defined by Thivillon [23] as the offset between two neighbouring melted tracks.

Thivillon [23] varied the hatch distance by 20µm, over a range from 60 -140µm, and evaluated its effect on density. Thivillon [23] goes on to call a line of re-melted powder as a Vector, and advise that for a laser spot size of 70µm, Power of 50W, speed of 0.13m/s and layer thickness of 50µm, the actual vector distance is 120µm, and thus is larger than the spot size of the laser. As such, when the laser passes over again, there is a partial re-melting of the same vector, and this re-melting cause breaks in the layers, which eventually leads to porosity of the sample. Figure 2.6 shows a graphical summary of the results of hatch distance to porosity, over the range being observed by Thivillon [23]. It is recommended to use a technique called Two-Zones technique, for improving porosity for an optimal hatch distance (around 120µm). This is a process in which every part of the hatch is melted twice, rather than just certain sections, reducing porosity to approximately 1%.

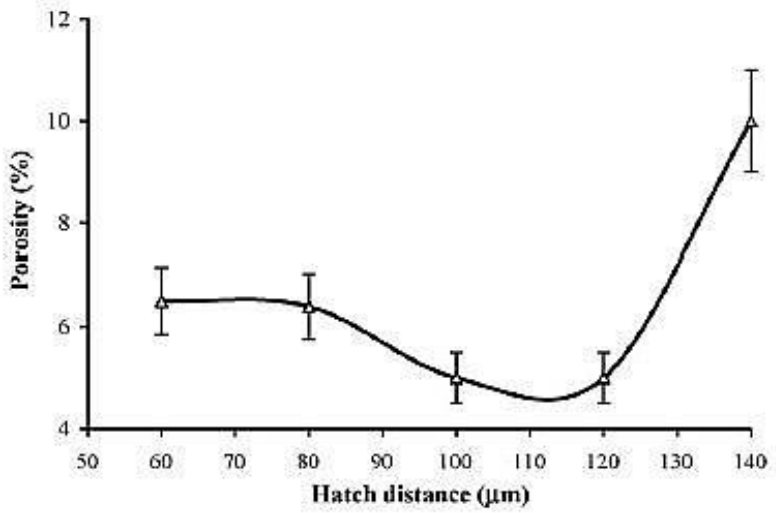

Figure 2.6 Hatch Distance against Porosity

Most of the research completed is on rather simple parts, with some referred to complex geometry. However, these so-called complex geometry parts are all open form (non-closed parts) where each surface is visible. These parts can then be fully reviewed for surface features, and can also undergo a finishing process that most of which would not be suitable for use with X-Stream and its closed nature geometry. It is also noted that there is little comparison of these SLM parts against parts manufactured from another method, particularly with a view to measure their performance characteristics.

As discussed, a great deal of research has been completed on the SLM method of manufacture, however, there is little physical evidence to prove that parts manufactured from this method can provide significant, or any cost and performance, advantage over other methods of manufacture that are currently being employed to make these parts. To investigate this is an aim of the present study.

2.3 Performance Characteristics of X-Stream and other similar disc stacks

X-Streams and other similar disc style trims use specific geometrical features to control pressure and velocity within the valve. This section reviews the research completed on these designs and looks at areas that have not been considered that may further affect, either positively or negatively, the performance of the trim.

2.3.1 Flow around Cylinders

There has been a great deal of published research regarding the effect of geometry on the performance characteristics of control valves. The doctoral thesis of Karen Morton [24] provides specific analysis of X-Stream against other disc stack designs available in the market.

As discussed in chapter 1, most conventional disc stack technologies use a series of sharp right angle turns, with constantly expanding areas as means of controlling the pressure drop. The X-Stream design however turns the fluid around a series of spaced columns, allowing for expansion and contraction of the fluid. Morton presented the use of cylinders as means of changing the direction of the fluid. The research was restricted to the use of incompressible fluids through a densely packed, low aspect ratio cylindrical array. Morton [24] reviewed research of fluid flow around a single cylinder assuming an ideal fluid flow whereby μ=0. Zukauskas [25] and Munson et al [26] both provided a mathematical description of the flow around a single cylinder. Zukauskas [25] showed that the velocity distribution, tangential to the surface of a cylinder, can be expressed as:

$$u_x = U_0 \sin\theta \left[1 + \frac{r}{r_1}^2\right] \tag{2.1}$$

where;
U_0 = Free stream velocity (m/s)
θ = Angle from the stagnation point (^{0})
r = Outer radius of the cylinder (m)
r_1 = Radial distance from axis of cylinder to where the velocity is calculated (m)

This equation can then be re-written to define the fluid velocity at the surface of the cylinder, when r_1=r, as:

$$u_x = 2U_0 \sin\theta \tag{2.2}$$

From this, Zukauskas [25] showed that the maximum velocity will occur when θ = ±π/2, where the surface velocity will reach a value of two times the upstream fluid velocity. Clearly, the geometry of the column has a significant impact on the velocity of the fluid, and as such has a considerable effect on the erosion of the column. Using Bernoulli's equation

(Equation 1.2) [2] a relationship can be formulated to find the static pressure at the surface of the cylinder using the fluid velocity. This can be formulated as follows, describing the static pressure over the cylinder as the dimensionless coefficient of pressure (Cp).

$$C_p = \frac{P_\theta - P_0}{0.5\rho {U_o}^2} \tag{2.3}$$

Where, P_θ = Gauge static pressure at angle θ, and P_0 is the free stream gauge static pressure. An ideal flow analysis would then suggest that

$$u_x = 1 - 4\,sin^2\,\theta \tag{2.4}$$

This theoretical method, devised by Zukauskas [25], when considering the viscous boundary layer that forms on the surface of the cylinder (for non-ideal cases), is a good representation of how the performance, relating to both the static pressure and the velocity, can vary with regards to changes in the geometry of the cylindrical column. Many heat exchanger designs use an array of cylinders. Most of these designs use an array, where the cylinders are directly in-line; however, some use an array of staggered cylinders, whereby the spacing of these cylinders, from one another, also has a significant effect on the performance of the heat exchanger. It is these types of staggered array heat exchangers that were analysed during the initial development of the X-Stream by Morton, who referenced the works of Zukauskas [25] and Zukauskas and Ulinskas [27]. Due to the wide use of heat exchangers, there is a significant amount of research available in these areas, relating column or cylinder spacing to performance. There has been significant research work carried out regarding the flow around cylinders, both in-line and staggered, however, there does not seem to be specific research related to the flow around these cylinders for a specific K factor, or how capacity can be increased. Further work also needs to be carried out in order to analyse the flow around the columns when the column is placed on a non-flat surface, or when the top wall is not flat.

2.3.2 Improvement of design using Numerical analysis

Young Joon et al [29] used numerical analysis to improve the design of a control valve on a LNG application by analysing the static pressure and velocity. They compared the design of a single cage trim with multiple wedges, allowing the fluid to pass through, against a design using single holes of similar sizes. Their analysis showed that a simple change of the geometry, associated with the hole, had a significant effect on the performance characteristics of the trim, showing how the change in trim increased the minimum static pressure on the outlet section of the valve body, and reducing the size of the low pressure region. Figure 2.7 depicts the pressure recovery measured across the valve length. The curves show the pressure drop variation from the final modified design, and clearly show the increase in minimum static pressure/vena contract.

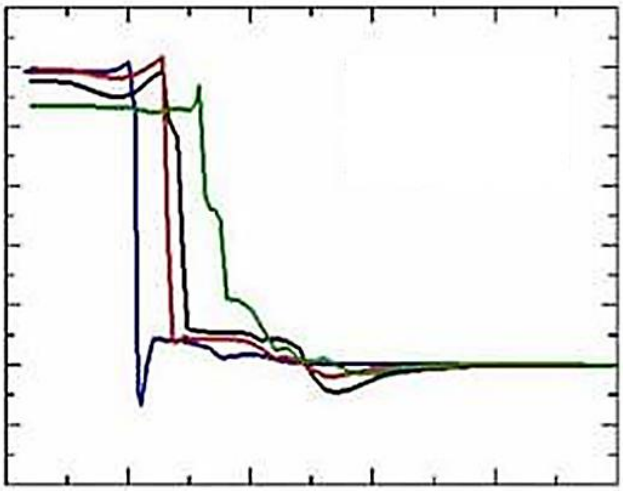

Figure 2.7 Pressure recovery across valve length

2.3.3 Comparison of Disc Styles

Morton [24] analysed the performance characteristics of competing right angled turn trim designs. This analysis specifically reviewed the comparisons of fluid flow through three geometrically different designs of disc stacks. i.e.:

1. Labyrinth Style – trim Stack 1 (Figures 2.8, 91, 2.10, 2.11)
2. Another Style of Right angle turn disc stack (Figures 2.12, 2.13, 2.14)
3. A cylindrical array single plane disc

Design 1 - Labyrinth Style – trim Stack

Morton [24] analysed that this design of trim produces a curved or snake-like flow pattern around the corners, and the velocity increases at the points where the fluid flow gets separated from the sharp corners. At this point (shown in figure 2.11) there is a large re-circulating flow region, showing a high velocity gradient across this area.

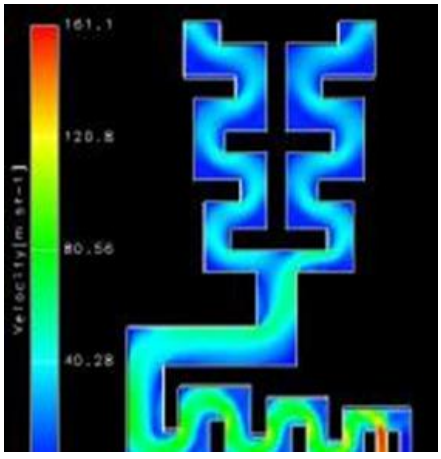

Figure 2.8 Fluid velocity

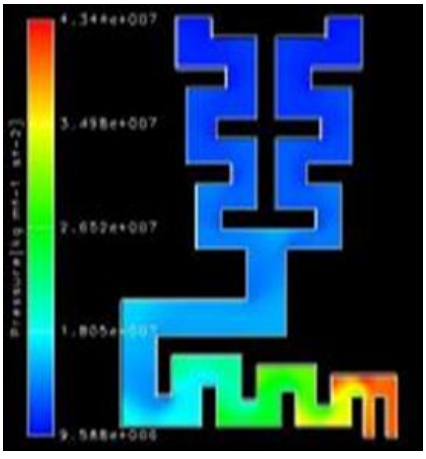

Figure 2.9 Static pressure

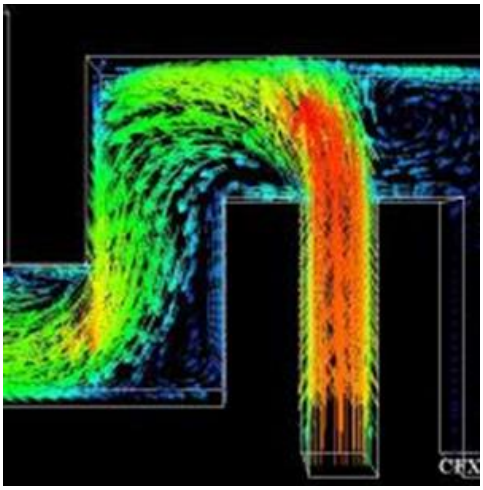

Figure 2.10 Area of re-circulating flow and high inlet velocity

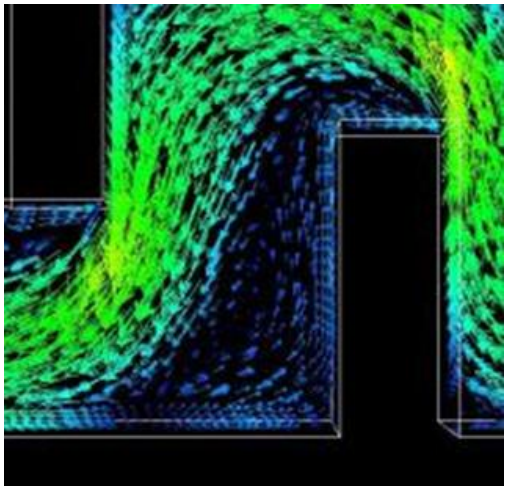

Figure 2.11 Re-circulation at Inlet

Morton [24] also noted that the velocities recorded using a three dimensional CFD analysis differed significantly from the estimated velocity predicted by [7]. Morton concluded that the high velocity gradients, caused by sharply turning of the fluid, limit the accuracy of the standard one dimensional approach proposed by Miller [7]. The contours of static pressure, shown in Figure 2.9, provide a good example of the effect of geometry on the static pressure, showing areas of low static pressure in the corners, away from the main flow stream. Morton argued that this area resulted in a high pressure recovery across this stage of pressure drop, and could be a potential area for the onset of cavitation.

Design 2 - Another Style of Right angle turn disc stack

Morton [24] analysed that with this design the presence of the walls split the fluid into 2 jet like formations whose growth was then prevented by the presence of the wall normal to the jet. The wall forced the fluid to turn sharply as had been shown in the first trim analysis. Again Morton analysed that this had led to area of re-circulating flow within the disc (shown in closer detail in figure 2.14) and that these formations and the similar area of peak velocity within the flow stream meant that this design was similar to the one above. It should be noted that Morton used the same inlet boundary conditions for each simulation and as can be seen from the analysis, the velocity magnitude plot on this second disc shows higher values for velocity than with the first design.

The areas of re-circulating flow, much like with the first design analysed were also identified as areas of high potential for cavitation. It was analysed that this design could suffer the effects of cavitation more as these re-circulating flow areas were more prevalent than with the first design and covered a larger area behind the flow separating walls.

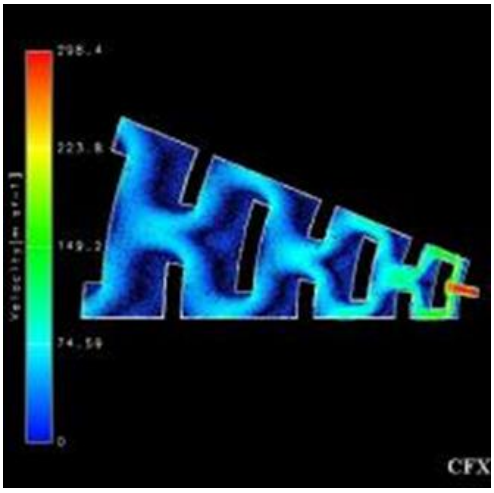

Figure 2.12 Fluid velocity magnitude

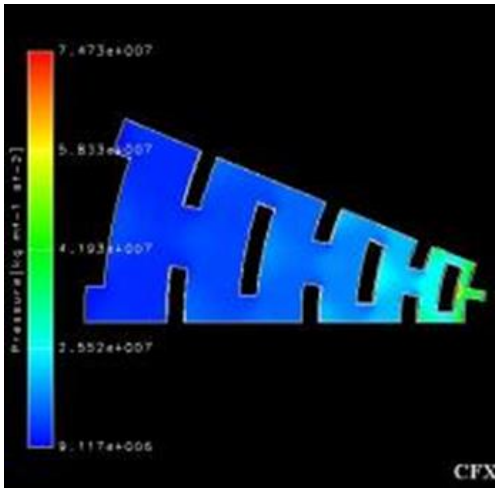

Figure 2.13 Static pressure

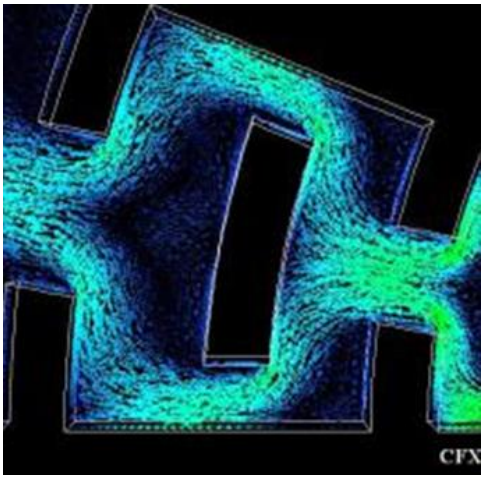

Figure 2.14 Re-circulating flow

Design 3 - A cylindrical array single plane disc

The final design is a columnar arrangement, similar to the current X-Stream design. As with the other designs Morton [24] used the same pressure conditions on this design analysis. Obviously this design does not rely on forcing the fluid through sharp right angles bends, the cylinder arrangement works to allow the fluid to take a more meandering path, which is as Morton identified, similar to the paths taken in the previous designs.

Morton [24] analyses that the areas of re-recirculating flow are reduced by the proximity of nearby (neighbouring) cylinders and that "this interference between adjacent cylinders appeared to cause the flow to reattach to the surface of each cylinder soon after the initial separation". She also states that "It was also expected that this would reduce the velocity levels at the point of separation". The large reduction in size of the re-circulating flow regions, minimised behind the columns, are discussed as being a significant reduction in the potential for cavitation to occur in these regions and that it would be restricted to a smaller

area. Morton completes her analysis of this design by noting that the reduction in recirculating flow area will support her requirement for the trim to prevent solid debris blockage, which she had not been able to achieve with either of the other designs shown.

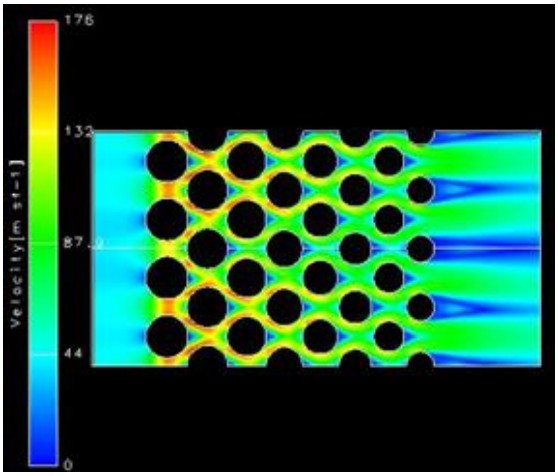

Figure 2.15 Re-circulating flow

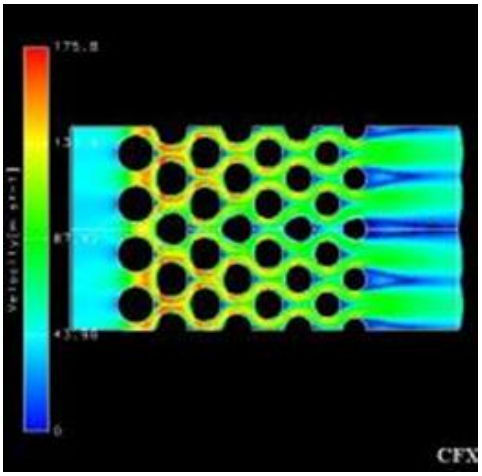

Figure 2.16 Re-circulating flow

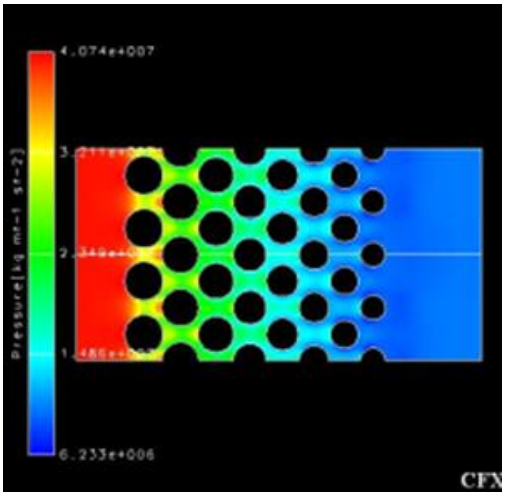

Figure 2.17 Static Pressure

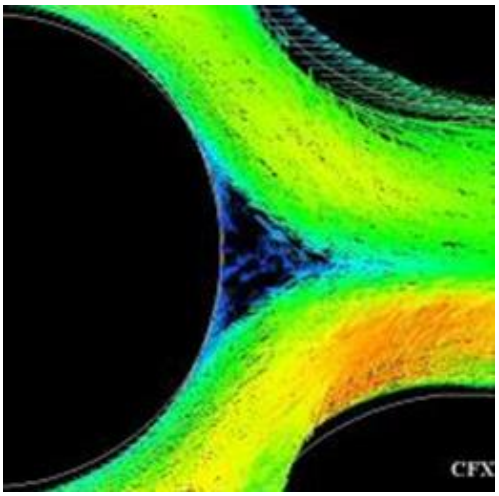

Figure 2.18 Re-circulating flow

Morton's [24] analysis was completed using the same boundary conditions for each of her trim designs, using specified inlet and outlet conditions only for the input parameters. However she rightly admits that the flow rates through each model vary significantly (Design 1=0.436m^3/hr, design 2=0.79m^3/hr and design 3 was = 2.97m^3/hr). As such a true comparison of the velocity control of each design cannot be completed. Further as with the work completed by Green et al, this analysis is only a study of a single flow path on a single disc and shows no interaction between multiple flow paths on the same disc.

It is also noted that Morton [24] made no considerations during her designs for manufacturing constraints, some of the gaps between columns on design 3, are very small and as can be seen from the analysis there is an increase in the velocity magnitude between the columns. As no

consideration had been made for manufacturing method, neither had there been any consideration for the effect of surface finish on the overall analysis.

2.3.4 Analysis of flow around cylindrical arrays in a control valve

Green et al [28] performed numerical analysis, using a commercial CFD code, on the performance of a geometrically complex control valve to determine the trim's ability to reduce erosion and cavitation. The work focused on the performance across one path of a linear (in the vertical direction) and symmetrical stack. The analysis took data from 7 points across the flow path and produced a graphical representation of normalised velocities across the flow path (shown in figure 2.19); the right hand view shows the location of the data points.

Green et al [28] observed that the radial velocities varied across the flow path, and the converging-diverging flow, in the neighbouring rows of columns, resulted in competing effects. Their analysis also depicted that the velocity was only uniform across the first row of cylinders. In subsequent rows, peak velocities were offset so that they were much closer to the column itself.

The peak velocities did reduce as the row numbers increased, as a result of an increase in spacing between the rows of columns, following the expansion design of the trim; allowing for an expansion of area to reduce the velocity magnitude. The research also showed that the fluid does not flow evenly around the cylinders as the second row is the only row which shows any significant asymmetry, with the flow velocities at one side of the channel being higher than the other. However, the results do show that this becomes much more evenly distributed in later rows (row 3 onwards). The plot of static pressure (figure 2.20) clearly shows that the static pressure in the first row is significantly different as compared to other rows, which appear more symmetric. The drop in the static pressure corresponds to the velocity peak, as shown in Figure 2.19.

The study concludes that the areas of separation, or re-circulating flow, are on the downstream surface of the cylinders, and are not at areas of peak velocity, improving the control of velocity and reducing the potential for cavitation, when compared with right angle turn trim designs. Control valves industry amended the design of the X-Stream disc, following this analysis, as the analysis showed that the peak velocities at the inlet of the trim (row 1) are high, and are caused by the half-column on the outer diameter of the disc. The revised design (similar to the latest design of X-Stream) now uses a full column on the entrance to the disc, recessed in from the outer edge. Analyses have shown that the reduction in the peak velocity at the entrance row reduces the erosive effects of the fluid.

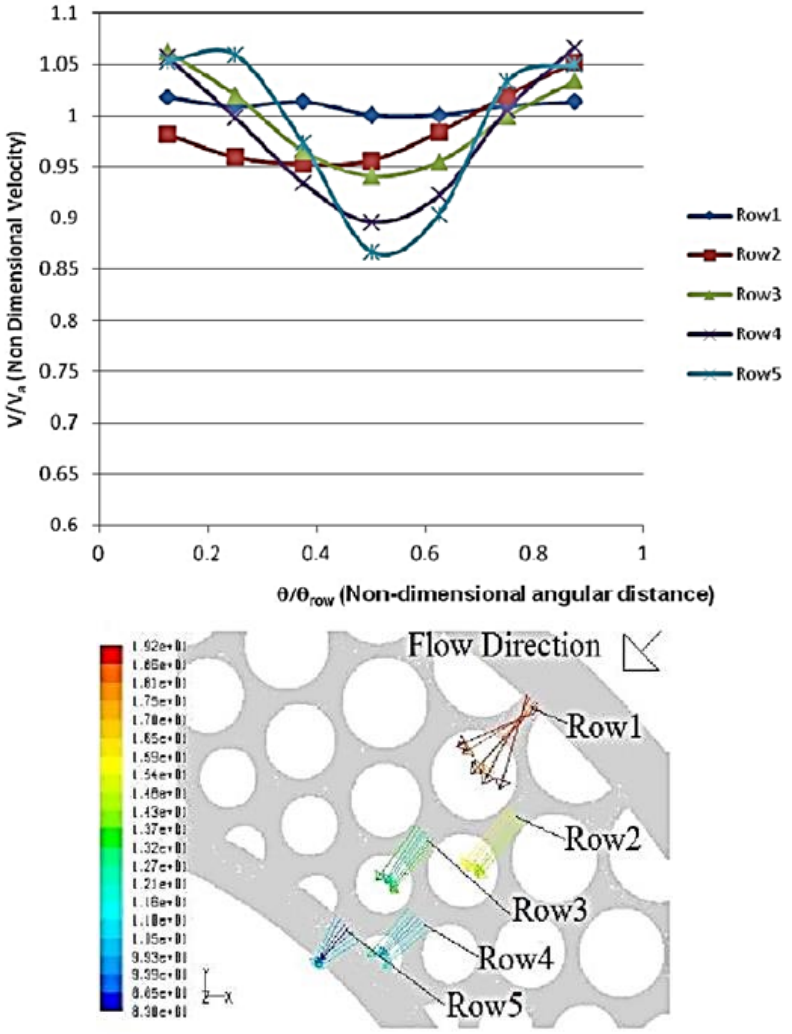

Figure 2.19 Graphical Representation of (a) Normalised Velocities and (b) Location of Data points

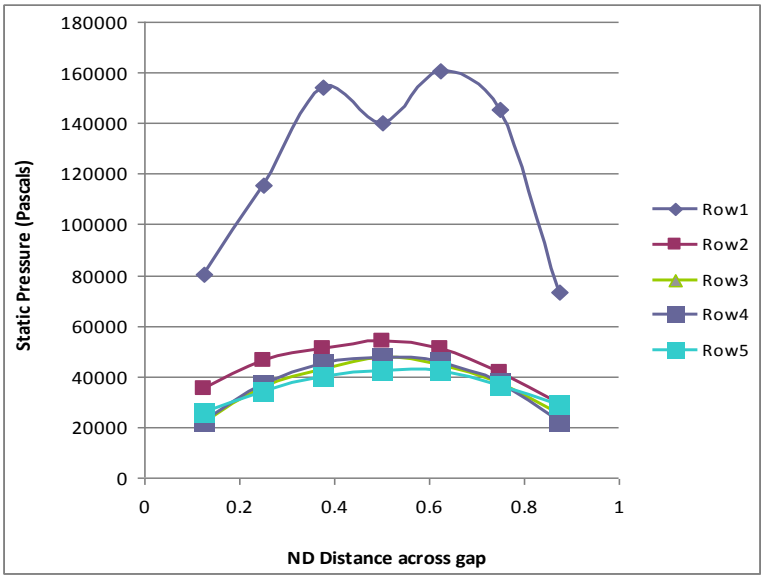

Figure 2.20 Static pressure variation across each row of columns

In the analysis by Green et al [28], there has been no consideration for the effects of the entire stack, and how the pressure, velocity and capacity vary when considering the full trim. The study assumes that the pressure drop, and the velocity, is linearly distributed between each disc and each flow path, which may not be the case. Furthermore, the analysis did not consider the effect of the valve body on the fluid flow.

2.4 Effect of surface roughness on fluid flow

The effect of surface finish to the flow passing through the X-Stream is important considering the previous attempts to use SLM with X-Stream have resulted in trims with poor surface finish. There have been some articles written that discuss the effect of surface finish on fluid flow. One such article by Taylor et al [30] reviewed previous work on the subject by Moody, Colebrook and Nikuradse, who had provided a method to include a first order estimate of roughness effects. However, this work was limited to small effects on fluid flow whereby reductions in fluid flow were reduced by minimal amounts (less than 5%).

Darcy had identified the importance of surface roughness on fluid flow, and had conducted a number of experiments where he varied the roughness of pipes in order to relate head loss, or pressure drop, to friction along any given length of pipe. Taylor et al [30] reviewed the work of each of the above, comparing the various expressions, but also defined the nature of a surface. Surface texture is the composite profile of certain deviations that are typical of a real surface. These include:

- Roughness: the finer irregularities of surface texture that is inherent in the materials or production process, i.e. cutting tool, spark, grit size, etc.

- Waviness: the more widely spaced component of surface texture and upon which roughness is superimposed. It may result from vibrations, chatter, etc.

- Error of form: the general shape of the surface neglecting roughness and waviness. It generally consists of the departure from the intended shape. It may be caused by lack of machine rigidity, etc.

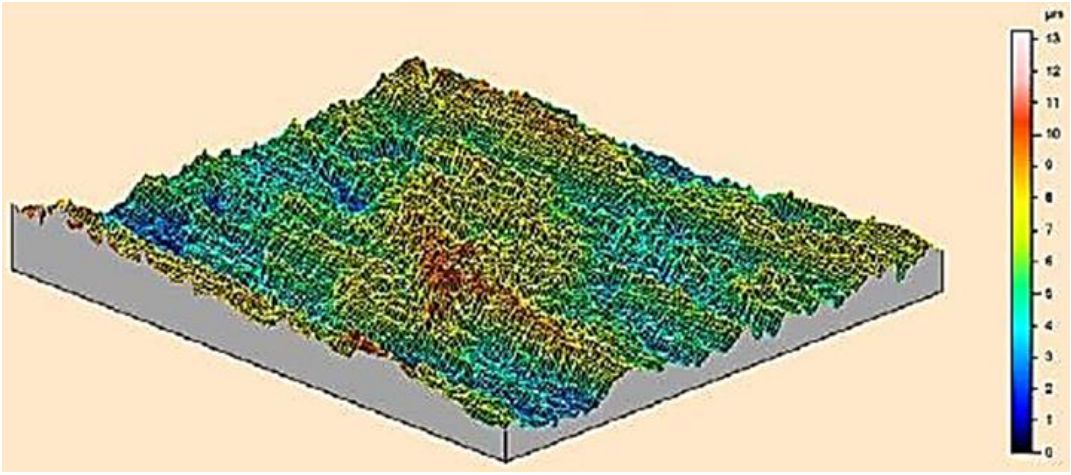

Figure 2.21 Surface Metrology Height Map [30]

Taylor discusses how these formulations may not be fully useable in current systems, where scales of components are reduced (parts are being made smaller and smaller). These micro surfaces are now of greater significance and the Moody diagrams, for example, cannot accommodate relative roughness in excess of 5%. The conclusions of this paper are that the work by Moody can be adapted for use up to 14% relative roughness, however, that future work, looking at the three dimensional surface, is more important as opposed to simple surface finish. Furthermore, mini and micro fluid systems, requiring a higher accuracy for the prediction of flow performance (or the optimisation of performance), will require significant further research. Figure 2.21 shows the height map included in the paper, and how height had varied over their sample.

It had been shown in many recent studies that the effects of surface finish on flow properties is affected more by large scale geometric features as compared to small scale features. Asim [31] completed a series of tests on a number of parts manufactured with a variety of columnar arrangements, but also on parts with identical geometry manufactured using differing techniques, more specifically EDM and SLM. The effects of these large peaks (as shown in Figure 2.22) are dominant on the flow characteristics within the control valve used within their study. These results were used within the CFD environment for the prediction of the flow variables with improved accuracy.

The study by Asim [31] reviewed the roughness of identical designed parts, however, one was manufactured using the standard EDM method, and the other via an SLM method of manufacture. The results show that the roughness amplitude in SLM trims can be as high as 1000microns. Furthermore, it can be seen in Figure 2.23 that the surface of an SLM trim is not only characterised by large peaks, but the core region of the surface is considerably rough as compared to EDM trims. This argument is further strengthened by the fact that the Sdr parameter of SLM surfaces is significantly higher than EDM trims. The Sdr parameter is the interfacial area ratio, which shows the percentage increase of the area of the actual surface

compared to an engineering drawing surface area (texture surface area minus cross sectional area divided by cross sectional area).

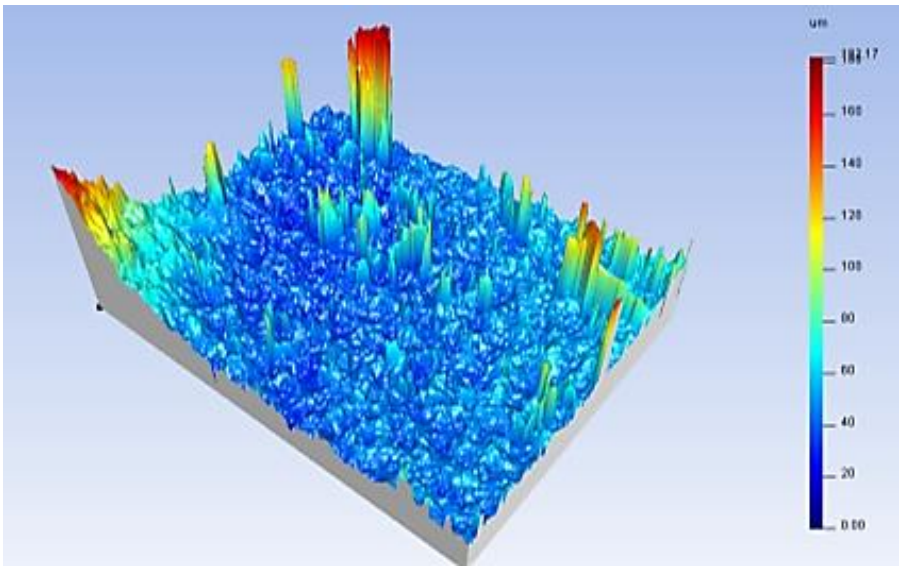

Figure 2.22 Surface Peak Analysis EDM part

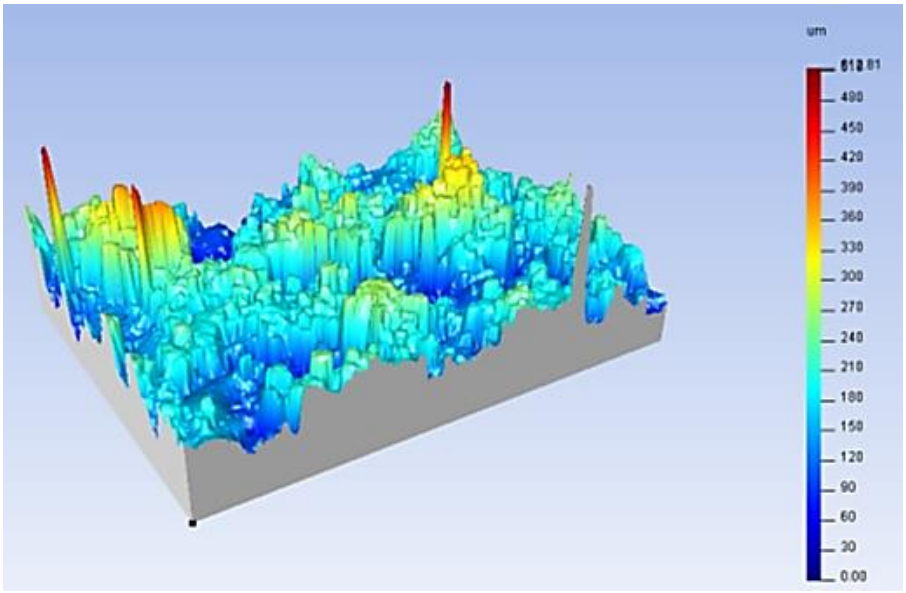

Figure 2.23 Surface Peak Analysis for SLM Part

Within the CFD environment, Asim [31] specified a roughness height of 8000microns. This value was much greater than 1000microns suggested by surface measurements. They did this deliberately to validate the results from a CFD analysis against experimental flow testing results, for the same boundary and flow conditions, which was one of the main aims of their study. However, it can be seen in Figure 2.20 that further geometrical imperfections are an inherent feature of the SLM trims, like asymmetry, chips formation, area reduction for flow etc. They conclude that these large scale features significantly affect the flow characteristics, and hence need to be incorporated into the CFD environment. Because no quantitative

analysis has been carried out in the present study to evaluate these imperfections geometrically, an estimated value has been specified based on the experimental results.

Table 2.1 shows the experimental result from the study by Asim [31]. As can be seen there is a significant difference between the results for total Cv between the two geometrically identical designs. Asim seem conclude that the manufacturing methods significant changes in surface parameters are related to this reduction Figure 2.24 shows the test piece of XLO8-040 SLM. It is quite clear that the difference in the surface finish between the model and the completed part. Figure 2.25 shows the corresponding part manufactured using EDM, note the difference in overall surface finish from a purely visual perspective. The work completed by Asim used an average method of surface roughness applied to the entire valve, rather than the trim only, and the performance calculations include the performance of other parts in the control valve, which in reality were cast surfaces of poor surface quality. Ideally the comparison for performance needs to consider the trims as individual components only for a better understanding of the variations in performance characteristics.

Table 2.1 Experimental Results for Cv_{Total} for EDM and SLM Trims [31]

Trim Style	Flow	Valve Opening (%)	T_1 (°C)	P_1 (Bar)	P_1 (psi)	Q (ltr/min)	ΔP (V)	Q (US Gal/min)	ΔP (psi)	Cv_{Total}
XLO8-40 (EDM Manufacture)	Max. Flow	100	16	3.6	66.7	862.6	5.71	227.9	49.72	32.3
		80		3.7	68.2	764.4	5.91	201.9	51.41	28.2
		60		3.9	71.1	610.2	6.19	161.2	53.85	22.0
		40		3.9	71.1	426.8	6.31	112.7	54.88	15.2
		20		4	72.5	185.2	6.22	48.9	54.16	6.6
		10		4	72.5	118.0	6.25	31.2	54.39	4.2
	50% of Max. Flow	100		N/A	N/A	446.2	1.52	117.9	13.19	32.5
		80		N/A	N/A	399.2	1.57	105.5	13.68	28.5
		60		N/A	N/A	313.6	1.63	82.8	14.22	22.0
		40		N/A	N/A	218.2	1.66	57.6	14.46	15.2
		20		N/A	N/A	122.0	1.68	32.2	14.60	8.4
		10		N/A	N/A	45.2	1.69	11.9	14.71	3.1
	25% of Max. Flow	100		N/A	N/A	250.2	0.45	66.1	3.92	33.4
		80		N/A	N/A	225.0	0.47	59.4	4.07	29.5
		60		N/A	N/A	174.2	0.49	46.0	4.23	22.4
		40		N/A	N/A	122.6	0.49	32.4	4.26	15.7
		20		N/A	N/A	53.2	0.50	14.1	4.35	6.7
		10		N/A	N/A	27.2	0.51	7.2	4.44	3.4
XLO8-40 (SLM Manufacture)	Max. Flow	100	16	3.8	69.6	674.6	6.07	178.2	52.81	24.5
		80		3.85	70.3	603.2	6.19	159.3	53.83	21.7
		60		3.9	71.1	472.6	6.28	124.8	54.67	16.9
		40		3.95	71.8	302.2	6.33	79.8	55.10	10.8
		20		4	72.5	160.0	6.23	42.3	54.23	5.7
		10		4	72.5	90.0	6.24	23.8	54.34	3.2
	50% of Max. Flow	100		N/A	N/A	346.6	1.62	91.6	14.08	24.4
		80		N/A	N/A	303.6	1.64	80.2	14.25	21.2
		60		N/A	N/A	239.8	1.66	63.3	14.41	16.7
		40		N/A	N/A	155.0	1.67	40.9	14.57	10.7
		20		N/A	N/A	87.2	1.67	23.0	14.57	6.0
		10		N/A	N/A	48.0	1.68	12.7	14.64	3.3
	25% of Max. Flow	100		N/A	N/A	201.2	0.49	53.2	4.25	25.8
		80		N/A	N/A	173.0	0.50	45.7	4.32	22.0
		60		N/A	N/A	137.0	0.50	36.2	4.35	17.4
		40		N/A	N/A	90.0	0.51	23.8	4.40	11.3
		20		N/A	N/A	50.4	0.51	13.3	4.44	6.3
		10		N/A	N/A	26.0	0.51	6.9	4.47	3.2

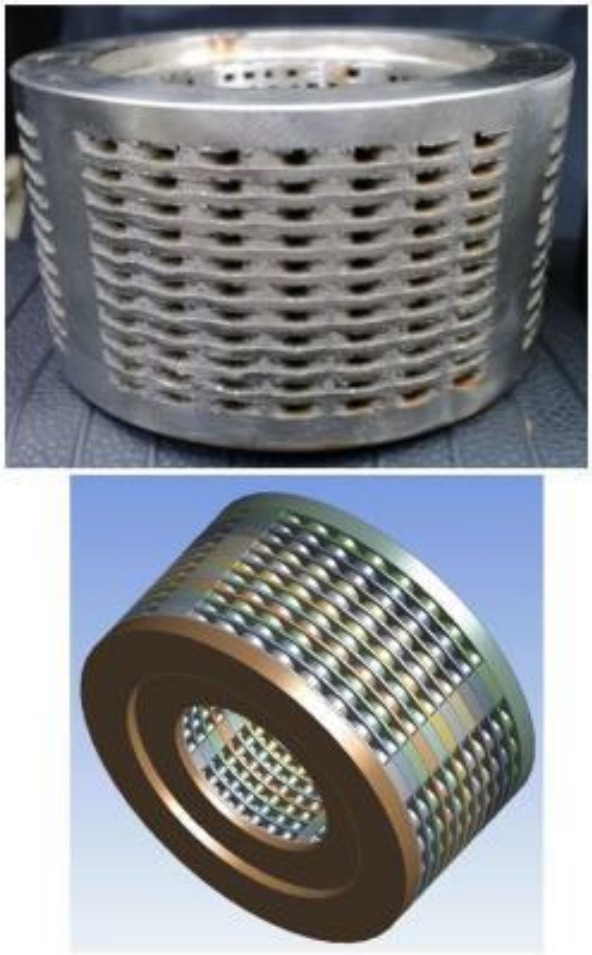

Figure 2.24 SLM Manufactured XLO8-040 (Top) and original CAD model (Bottom)

Figure 2.25 EDM Manufactured XLO8-040

2.5 Specific Research Objectives

From the literature review completed it is now known which areas require further research before a definitive decision can be made on the use of ALM/SLM for manufacturing X-Stream trims.

Five main research goals have been defined for this project for further study, they are;

1. To perform a critical analysis on improving the manufacturability of an X-Stream trim by altering the manufacturing process or the design of the trim. The research reviews which of these methods is preferred.

2. To review the performance characteristics between a trim manufactured using process improvements against a trim with design modifications; to aid the manufacturing process. This involves experimental testing for the values of Cv_{Total}, Cv_{Trim} and K_{Trim} for each design.

3. To perform a numerical analysis on the effects of surface roughness induced by the different manufacturing methods on new variations of the X-Stream design, reviewing individual features of geometry for these designs and comparing them against the standard trim design of XLO8-040.

4. This study will also review the impact of surface uniformity on Cv via means of numerical analysis. The study will also look at specific geometrical features that may be affected by a non-linear application of surface roughness.

5. Review of other performance characteristics of the trims by analysis of contours of static pressure and velocity to identify potential areas for cavitation and areas with increased potential for premature erosion

CHAPTER # 3
DETAILS OF NUMERICAL ANALYSIS

This chapter sheds light on the experimental and the numerical formulations that have been followed/specified in the present study. The experimental studies have been carried out in accordance to the industrial standard/s, the details of which have been clearly discussed. Basic concept of CFD has been provided, with its implementation to the control valves and their associated trims. Furthermore, scope of the work has been defined.

3.1 Experimental Formulation

A 100mm control valve has been used in the present study for capacity testing of two of the manufactured X-Stream trims, using the flow loop set-up and water as the working fluid, in general accordance with BS EN 60534-2-3, and as per test procedure VT-QC-SP503. Only two X-Stream trims have been flow tested in this study, out of a total of 5, due to the various limitations such as the availability of the test setup etc. The main objective of the test programme is to determine the Cv of the trims installed within it. The tests have been conducted at various valve opening positions i.e. fully open, 75%, 50% and 25%. The tests have been performed at three differential pressure conditions corresponding to 75% of the maximum available flow, 50% of the maximum available flow and 10% of the maximum available flow. These operating conditions are in accordance with BS EN 60534-2-3's recommendations. Furthermore, k factor values at the aforementioned valve openings and flow conditions have also been computed.

3.1.1 Test Setup

In accordance with BS EN 60534-2-3, the test setup consists of two straight lengths of pipe, connected at either ends of the valve, as shown in Figure 3.1. The upstream pipe is 20 times longer than the nominal diameter of the pipe while the downstream pipe is 7 times longer than the nominal diameter of the pipe.

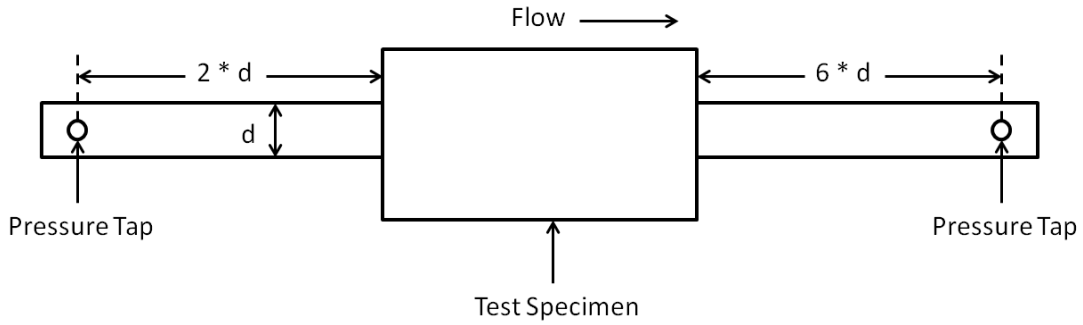

Figure 3.1 Dimensions of Upstream and Downstream sections

Clean mains water is supplied to the 37kW centrifugal pump from the water storage tank, once the upstream butterfly valve is opened. The pump is controlled via an electrical invertor that can adjust the motor speed within 0.1% of the total 50Hz output frequency. A turbine flow meter is positioned downstream of the pump, and upstream of the test valve, to monitor flow rate. The flow meter readings are continuously logged via an Omega USB-4718 data acquisition module onto the computer network. Ten manual readings are also taken at 30 second intervals for each pressure differential. Further details including Figures of the flow loop setup are included in Appendix 2 and a simple schematic of the loop is shown in Figure 3.2.

Pressure tapings in the flow loop pipework are used to record an average pressure in the pipe, and are installed as follows:

- Inlet tapings at a minimum of two pipe diameters (2d) upstream of the test valve
- Outlet tapings at a minimum of six pipe diameters (6d) downstream of the test valve

There are no bends within eighteen diameters (18d) downstream of the test valve. All entry points into the pipework are a minimum of 3mm in diameter and free from burrs. A pressure transducer is connected to the upstream tapings to monitor gauge inlet pressure, and a differential pressure transducer, installed between the upstream and downstream tapping, monitors the differential pressure. Both these pressure transducers are connected to the flow loop software via an Omega USB-4718 data acquisition module. Pressures are also recorded manually in order for third party inspection verification against logged data. A thermocouple is located within the IBC to measure the temperature of the test fluid. It is positioned to have a negligible effect on flow and pressure.

Flow rates and differential pressures through and across the valve are measured at three widely spaced pressure differentials. No differential pressure of less than 0.1barg was used. Flow conditions were all within the turbulent, non-vaporising region. The invertor was taken up in 5% increments to increase flow rates and calculations made to ensure the onset of cavitation was not reached, once the maximum flow rate was established below this point the initial test was performed. The other two flow rates were then set at approximately 50% and 25% respectively of this value.

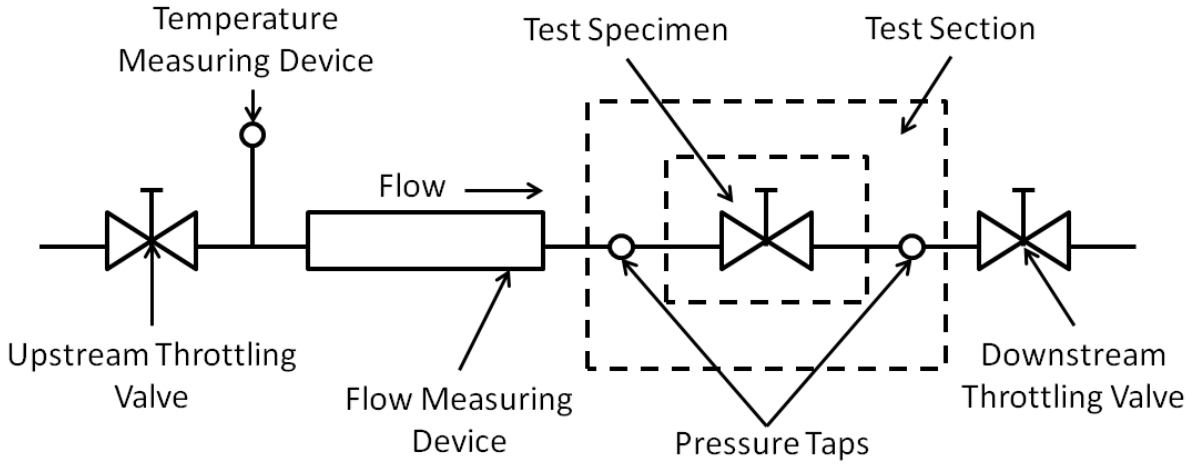

Figure 3.2 Schematic of the Test Setup

Figure 3.3 depicts a typical flow loop setup installed for the capacity testing of X-Stream valves. The actuator, sitting on the top of the valve, is connected to an air supply at 4 bar (g), which controls the valve opening position. It can be seen in the Figure that four equally spaced pressure tapings have been installed circumferentially at both upstream and

downstream locations. These pressure tapings measure the average pressure at the specified location, and hence the three dimensional effects can be recorded more accurately.

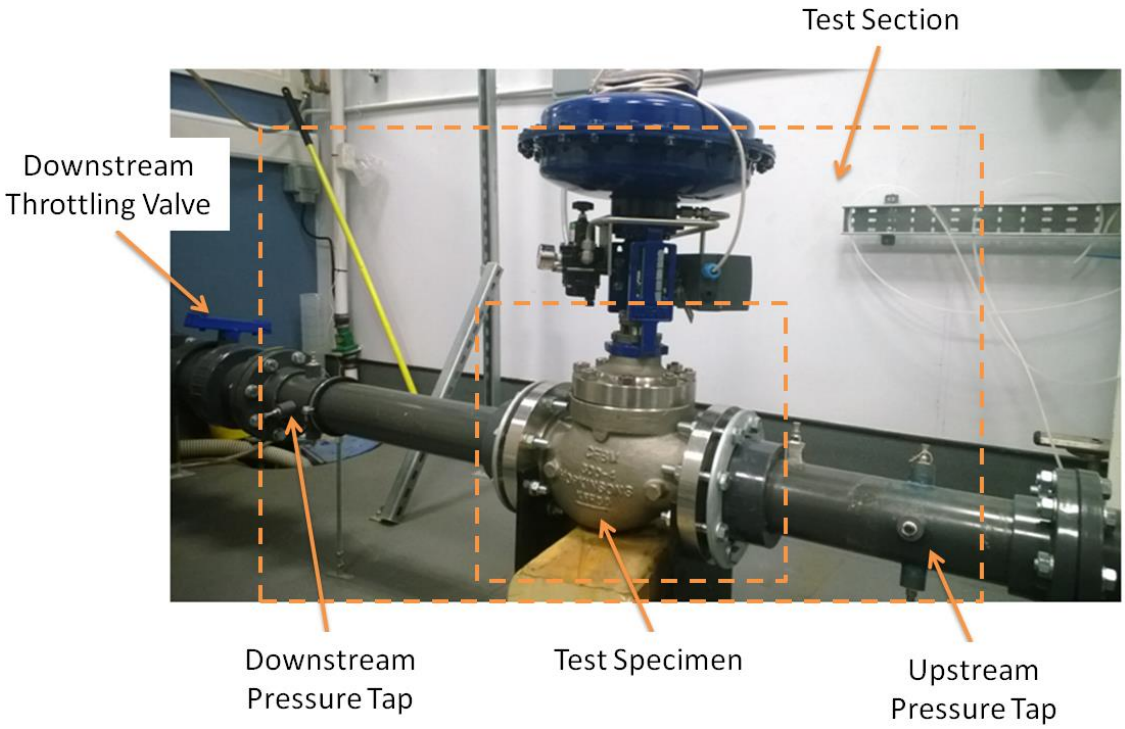

Figure 3.3 Flow Loop Setup

The data sheet of the valve used is shown in figure 3.4. The data sheet contains important information about the value that has been used, such as its type, range, size etc. It also indicates the type of trim/s that can be used with this type of valve, and information on the material of the seat, plug, disc etc.

3.1.2 Test Procedure

Flow tests have been conducted at three different flow conditions which represent operating conditions for these valves. These flow conditions correspond to:

1. 75% Pump speed
2. 38% Pump speed
3. 10% Pump speed

Tests have been performed in turbulent, non-vaporising conditions. At each flow condition, tests have been performed at the following valve opening positions to cover a wide range of operation:

1. 100%
2. 75%

3. 50%
4. 25%

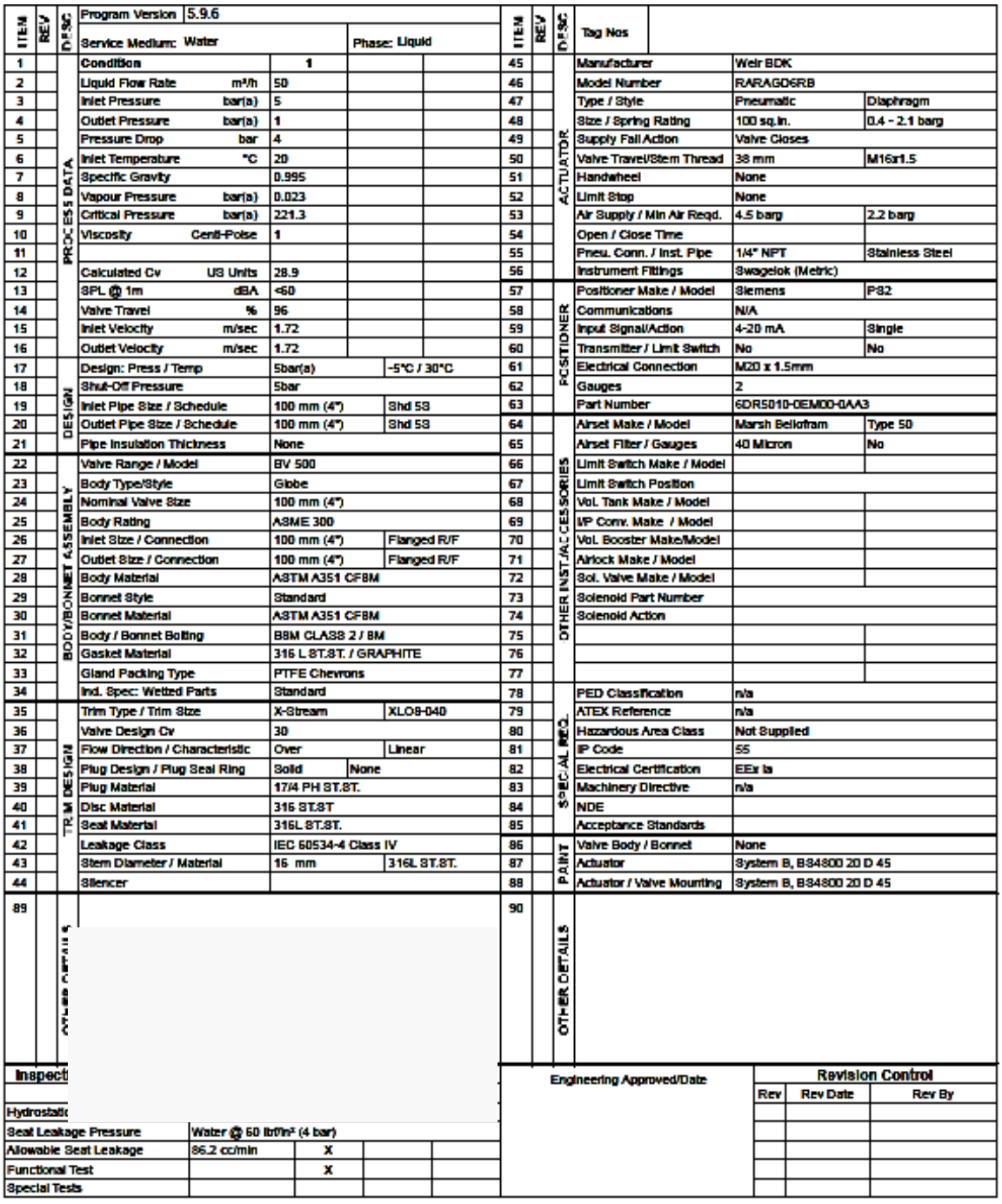

ITEM	REV	DESC						ITEM	REV	DESC			
			Program Version	5.9.6							Tag Nos		
			Service Medium: Water		Phase: Liquid								
1		PROCESS DATA	Condition		1			45		ACTUATOR	Manufacturer	Weir BDK	
2			Liquid Flow Rate	m³/h	50			46			Model Number	RARAGD6RB	
3			Inlet Pressure	bar(a)	5			47			Type / Style	Pneumatic	Diaphragm
4			Outlet Pressure	bar(a)	1			48			Size / Spring Rating	100 sq.in.	0.4 - 2.1 barg
5			Pressure Drop	bar	4			49			Supply Fail Action	Valve Closes	
6			Inlet Temperature	°C	20			50			Valve Travel/Stem Thread	38 mm	M16x1.5
7			Specific Gravity		0.995			51			Handwheel	None	
8			Vapour Pressure	bar(a)	0.023			52			Limit Stop	None	
9			Critical Pressure	bar(a)	221.3			53			Air Supply / Min Air Reqd.	4.5 barg	2.2 barg
10			Viscosity	Centi-Poise	1			54			Open / Close Time		
11								55			Pneu. Conn. / Inst. Pipe	1/4" NPT	Stainless Steel
12			Calculated Cv	US Units	28.9			56			Instrument Fittings	Swagelok (Metric)	
13			SPL @ 1m	dBA	<60			57		POSITIONER	Positioner Make / Model	Siemens	PS2
14			Valve Travel	%	96			58			Communications	N/A	
15			Inlet Velocity	m/sec	1.72			59			Input Signal/Action	4-20 mA	Single
16			Outlet Velocity	m/sec	1.72			60			Transmitter / Limit Switch	No	No
17		DESIGN	Design: Press / Temp		5bar(a)		-5°C / 30°C	61			Electrical Connection	M20 x 1.5mm	
18			Shut-Off Pressure		5bar			62			Gauges	2	
19			Inlet Pipe Size / Schedule		100 mm (4")		Shd 5S	63			Part Number	6DR5010-0EM00-0AA3	
20			Outlet Pipe Size / Schedule		100 mm (4")		Shd 5S	64		OTHER INST./ACCESSORIES	Airset Make / Model	Marsh Bellofram	Type 50
21			Pipe Insulation Thickness		None			65			Airset Filter / Gauges	40 Micron	No
22		BODY/BONNET ASSEMBLY	Valve Range / Model		BV 500			66			Limit Switch Make / Model		
23			Body Type/Style		Globe			67			Limit Switch Position		
24			Nominal Valve Size		100 mm (4")			68			Vol. Tank Make / Model		
25			Body Rating		ASME 300			69			I/P Conv. Make / Model		
26			Inlet Size / Connection		100 mm (4")		Flanged R/F	70			Vol. Booster Make/Model		
27			Outlet Size / Connection		100 mm (4")		Flanged R/F	71			Airlock Make / Model		
28			Body Material		ASTM A351 CF8M			72			Sol. Valve Make / Model		
29			Bonnet Style		Standard			73			Solenoid Part Number		
30			Bonnet Material		ASTM A351 CF8M			74			Solenoid Action		
31			Body / Bonnet Bolting		B8M CLASS 2 / 8M			75					
32			Gasket Material		316 L ST.ST. / GRAPHITE			76					
33			Gland Packing Type		PTFE Chevrons			77					
34			Ind. Spec: Wetted Parts		Standard			78		SPECIAL REQ.	PED Classification	n/a	
35		TRIM DESIGN	Trim Type / Trim Size		X-Stream		XLO8-040	79			ATEX Reference	n/a	
36			Valve Design Cv		30			80			Hazardous Area Class	Not Supplied	
37			Flow Direction / Characteristic		Over		Linear	81			IP Code	55	
38			Plug Design / Plug Seal Ring		Solid	None		82			Electrical Certification	EEx ia	
39			Plug Material		17/4 PH ST.ST.			83			Machinery Directive	n/a	
40			Disc Material		316 ST.ST			84			NDE		
41			Seat Material		316L ST.ST.			85			Acceptance Standards		
42			Leakage Class		IEC 60534-4 Class IV			86		PAINT	Valve Body / Bonnet	None	
43			Stem Diameter / Material		16 mm		316L ST.ST.	87			Actuator	System B, BS4800 20 D 45	
44			Silencer					88			Actuator / Valve Mounting	System B, BS4800 20 D 45	
89		OTHER DETAILS						90		OTHER DETAILS			

Inspect				
Hydrostatic				
Seat Leakage Pressure	Water @ 60 lbf/in² (4 bar)			
Allowable Seat Leakage	86.2 cc/min	X		
Functional Test		X		
Special Tests				

Engineering Approved/Date	Revision Control		
	Rev	Rev Date	Rev By

Figure 3.4 Data sheet of the valve

The following data has been recorded during the tests:

1. Valve Opening Position (VOP in %)
2. Inlet Absolute Pressure (p_1 in barg)

3. Pressure Differential across the upstream and downstream pressure tapings ($\Delta p=(p_1-p_2)$ in barg)
4. Inlet Water Temperature (T_1 in ºC)
5. Volumetric Flow Rate (Q in m^3/hr)
6. Barometric Pressure (bar)

3.1.3 Method to find C values

The basic flow equation for non-choked, incompressible fluids is:

$$Q = N_1 F_R F_P C \sqrt{\frac{\Delta p}{\frac{\rho}{\rho_o}}} \tag{3.1}$$

where;

N_1 = Numerical constant that depends on the units used. $N_1 = 0.865$ to find Cv
F_R = Reynolds number factor. For turbulent flows its value = 1
F_P = Piping geometry factor. With no fittings attached to the piping (such as expander, reducer etc.), its value = 1. Hence, $F_P = 1$ has been used in the sizing equations
C = Flow coefficient. It can be C_v or K_v
ρ/ρ_o = Relative density. For water its value = 1

Hence, equation (3.1) becomes:

$$C = \frac{Q}{N_1}\sqrt{\frac{\frac{\rho}{\rho_o}}{\Delta p}} \tag{3.2}$$

assuming that the flow is always within a turbulent regime. It has been mentioned in BS EN 60534-2-3 that with the exception of valves with very small values of C, turbulent flow will always exist. It has been observed, that while conducting the experiments, that flow rates are not small enough to warrant modifications for non-turbulent flow, thus this assumption looks reasonable. Eq. (3.2) therefore becomes the primary sizing equation for the X-Stream valves. It is noteworthy at this point that Eq. (3.2) is valid only for:

- Newtonian fluids
- Non-vaporizing conditions

3.1.4 Method to find Cv_{Trim} values

Cv can be calculated from the experimental data directly. The values for Cv_{Trim} are calculated using the formulae detailed in Chapter 1, which is:

$$Cv_{Total} = \frac{1}{\sqrt{\left(\frac{1}{Cv_{Trim}{}^2}\right)+\left(\frac{1}{Cv_{Valve\ Body}{}^2}\right)+\left(\frac{1}{Cv_{Seat}{}^2}\right)}} \quad (3.3)$$

where,

$$Cv_{Valve\ Body} = K_{Body} \times \pi \times \frac{D_{Body}{}^2}{4} \quad (3.4)$$

and,

$$Cv_{Seat} = K_{Seat} \times \pi \times \frac{D_{Seat}{}^2}{4} \quad (3.5)$$

Note that the diameters in Eqs. (3.4) and (3.5) are measured in inches. In the current study, D_{Valve} = 101.6mm and D_{Seat} = 38mm.

3.1.5 Method to find K_{Trim}

K_{Trim} can be calculated using the following expression:

$$k_{Trim} = \frac{Cv_{Trim}}{A} \quad (3.6)$$

where A is the area available to flow within each trim. Table 3.1 Shows the values of A for the two trims used in the present study.

Table 3.1 'A' values of various trims

Trim	A (m)
XLO8-040 (Original Design)	8.46818 x 10^{-6}
XLO8-040 (Version 5.2)	8.46818 x 10^{-6}

3.1.6 Scope of Experimental work

As mentioned in section 3.1, flow loop tests of X-Stream valve have been conducted at various flow and geometric conditions (VOP). Table 3.2 summarises the scope of the experimental work. The valve will be tested at various opening positions with a varied pump speed to amend the flow parameters (pressures drop and mass flow rate) passing through the valve.

Table 3.2 Scope of experimental work

Stack	Flow Condition	Valve Opening Position (%)
XLO8-040 (Original Trim)	75% Pump Speed	100
		75
		50
		25
	38% Pump Speed	100
		75
		50
		25
	10% Pump Speed	100
		75
		50
		25
XLO8-040 (Version 5.2)	75% Pump Speed	100
		75
		50
		25
	38% Pump Speed	100
		75
		50
		25
	10% Pump Speed	100
		75
		50
		25

3.2 Numerical Formulation

Computational Fluid Dynamics, or CFD, has been used for the numerical analysis of the fluid flow within the X-Stream valve. CFD is the analysis of systems involving fluid flow, heat transfer and associated phenomena, such as chemical reactions, by means of computer-based simulation. The technique is very powerful and spans a wide range of industrial and non – industrial application areas. From 1960s onwards, the aerospace industry has integrated CFD techniques into the design, R &D and manufacture of aircraft and jet engines. More recently, the method has been applied to the design of internal combustion engines, combustion chambers of gas turbines and furnaces. Furthermore, motor vehicle manufacturers now

routinely predict drag forces, under–bonnet air flows and the in–car environment with CFD. CFD is becoming a vital component in the design of industrial products and processes.

3.2.1 Working of CFD Codes

There are three distinct streams of numerical solution techniques. They are finite difference, finite element and spectral methods. Finite volume method, a special finite difference formulation, is central to the most well established CFD codes. The numerical algorithms include integration of the governing equations of fluid flow over all the control volumes of the domain, discretisation or conversion of the resulting integral equations into a system of algebraic equations, and the solution of these equations by an iterative method.

CFD codes are structured around the numerical algorithms that can tackle fluid flow problems. In order to provide easy access to their solving power, all commercial CFD packages include sophisticated user interfaces to input problem parameters and to examine the results. Hence, all codes contain three main elements. These are:

- Pre – Processor
- Solver Execution
- Post – Processor

Pre-processing consists of the input of the flow problem to a CFD programme by means of an operator-friendly interface, and the subsequent transformation of this input into a form suitable for use by the solver. The user activities at the pre-processing stage include definition of the geometry of the region of interest (called the computational domain) and the grid generation, which is the sub-division of the domain into a number of smaller, non-overlapping sub-domains. This is also called the Mesh. Selection of the physical or chemical phenomena that needs to be modelled, definition of fluid properties and the specification of appropriate boundary conditions at cells, which coincide with or touch the domain boundary, are also included in pre – processing. The solver primarily consists of setting up the numerical model and the computation/monitoring of the solution. The setting up of the numerical model includes the following:

- Selection of appropriate physical models. These included turbulence, combustion, multiphase etc.
- Defining material properties like the fluid, solid, mixture etc.
- Prescribing operating conditions
- Prescribing boundary conditions
- Prescribing solver settings
- Prescribing initial solution
- Setting up convergence monitors

The computation of the solution includes:

- The discretised conservation equations are solved iteratively. A number of iterations are required to reach a converged solution.
- Convergence is reached when change in solution variables from one iteration to the next is negligible. Residuals provide a mechanism to help monitor this trend.
- The accuracy of the converged solution is dependent upon problem setup, grid resolution, grid independence, appropriateness and accuracy of the physical model.

Figure 3.5 describes the working of the solver. Post processing comprises the examination of the results obtained and revision of the model based on these results. These can be further elaborated into:

- Examine the results to view solution and extract useful data.
- Visualization tools can be used to extract the overall flow pattern, separation, shocks, shear layers etc.
- Numerical reporting tools are used to calculate quantitative results like forces, moments, and average heat transfer co-efficient, flux balances, surface and volume integrated quantities.
- Are physical models appropriate?
- Are boundary conditions correct?
- Is the grid adequate?
- Can grid be adapted to improve results?
- Does boundary resolution need to be improved?
- Is the computational domain large enough?

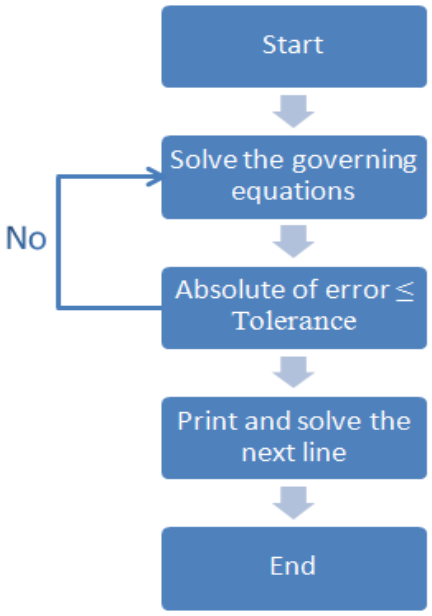

Figure 3.5 CFD Solver

Due to the increased popularity of engineering workstations, many of which have outstanding graphic capabilities, the leading CFD packages are now equipped with versatile data visualisation tools. These include domain geometry, grid display, vector plots, line and shaded contour plots, 2D and 3D surface plots, particle tracking, view manipulations, colour post – script output etc. more recently these facilities may also include animation for dynamic result display, and in addition to graphics, all codes produce trusty alphanumeric output and have data export facilities for further manipulation external to the codes. As in many other branches of CAE, the graphics output capabilities of CFD codes have revolutionised the

communication of ideas to the non- specialists. An overview of CFD modelling is presented in Figure 3.6.

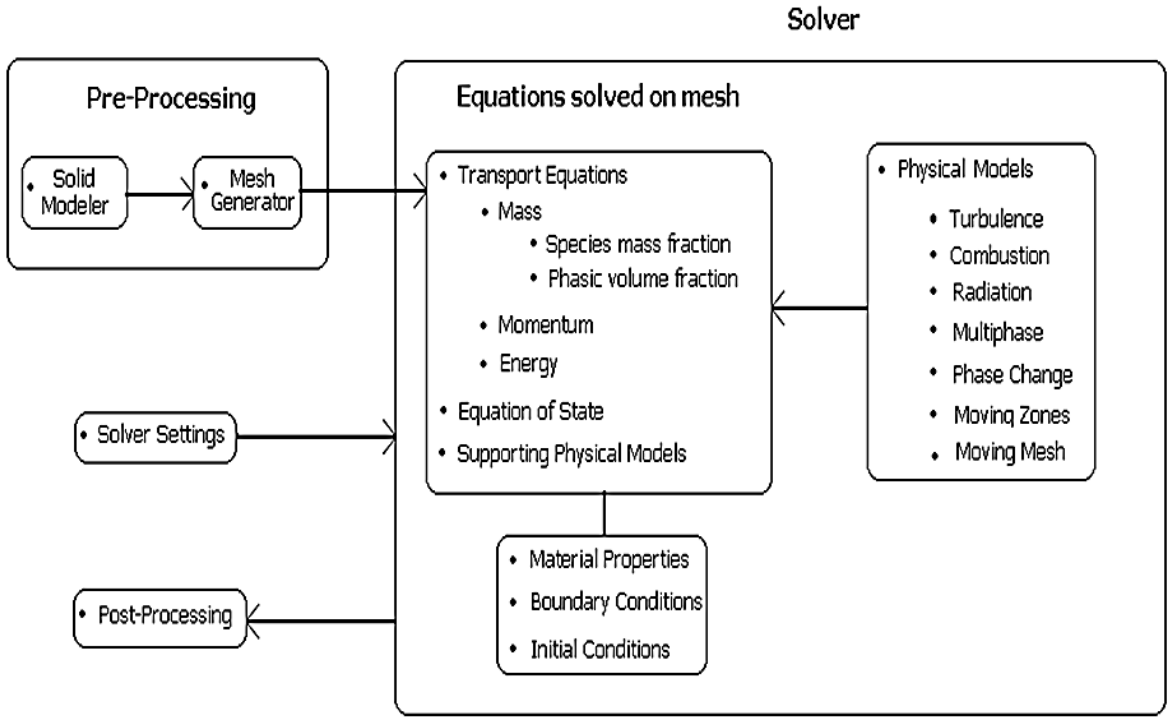

Figure 3.6 Overview of CFD Modelling

3.2.2 Geometry of X-Stream Models

All the five X-Stream models were created using Solid Edge ST5. Because the numerical testing of the trims has no such constraints as the availability of the test setup etc., all five X-Stream trims have been numerically analysed. However, due to the aforementioned reasons, only two trim models had been flow tested. The standard Solid Edge models were saved as an IGES file type for direct import into ANSYS. The ANSYS design modeller can import many different types of file, however, there are some advantages of using IGES files, i.e.:

- The file size is smaller in comparison to some other file types
- They do not need any part files that associate with model

ANSYS is a commercial software that is used extensively for CFD related numerical simulations, and hence has been used in the present study for X-Stream performance testing. The package consists of a CAD program (design modeler), a meshing program and a CFD solver program. The design modeler offers a unique method of computer aided design. Like any other CAD program design, the design modeler has certain advantages for some methods of design. For example, depending on the complexity of the model that is being imported, the

time to import the file can vary significantly, from a few minutes to a few hours. In this scenario, the models that require importing into ANSYS were of high complexity, and therefore, to reduce the importing time, all five of the XLO8-040 models were re-created in the ANSYS design modeller using the exact geometry of the solid edge models. The five Solid Edge CAD models used for the Numerical Analysis are shown in Figures 3.7-3.11. Details of their designs, methods and reasoning are discussed in chapter 4.

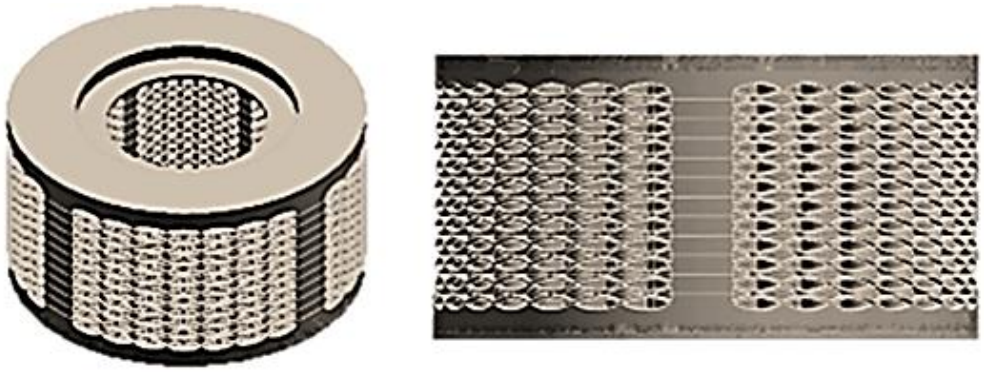

Figure 3.7 V4.1 ANSYS numerical models + flow domain information

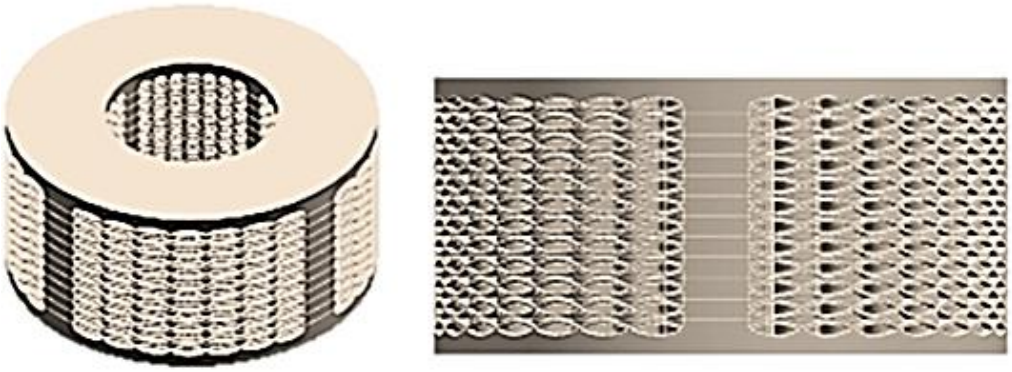

Figure 3.8 V4.2 ANSYS numerical models + flow domain information

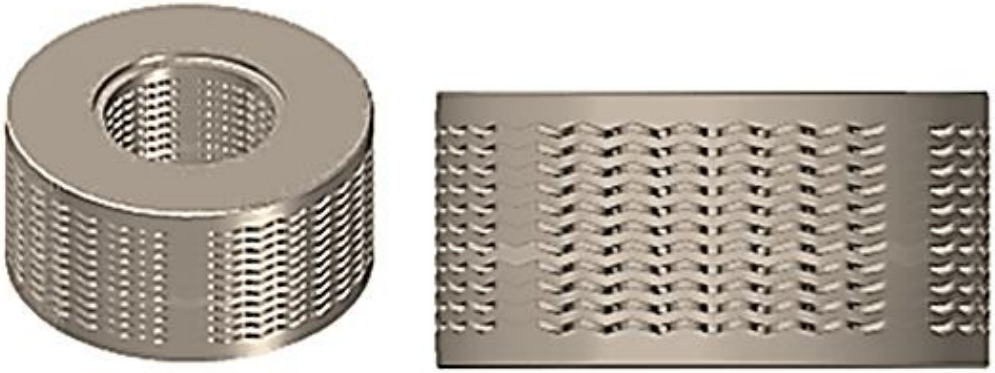

Figure 3.9 V5.0 ANSYS numerical models + flow domain information

Figure 3.10 V5.1 ANSYS numerical models + flow domain information

Figure 3.11 V5.2 ANSYS numerical models + flow domain information

3.2.3 Meshing Condition of models

This section provides details of the meshing parameters used for each of the five trim designs.

Version 4.1 CFD Meshing condition

Table 3.3 summarises the mesh condition of V4.1.

Table 3.3 Meshing Details V4.1

Model Version	Mesh element	Mesh size		Face size of chamfers
		Max	Min	
V4.1	8305152	1mm	N/A	0.2mm

The above table depicts the mesh condition of V4.1. The maximum mesh size is 1mm; the minimum mesh size is not applicable as the advanced meshing option is switched off. The reason for not including the advanced meshing option is that the function of advanced

meshing automatically recognises ‘important features’, however the program is not aware of what features are important from the application of the product point of view (for example an area where the pressure is reduced). The advanced meshing option is automatic and generates fine meshing areas around ‘important areas’.

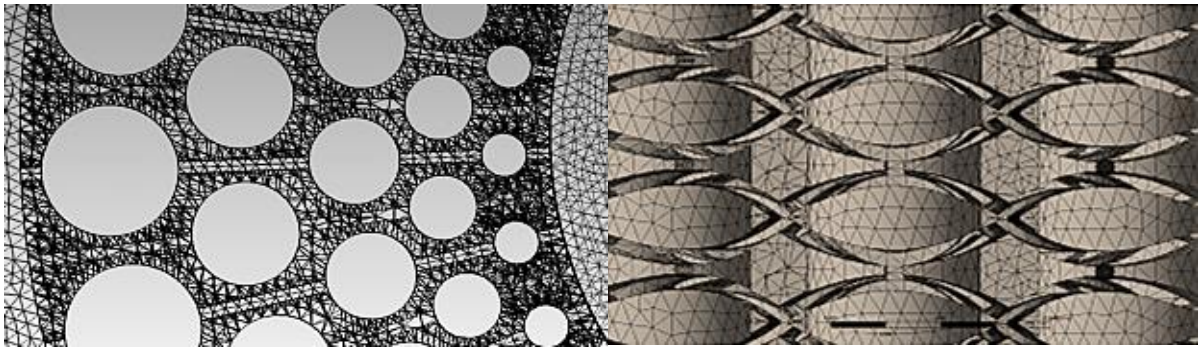

Figure 3.12 Mesh generation of V4.1 (Left) top view, (Right) cross-section view

With the design of V4.1, when advanced meshing was switched on the program recognised areas of the trim designs that included chamfers and defined these areas as important, thus generating very fine mesh areas at these points. As a result the mesh elements for the trim increased to over 20million elements greatly increasing the computer power required to process the mesh. The advanced meshing feature was switched off so that a reasonable mesh size could be implemented, meshing for this particular trim relied on experience from previous research on X-Stream, with at least two elements specified around chamfers each with a 0.2mm element size.

Version 4.2 CFD Meshing condition

Table 3.4 summarises the mesh condition of V4.2.

Table 3.4 Meshing Details V4.2

Model Version	Mesh element	Mesh size		Face size of chamfers
		Max	Min	
V4.2	11350217	0.25mm	N/A	2mm

The mesh condition of V4.2 maximum size was reduced to 0.25mm and the face size of the elements around any chamfers was increased to 2mm due to design similarity with V4.1. The size of the maximum mesh element was reduced to increase the total number of elements to around 10million, when larger sizes were used the total number of elements was much deemed too low to achieve the required accuracy for analysis.

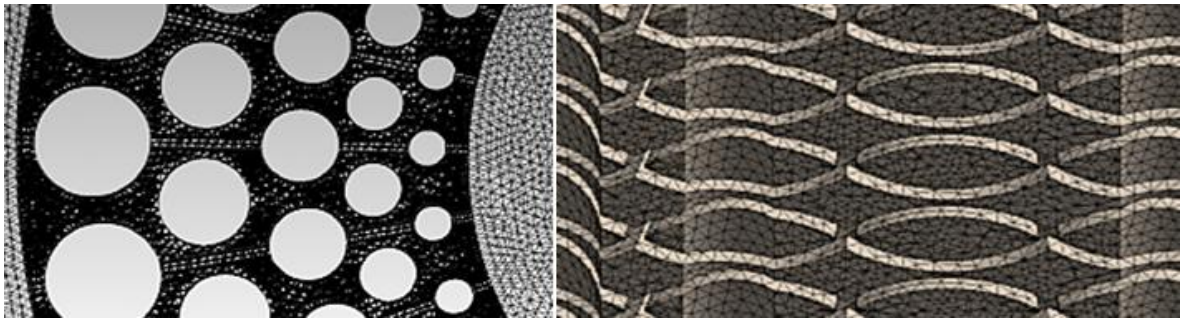

Figure 3.13 Mesh generation of V4.2 (Left) top view, (Right) cross-section view

Version 5.0 CFD Meshing Condition

Table 3.5 summarises the mesh condition of V5.0.

Table 3.5 Meshing Details V5.0

Model Version	Mesh element	Mesh size		Face size of chamfers
		Max	Min	
V5	11663136	0.5mm	0.25mm	N/A

There were no chamfers included in the design of V5.0 and as a result advanced meshing option was included. As a result the minimum size of element was defined by ANSYS and the corresponding number of elements and element spacing suggested by advanced meshing was deemed acceptable. The overall four elements are placed in the fluid zone of trim.

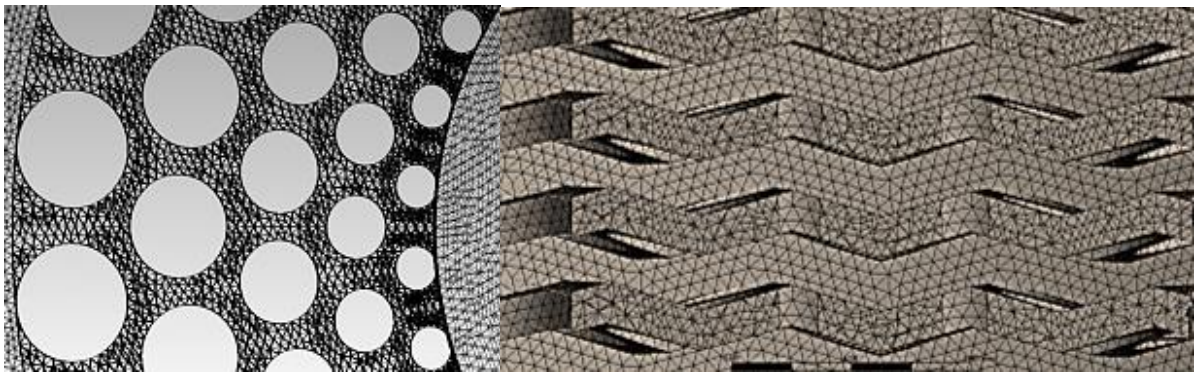

Figure 3.14 Mesh generation of V5.0 (Left) top view, (Right) cross-section view

Version 5.1 CFD Meshing Condition

Table 3.6 summarises the mesh condition of V5.1.

Table 3.6 Meshing Details V5.1

Model Version	Mesh element	Mesh size		Face size of chamfer
		Max	Min	
V5.1	12851376	0.5mm	0.1mm	N/A

Similarly to design V5.0, V5.1's design does not include chamfers and therefore advanced meshing is applied, the minimum element size was set to 0.1mm and the total number of elements and their spacing was deemed acceptable.

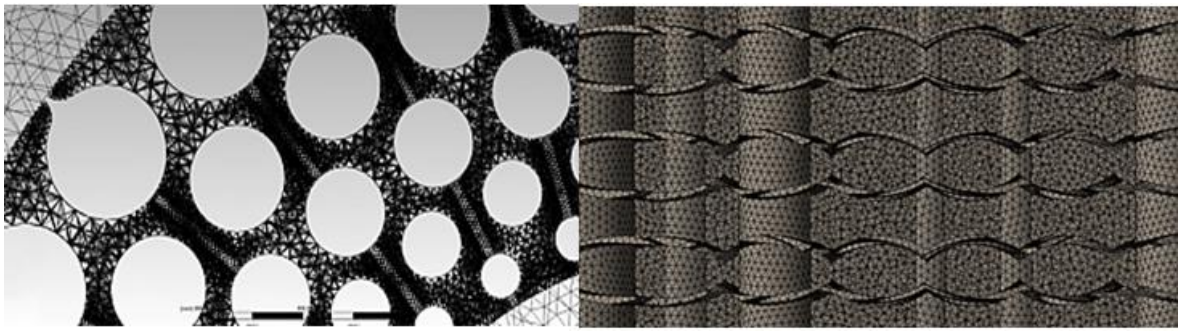

Figure 3.15 Mesh generation of V5.1 (Left) top view, (Right) cross-section view

Figure 3.15 shows two elements placed in the smallest area and six elements are placed in the largest area of the trim.

Version 5.2 CFD Meshing Condition

Table 3.7 summarises the mesh condition of V5.2.

Table 3.7 Meshing Details V5.2

Model Version	Mesh element	Mesh size		Face size of chamfers
		Max	Min	
V5.2	9959979	2mm	0.2mm	N/A

Similarly to V5.0 and V5.1, there are no chamfers on this design and as a result advanced meshing was enabled. The minimum mesh size is 0.2mm and the total number of elements is almost 10million and deemed acceptable for analysis.

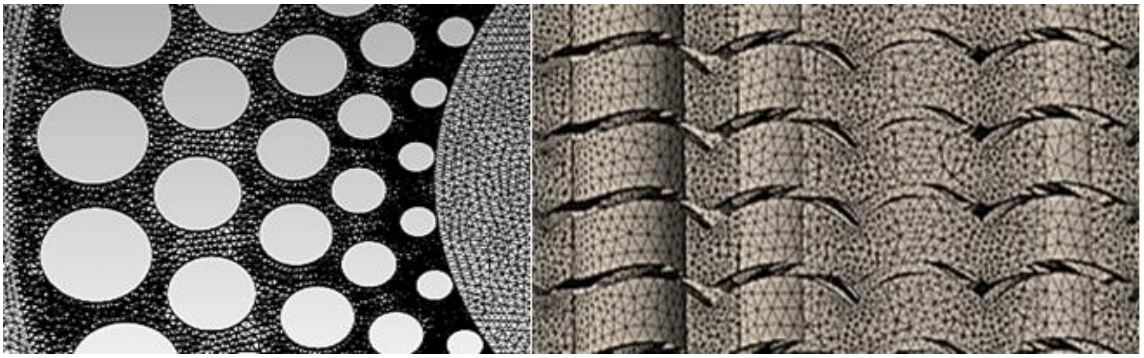

Figure 3.16 Mesh generation of V5.2 (Left) top view, (Right) cross-section view

Figure 3.16 shows the mesh generation of V5.2. In the fluid zone of the trim, four elements are placed between the discs.

3.2.4 Selection of Physical Models

In case of incompressible flow analysis, the pressure based solver has been used to carry out analysis. This is because the flow velocity in case of incompressible flow analysis is much lower than the speed of sound, and hence the compressibility effects are negligible. It is recommended to use pressure based solver in such cases. In this approach, the density of the fluid remains constant and the primary fluid flow parameter, that is being solved iteratively, is the pressure within the flow domain. The control valve used in the present study is designed such that it can deliver a constant flow rate at a specific valve opening position. Hence, the flow within the pipeline is considered to be steady. This argument is further strengthened by the fact that all the boundary condition, including the geometrical variables, during a CFD test remains constant. Therefore, a steady state solver has been used in the present study.

Further to the aforementioned solver settings, it has been observed, and also according to the industrial standards, that these types of valves almost certainly contain turbulent flows within them. Hence, turbulence modelling is essential for accurate prediction of the capacity of the valve and the trims. There are many turbulence models available in the commercial CFD package that has been used in this study. Each one of these turbulence models has its own advantages and disadvantages, which can be found out in any CFD text book. As far as the flow within control valves is concerned, k-ω model has been chosen for the modelling of turbulence within such valves. The primary reason behind choosing k-ω model is its superiority in accurately modelling the severe velocity gradients, which are expected to occur within the trims due to reduction and expansion of area available for the flow to take place.

The k-ω is a two equation model that is further divided into two types. The first type is called Standard k-ω model whereas the second type is called Shear-Stress Transport (SST) k-ω

model. In the present study, SST k-ω model has been chosen because it includes the following refinements:

- The standard k-ω model and the transformed k-ε model are both multiplied by a blending function, and both models are added together. The blending function is designed to be one in the near-wall region, which activates the standard k-ω model, and zero away from the surface, which activates the transformed k-ε model.

- The definition of the turbulent viscosity is modified to account for the transport of the turbulent shear stress.

These features make the SST k-ω model more accurate and reliable for a wider class of flows (e.g., adverse pressure gradient flows, aerofoils, transonic shock waves) than the standard k-ω model. Other modifications include the addition of a cross-diffusion term in the ω equation and a blending function to ensure that the model equations behave appropriately in both the near-wall and far-field zones. Further details of SST k-ω model can be found in any turbulence modelling text book and hence have not been included in this report.

3.2.5 Material Properties

Table 3.8 summarises the material properties used in the current study.

Table 3.8 Material Properties

Material	State	Density	Viscosity	Specific Heat	Thermal Conductivity
		(kg/m^3)	(kg/m-sec)	(J/kg-K)	(W/m-K)
Water	Liquid	998.2	0.001003	N/A	N/A

3.2.6 Operating Conditions

Table 3.9 summarises the operating conditions used in the current study.

Table 3.9 Operating Conditions

Parameter	Condition	Comments
Gravity	On	For accurate prediction of mass flow rate

Operating pressure	14.7 psi absolute	Atmospheric condition
Specified operating density	0 kg/m^3	For accurate vertical flow modelling

3.2.7 Boundary Conditions

The boundary types that have been specified are listed in table 3.10

Table 3.10 Boundary Types

Boundary Name	Boundary Type	Value
Inlet to the suction trim	Pressure Inlet	Variable
Outlet of the discharge trim	Pressure Outlet	0 psi gauge
Walls of the trims	Stationary Wall	Roughness height specified and roughness uniformity specified

3.2.8 Solver Settings

Application based solver settings are required to accurately predict the fluid flow behaviour in the flow domain. These settings comprise:

- Pressure – Velocity Coupling
- Gradient
- Spatial Discretisation

Time averaged Navier-Stokes equations are solved in discretised form. Pressure–velocity coupling is required to predict the pressure distribution in the flow domain with reasonable accuracy. In the present study, SIMPLE algorithm for pressure–velocity coupling has been incorporated because it converges the solution faster and is often quite accurate for flows in and around simple geometries such as spheres, cylinders etc. In SIMPLE algorithm, approximation of the velocity field is obtained by solving the momentum equation. The pressure gradient term is calculated using the pressure distribution from the previous iteration or an initial guess. The pressure equation is formulated and solved in order to obtain the new pressure distribution. Velocities are corrected and a new set of conservative fluxes is calculated.

Gradients are needed for constructing values of a scalar at the cell faces, for computing secondary diffusion terms and velocity derivatives. Green–Gauss Node–based gradient evaluation has been used in the present study. This scheme reconstructs exact values of a linear function at a node from surrounding cell–centred values on arbitrary unstructured meshes by solving a constrained minimization problem, preserving a second-order spatial accuracy.

The CFD solver stores discrete values of the scalars at the cell centres. However, face values are required for the convection terms and must be interpolated from the cell centre values. This is accomplished using an upwind spatial discretisation scheme. Upwinding means that the face value is derived from quantities in the cell upstream, or upwind relative to the direction of the normal velocity. In the present study, 2^{nd} order upwind schemes have been chosen for pressure, momentum, turbulent kinetic energy and turbulent dissipation rate. The use of 2^{nd} order upwind scheme results in increased accuracy of the results obtained.

3.2.9 Convergence Criteria

Getting to a converged solution is often necessary. A converged solution indicates that the solution has reached a stable state and the variations in the flow parameters, w.r.t. the iterative process of the solver, have died out. Hence, only a converged solution can be treated as one which predicts the solution of the flow problem with reasonable accuracy.

The default convergence criterion for the continuity, velocities in three dimensions and the turbulence parameters in the CFD solver is 0.001. This means that when the change in the continuity, velocities and turbulence parameters drops down to the fourth place after decimal, the solution is treated as a converged solution. However, in many practical applications, the default criterion does not necessarily indicate that the changes in the solution parameters have died out. Hence, it is often better to monitor the convergence rather than relying on the default convergence criteria.

In the present study, mass flow rate at the inlet and the outlet faces of the flow domain has been monitored throughout the iterative process. The solution has been considered converged once the mass flow rate at both these faces has become stable. Here, a stable solution can be either one; in which the mass flow rate fluctuations have died out completely or have become cyclic having same amplitude in each cycle.

3.2.10 Scope of Numerical Work

As mentioned in sections 3.2.3 to 3.2.8, solver settings and conditions have been specified to predict mass flow rate at a number of pressures, roughness heights and roughness uniformities. Table 3.11 summarises the scope of the numerical work. The five designs, shown above and detailed in Chapter 4, will each be tested in the full open position at three

defined differential pressures across the trim. Surface roughness and uniformity of the surface will also be varied to see the effect of these parameters following the specific research goals. Values of 100 and 1000 microns have been chosen based on results by Asim that showed SLM with roughness peaks up to 1000microns.

Table 3.11 Scope of Numerical Work

ΔP (bar)	**ε (μm)**	**Roughness Constant (-)**	**Model**
25	N/A	N/A	4
			4.2
			5
			5.1
			5.2
25	100	0.5	4
			4.2
			5
			5.1
			5.2
25	100	1	4
			4.2
			5
			5.1
			5.2
25	1000	0.5	4
			4.2
			5
			5.1
			5.2
25	1000	1	4
			4.2
			5
			5.1
			5.2
50	N/A	N/A	4
			4.2
			5
			5.1
			5.2
50	100	0.5	4
			4.2

			5
			5.1
			5.2
50	100	1	4
			4.2
			5
			5.1
			5.2
50	1000	0.5	4
			4.2
			5
			5.1
			5.2
50	1000	1	4
			4.2
			5
			5.1
			5.2
100	N/A	N/A	4
			4.2
			5
			5.1
			5.2
100	100	0.5	4
			4.2
			5
			5.1
			5.2
100	100	1	4
			4.2
			5
			5.1
			5.2
100	1000	0.5	4
			4.2
			5
			5.1
			5.2
100	1000	1	4

			4.2
			5
			5.1
			5.2

CHAPTER # 4
MANUFACTURING METHODS FOR X-STREAM TRIMS

This chapter presents a critical comparison of either a geometric modification or a modification to the process of manufacture of severe service valves on capacity of the valve trims. The chapter details a number of concept designs prepared for testing and an analysis on the process of manufacture to produce samples of each, ready for flow capacity testing.

4.1 Current Manufacturing Methods and Current Design

The X-Stream trim has been in production by for a number of years. As previously discussed, the trims have been manufactured predominantly using the EDM method, which had been identified as a very suitable method for the trims' original design. However it limited the overall size of valve that could house the X-Stream. Furthermore, the X-Stream flow paths were restricted to a small portion of the disc (as can be seen in Figure 4.1).

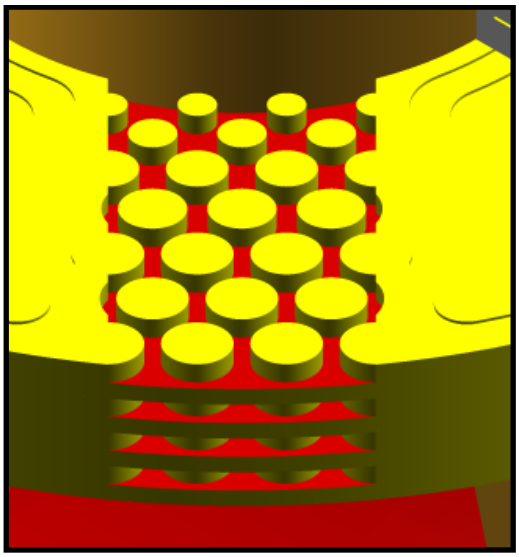

Figure 4.1 Earliest example of X-Stream flow path

Developmental activities have been taking place on the trim over the past three years, and as a result, the general design has been altered to include many more features which can increase the available flow area. The cost for manufacture has increased significantly with these revised designs. EDM continues to be the main method of manufacture for the revised design (figure 1.5), all testing performed for the production trims has been completed on trims manufactured using EDM.

Qualitatively, the X-Stream in its current design has a defined average surface roughness value (Ra) of approximately 32 microns and the K factor, based on area, is averaged for design changes, like increase in number of stages and is specific to the EDM method of manufacture. A full analysis of the surface of a disc, manufactured using EDM, was completed and the results are shown in Appendix 1. Appendix 1 also shows other surface parameters for the EDM trim, including important parameters like Sp and Sv, which are the height of the highest peaks in three dimensions and the depth of the lowest valley. The value of K is, in reality, a combination of various restriction factors to fluid flow through the trim, including losses as a result of friction with the surface of the trim. Analysing the results by Asim [31] values of K for the trims can be calculated when the area and K values for the other elements of the valve are known, in order to satisfy equation 1.6. Values for Cv of the body and Cv of the seat can be calculated as follows:

$$Cv_{Seat} = A_{Seat} \times K_{Seat} \qquad Cv_{Body} = A_{Body} \times K_{Body}$$

$$= \left((\frac{38}{25.4})^2 \times \frac{\pi}{4} \right) \times 38 \qquad = ((\frac{101.6}{25.4})^2 \times \frac{\pi}{4}) \times 24$$

$$Cv_{Seat} = 66.8 \qquad Cv_{Body} = 301.6$$

Thus, using equation 3.3, a value for Cv of the trim can now be calculated for the Cage/Stack, when made using EDM.

$$Cv_{Cage} = \frac{1}{\sqrt{\frac{1}{Cv_{Valve}{}^2} - \frac{1}{Cv_{Body}{}^2} - \frac{1}{Cv_{Seat}{}^2}}}$$

$$= \frac{1}{\sqrt{\frac{1}{32.3^2} - \frac{1}{301.6^2} - \frac{1}{66.8^2}}}$$

$$Cv_{Cage} = 37.2$$

Knowing that the Cv of the trim is 37.2, the K factor can be determined. The K Factor has been calculated as being 65 for this particular disc design, using EDM as the method of manufacture.

4.2 Proposed Manufacturing Method, Current Design

The author had begun trials using SLM as the method of manufacture for the X-Stream trim, however, the tests that have been completed to-date have shown significant differences in the results between the trims manufactured from the two methods. Flow tests completed by Asim [31]summarised in table 2.1, show that for a like-for-like design, the Cv of the SLM X-Stream is significantly lower than EDM; a value of 24.5 for the like-for-like flow rates and valve opening percentage. This represents a decrease in Cv of 31.8%.

As can be seen, the results have been obtained at various openings and flow rates, to ensure that the results are not anomalies. Furthermore, further samples had been manufactured and flow tested, with very similar reductions in Cv. Values for surface roughness were measured (as shown in Appendix 1), and average area roughness values for this design in three dimensions (Sa) were determined over a two position average to be 37.7µm; an increase of 410% from EDM. As with the design from EDM, a K factor can be worked out for the SLM

trim, knowing that the Cv for the body and the seat has remained constant. The Cv of the SLM cage is calculated from Asim's results as follows:

$$Cv_{Cage} = \frac{1}{\sqrt{\frac{1}{Cv_{Valve}{}^2} - \frac{1}{Cv_{Body}{}^2} - \frac{1}{Cv_{Seat}{}^2}}}$$

$$Cv_{Cage} = 26.6$$

Resulting in a K factor of just 46; a decrease of 41% from EDM (one tenth of the increase in area roughness)

4.3 SLM Method – Improvements to method of manufacture and design

There are other performance characteristics that must be considered for the control valve in order to determine its suitability to control a service. However values of Cv are possibly the most important factor to valve companies, as this can result in a competitive price advantage over their competitors. The SLM method shows promise, based on the reduction of costs for manufacture and lead times, when comparing like-for-like sizes against EDM, however, the significant reduction in overall Cv means that this cost advantage could be offset by the reduction in flow capacity through the valve. Thus the first research goal for this project is to perform a critical analysis on improving the manufacturability of the X-Stream by altering the process of manufacture, or by altering the design.

Literature suggests that structural deformities can occur when the distance from the base plate increases. This is evident in samples produced previously, that present deformities in shape towards the top of the stack and that the methods of reducing these deformities, (proposed by Osakada and Shiomi [20] are to increase scan speed, or to modify the geometry of the part in order to reduce the effects of the thermal gradients across the parts. Previous work had aimed to reduce the deformities by adding additional strength to the component, via means of an inner and outer sleeve, added to the part during the printing phase, which would then need to be removed during the finishing phase (example shown in Figure 4.2), and also through printing the stack at angles.

It was this method that was used when producing earlier samples, allowing for the part to be manufactured as close to the requirements as possible, to the extent that flow results could be gathered on a fully completed trim. Without this method, previous build attempts had failed to construct the part as the deformities were so large that the laser was unable to continue the printing phase, The surfaces had deformed to an extent that laser was unable to work in these areas. Further review has also identified that there are possibilities that the removal of these

features may have an effect on fluid flow, as removal using a standard turning machining operation leaves flashing/burring of the metal, which requires significant de-burring operations.

The deformities were still evident in the trim after the removal of these features. During the machining phase, flow paths were opened in some areas before others i.e. the shroud itself did not appear to be of a constant thickness, around the circumference of the stack. Therefore, as a result of previous attempts in these areas, the performance characteristics were reduced, but allowed for completed builds. It is the aim of this study to review further geometrical designs, and assess these components.

4.3.1 Design Improvements

Discussions were held with TWI (The Welding Institute), the company used to produce the original sample trim designs, to understand manufacturing constraints with the SLM equipment, specifically, discussions related to the minimum thickness of solid sections, limitations of powder thickness etc.

TWI also advised that there were issues, when attempting to deposit powder on to areas where there was no metal structure beneath and that this was one of the reasons why the parts were manufactured at an angle (as can be seen in figure 4.2). Figure 4.3 shows an example of unsupported powder layers, which they had previously attempted to overcome by printing the parts at an angle (approximately 45^0), however, other angles had been attempted. Angular printing did not solve the issues that Osakada and Shiomi [20] had identified i.e. the increase in stress of the material. In fact, printing at an angle actually worsened this effect, due to the gravitational force tending to move the powder.

Figure 4.2 Example of X-Stream with shroud added on OD for support

TWI thus advised that the part would benefit from having any unsupported flat surfaces removed, and as a result, a number of designs were developed to be presented to TWI for manufacture and testing.

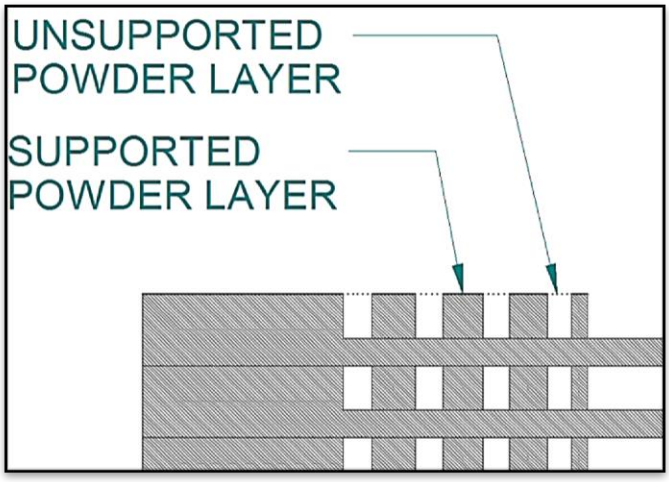

Figure 4.3 Examples of supported and unsupported areas

Five different models of X-Stream trims have been generated in the present study using SLM method of manufacture. These trim models depict the range of operations an SLM process can carry out, in order to create X-Stream trims. Furthermore, these models have been generated based on the range of operations required to manufacture X-Stream trims. The created models show the capabilities of the SLM process. In order to characterise the created models, both experimental and numerical investigations have been carried out. The experimental investigations have been limited to only two of the models because of limited testing facilities available at the time when the experimental investigations were carried out. However, detailed numerical investigations have been carried out on all the trim models. Numerical investigations are not only capable of predicting the global performance characteristics of these trim models (like Cv), but can also predict the various flow related parameters within the flow domain (like pressure, velocity etc). This information is very useful for the trim designer as this information can be used to decide design alterations/modifications to create better performing trims.

A comparison between the performance characteristics of the various trim models considered in the present study has been included in Chapter 5, where the performance characteristics have been predicted through the use of illustrative numerical investigations. Furthermore, an in-depth analysis, and comparison, between the flow characteristics of these trim models has also been discussed in detail. The objective is to determine which one of the trim models performs the best amongst the models considered in the present study. For each of the designs presented, there was a standard method to the placement of the columns on the X-Stream disc. The CAD modelling strategy employed has also been similar for each design and follows a standard procedure for the placement of the columns on the disc. Each design uses a number of steps for the modelling phase, of which the first five steps are identical for

each concept design and all used the same gaps between the columns defined by the standard XLO8-040 trim design. The modelling procedure, as follows, was implemented:

1. Initially, the geometry for a single flow path was modelled using a lofted protrusion constructed from two sketches, one on the outer diameter and one on the inner diameter

2. The flow path was patterned through a 90° arc, to produce the flow path for a quarter of the disc

3. Columns were modelled, extruded and patterned through a 90° arc

4. The blank paths were constructed by extrusions, before the quarter disc was patterned symmetrically four times around the full 360° of the disc

5. The disc was completed by cutting the inner and outer diameter to size

The above method produces a disc stack with minimum features in order to reduce modelling time. The majority of the design process that follows this section focuses on the reasons for the choice of geometry in step 1. Once this geometry was correctly constructed, steps 2-5 were repeated identically for each model. The disc stack was initially constructed as an assembly part, using the following method:

6. The disc part was imported into an assembly file

7. A rectangular pattern sketch was constructed, with a node number equal to the number of discs in the vertical direction

8. Discs were patterned to the sketch in step 2

9. Existing end discs were mated to the discs completing the stack

Using an assembly method (steps 6-9), to construct a model using SLM produces, an undesired effect of having micro spaces between the parts in the assembly. This was identified using the Magics software used by the SLM manufacturer. To overcome this issue, it was decided that rather than using the standard assembly method (as used for all trims manufactured from the EDM method), the micro gaps could be removed by using a single part file, whereby the following steps were used (instead of steps 6-9):

10. The disc was part copied into a new part file

11. A body pattern was used to produce a disc stack of the required number of discs

12. Extrusions were made on the top and bottom of the stack to produce the end discs. The inner and outer diameters were given a tangential and concentric relationship to the discs

13. A revolved cut was used to construct the desired disc stack, identical to that of a machined disk stack

Using a separate part model for the stack allows quick replacement of the discs, with the relationships within the stack model adjusting to the new disc internal and outer diameters. This means that multiple discs can be produced while using the same disc stack model, and in actual fact, made the process no more complicated or time consuming than the standard method. Using this method, when applied for each new design, would save modelling time over the standard, as the standard method requires the addition and mating of multiple parts to manufacture the stack, In standard method, when dealing with stacks of greater height, the total number of discs to import into the assembly can become rather large, thus requiring a large number of mates.

There were a number of preliminary designs developed that are not shown in this report, which led to the creation of the concepts put forward. These designs were simpler designs that were not intended to improve performance (or ease of manufacture), but rather to test various modelling constraints, and to develop the steps above. The first complete stack design produced is called Version 4.1

Design Concept 1 – Version 4.1

The first design concept developed came through discussions with manufacturer, who advised that this structure would provide optimum build quality and strength for the part. This design uses an oval design feature with a flat surface at the top of each oval to allow for completion and assembly of the part. This was the first design put forward for manufacture.

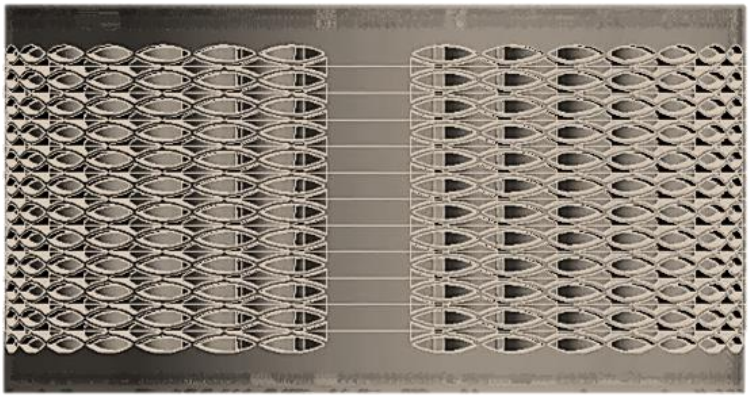

Figure 4.4 V4.1 Side View

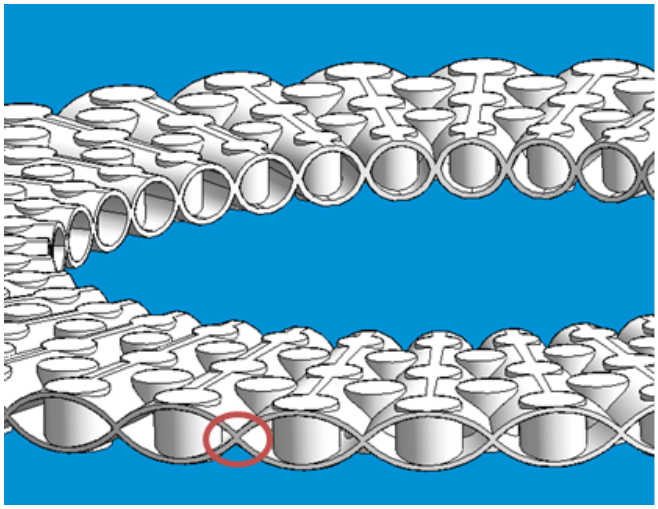

Figure 4.5 V4.1 single disc view from Solid Edge

Figures 4.5 and 4.6 show what is now defined as a single disc and the assembled stack. The design uses a thin wall feature and a mirror body feature to produce the flow path rather than a standard lofted cut. This reduced the amount of complex sketches required for the lofted cuts. The total number of features for the disc was thus limited to 13, and the file size 21.5Mb, rising to 93Mb for the complete stack.

The flat surface feature on the top and underside of each disc (circled in red in figure 4.5), had a thickness of 0.25mm, advised by the manufacturer as the minimum thickness for a ligament. As a result, it reduced the minimum gaps between the columns by the same amount, and forced the splitting of the flow paths. As the flow paths were distinctly split, this would prevent jet impingement to some extent, which had been an inherent design feature of the original X-Stream trim.

Design Concept 2 – Version 4.2

This design, shown from a side view in figure 4.6, is very similar to 4.1 and follows the steps 1-12 laid out above. The significant change in this design is the removal of the ridge section at the top of the oval. This feature has been removed because it is thought that this may cause an issue with velocity peaks and areas of re-circulating flow, contributing to erosion and cavitation, this ridge section is shown, circled, in figure 4.5.

The ridge surface was restricting the minimum gap between the columns, below the company design standard of 1.2mm. Although this design limit had been specified due to the machining limits of spark eroding, it was thought that a comparison between the two designs without this surface may show interesting results, with only minimum effect on the manufacturability of the trim. The design would then allow impingement on the top and lower surfaces of the disc, but would still prevent this feature in the middle section (through the disc).

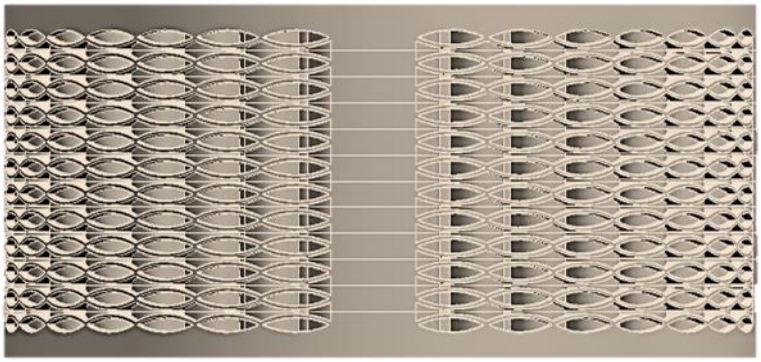

Figure 4.6 V4.2 Side View

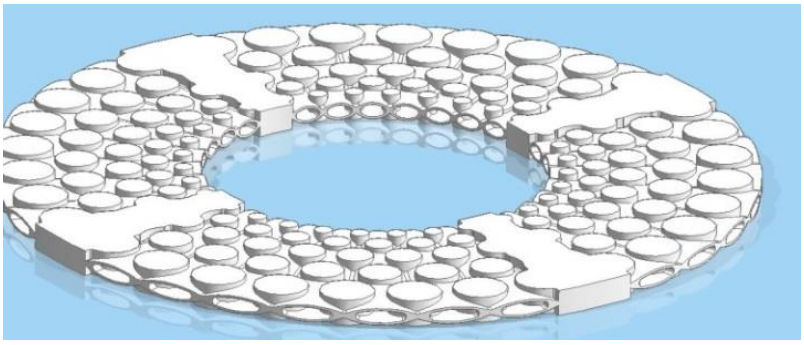

Figure 4.7 V4.2 single disc view

The removal of the flat surface, shown in figure 4.7, is not related to the requirement to remove flat surfaces from the design for manufacturing purposes, as this was in fact a supported flat surface. The design also lowered the height of the oval to allow a minimal width between columns and a minimum height of the flow path. This design uses fifteen features and results in an overall increase in size from 21.5 to 32.35Mb for the individual disc and the stack rising to 109Mb – warranted by the overall increase in number of features. The stack is made up of the same number of discs resulting in the same overall height.

Design Concept 3 – Version 5.0

This design is considerably different to that of the previous two design concepts and is more like some of the basic shapes that had been considered during the method development phase. Rather than using oval shapes for the main flow path shape; flowing the process fluid through the discs as well as on the top and bottom surfaces of the disc, this design was much similar in basic shape to the standard X-Stream design, simply exchanging flat surfaces for surfaces at a 15 Degree angle, figures 4.8 and 4.9 show the side and single disc design views for version 5.0. .

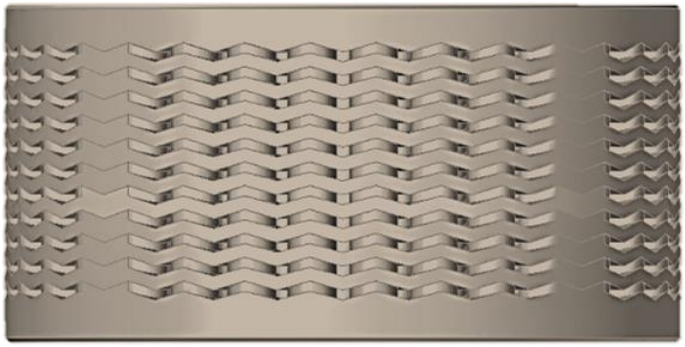

Figure 4.8 V5.0 Side View

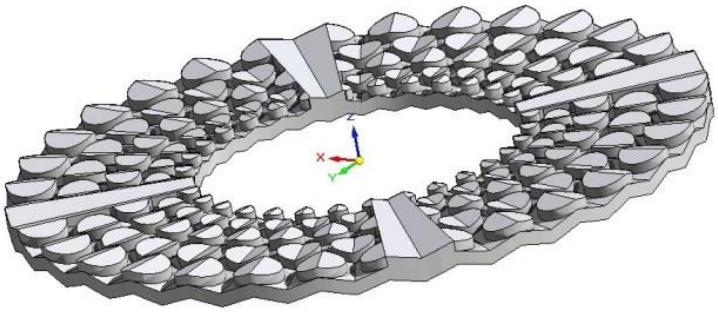

Figure 4.9 V5.0 Single disc view

This design is complex assembly of features grouping multiple sketches and planes together to form the angles at the top of the columns and on the undersides of the discs. The faces of the blank channels are done using replace face and are patterned and protruded around the surface of the disc. In total the individual disc is made up of over 40 features and rather than following steps 10-13 for creation into a stack, it uses the standard assembly method from 6-9. This design, was actually completed much earlier than concepts 1 and 2 and as such was not modelled in the same way as those design, it was initially rejected as a suitable design due to its more complicated design process but was later included following discussions with the SLM manufacturer who advises that this shape would be manufacturable.

Version 5.0 of the trim is the first of the new trim designs to be successfully manufactured, but as shown in Figure 4.10 the part is still showing deformities in its physical shape. As can be seen the right edge of the part is appearing non circular. The part slipped during the manufacture phase. It is confirmed, by TWI, that this deformity could be eliminated with a further refinement in the manufacturing process, rather than through the design process.

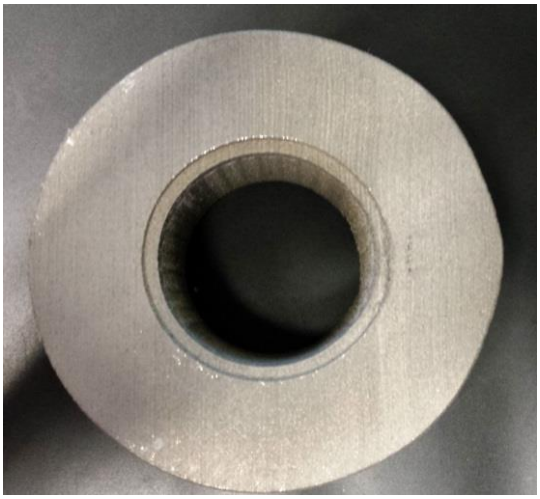

Figure 4.10 V5.0 view of manufactured trim showing deformity

Design Concept 4 – Version 5.1

Design 5.1 simplifies the design process of 4.2 by producing a simple arced disc of ten features as opposed to a straight, angled or extruded disc. This wave design requires simple geometry which is then patterned into a disc. A new method of design for the stack is used by copying the disc into a part file and producing the stack. This method allows for the easy replacement of a disc, by using the replace part feature. This method increases the overall file size to 89Mb, thus increasing the construction time and consequently the computer power required.

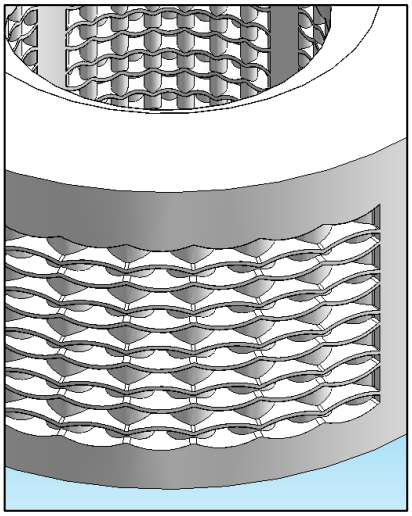

Figure 4.11 V5.1 Solid model view

This method of design reduced the strength of the component; the arc angle decreased as the diameter increased, which is similar to to the design of the angle feature in version 4.1. The design as with versions 4.1 and 4.2 allows for fluid flow within the disc and on top of it. However some of the gaps between these areas were minimal, restricted to the manufacturing

constraints, which restricted the minimum feature thickness of 0.25mm. It is also thought that the opposing discs would restrict the flow path.

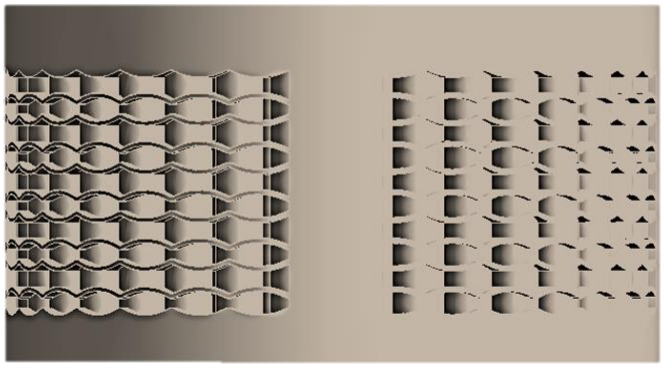

Figure 4.12 V5.1Side View

As such some of the gaps between columns and edges of the flow path which have been designed for a standard gap of 1.2mm at the minimum points, were now reduced to less than 1mm. As can be seen from Figures 4.11 and 4.12, the design varies from versions 4.1 and 4.2, by not closing the arc between the columns, meaning that the fluid is free to flow around the columns and is not restricted to an individual route. This means that one of the original key features (jet impingement) is not restricted like in the previous designs. Fluid is now free to flow around all columns on the top, underside and through the center of the disc. This maximises the effect of jet impingement as a method of both velocity control and pressure reduction, but also on the premise that previous testing had shown that this feature reduced areas of re-circulating flow. It is considered that this design may have unsupported areas at the tips at the edge of the arcs, where the bottom surface was flat and as such a final design was proposed.

Design Concept 5 – Version 5.2

The final design concept aims to use features inherent with all four of the previous designs. The curved arcs of 4.1, 4.2 and 5.1, the standard design of flow only through the trim like in design 5.0 and the original concept rather than the flow paths for designs 4.1 and 4.2. Finally the design aims to remove the restrictions that have been identified with design 5.1, whereby the arc angle decreased as the diameter increased.

It is identified that this occurred as a result of the changing hydraulic diameter and as such this design (V5.2) is constructed in translation symmetry. A further design alteration includes the addition of a tear drop / aerofoil shape adding to the largest outer diameter column on the side linking to the outer edge of the trim. This feature is added to increase with support, but also to assist the performance of the trim by potentially removing the sharp angle for entry of the process fluid to the trim.

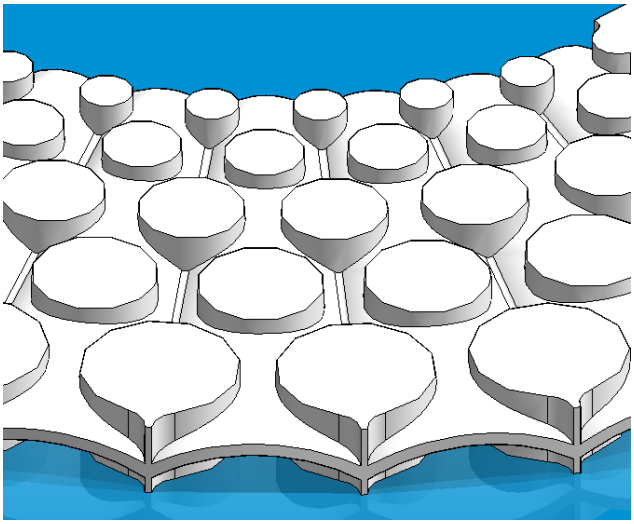

Figure 4.13 V5.2 single disc view

Earlier analysis identified that this area; the minimum area within the trim, is subject to the highest pressure drops and as such the highest velocity's. A streamlined entrance, is thought, would reduce the velocity peaks at the entrance and as such improve the trims overall performance.

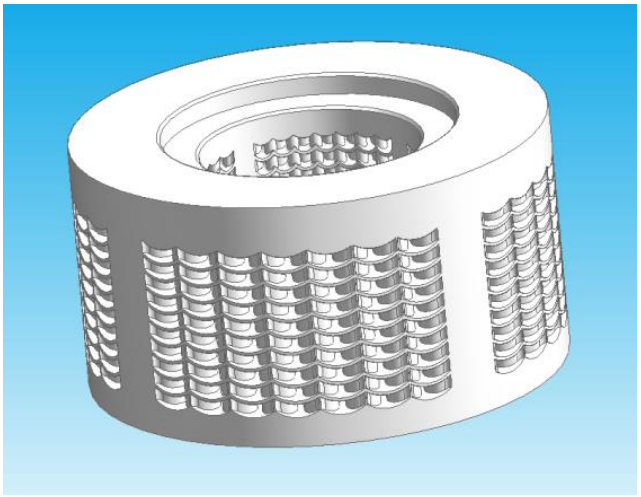

Figure 4.14 V5.2 solid model full view

The aerofoil shape at the entrance could potentially improve the overall surface finish at the trim, by adding a further feature at this area to improve the strength, thus reducing the residual stress and restricting deformation of the surface. The idea of using aerofoils within the trim specifically at the entrance had been considered previously, however had never been successfully implanted when using the EDM manufacturing method, due to the accuracy/size of the feature. It may have been possible to do this shape on much larger discs; however the author was interested in this feature being applied across the standard range which restricted minimum features to 1.2mm. However as these restrictions were not the same with SLM, it was trialled with this concept, where successful application may allow for the application of full aerofoil shapes to replace all the standard column design.

Figure 4.13, shows the individual profile of the disc and Figure 4.14 the assembled stack, which uses the second method of stages 10-13 to assemble. Although not noticed, during the extrusion of the final disc to form the end pieces of the standard stack, a whole disc was lost from the stack, meaning that the stack finished with only ten disc paths, compared to the eleven with version 5.0 and twelve with versions 4.1, 4.2 and the original design XLO8-040. This design has also been successfully manufactured using the SLM process, the part is the most successful shape that has been manufactured using SLM. Figure 4.15 shows the completed part, where the line slightly above centre is where the part has been sectioned for inspection.

Figure 4.15 Manufactured sample of V5.2

4.3.2 Process Optimisation

The next stage of the programme requires the review of various features within the manufacturing process and the observation of their effect(s) on the successful creation of the part; whereby the definition of successful creation was dependent on a number of parameters;

- Density
- Surface finish
- Feature Size
- Laser Spot Size
- Hatch Distance
- Point Distance
- Laser Power
- Exposure time
- Finally, overall production time (also known as build rate)

Various trials were completed on test block samples, whereby larger variations could be made with regards to certain parameters that would have not been possible for commercial cost reasons, if this analysis had been done on full production samples of the X-Stream trim.

Each of these features was important to monitor, analyse individually and also collectively with the build trials. The density of the part is obviously important to ensure that the columns and features on the disc are not porous and to ensure that the material meets the required material properties, like Tensile and Yield strength but also that the hardness of the material conforms to the material standards.

Hardness is one of the main considerations for the resistance to erosion of the material. Materials are selected for the X-Stream trim considering required hardness for the specific application. Parts that are manufactured under the required values, as a result of poor density, could be prone to premature wear/failure.

4.3.3 Equipment Used

The manufacturing trials and optimisation tests were performed using 3 different machines;

- Realizer SLM 100
    - This is a 200W Ytterbium fibre laser
    - It can deposit powder layers between 20 -100 Microns
    - The optical train allows a spot size (for the laser) of 20 microns
    - The processing area is 100mm^3
    - It uses an Argon inert atmosphere

- Renishaw AM250
    - This is (up to) a 1000W Ytterbium fibre laser
    - It can deposit powder layers from 50-200 Microns
    - The optical train allows spot size of 100 microns
    - The processing area is 250mm^3
    - It uses a vacuum processing chamber

- M1 Concept Laser 200W
    - This is a 200W Ytterbium fibre laser
    - It can deposit powder layers from 50-200 Microns
    - The optical train allows spot size of 90 microns
    - The processing area is 300mm^3
    - It uses an Argon inert atmosphere

4.3.4 Features Explained

Information, detailed in chapter 1, on SLM parameters covered the basic fundamentals of what these main process parameters were. In order to optimise the process these parameters have been investigated for their effects on the build and are explained as follows. Density is simply the density of the part/feature post laser melting. The density of the part is important

to understand the strength of the component and its porosity. Density is controlled by a number of features predominantly point distance and hatch distance, but also by layer thickness and exposure time.

The feature of surface finish is measured purely as an average surface roughness value. During the SLM process surface finish is mainly controlled by laser Spot size, but also by the layer thickness and the thickness of the powder used. Feature size is the accuracy of the process, more specifically the smallest feature that can be produced using the current equipment. Typically, the feature size will be at least double the laser spot size, as a single feature will need a minimum of two spots to melt the powder to form the feature. Laser spot size is the size of the laser beam at the application point. This is totally defined by the lenses and other parts of the optical train used in the machine. Laser spot size is a very important parameter in the manufacturing process. It is a key parameter for the accuracy of features/parts, the surface finish of the parts and also the speed/build rate. Typically a smaller laser spot size will mean that the part build rate is lower, however when worked in conjunction with other features, this may not be to a linear rate.

Hatch distance is the distance between lines of spots/points that the laser will make. As discussed during the literature review most modern SLM machines will use the spot laser method of manufacture and the spacing of lines (hatch) is important to build rate and density of the part. Point distance is the distance between each laser spot/point in a single line. Point distance is very important feature to determine build rate and density. Laser power, is simply the power of the laser determining the amount of heat that can be applied to the powder in a given exposure time. Most systems will work up to a minimum of 200W, but may actually run with a much reduced laser power. Laser power is one of the most over appreciated parameters in the system. It is a common misconception that the higher the laser power the faster the build rate. To some extent this is true, although it is more reliant on most of the other features, specifically layer thickness, exposure time, hatch and point distance.

Exposure time is simply the time a specific area (spot size) is exposed to the laser. The exposure time is a very important parameter for density, as insufficient exposure time could mean that the part is not fully melted/formed. Exposure time will also impact the build rate. Overall production time / build rate is controlled by most of the features mentioned above. Faster build rates will usually have a detrimental effect on surface finish, while slower build rates may allow for better surface finishes at increased costs. Production time is important to determine the overall cost of the component; however it should not be considered the highest priority of the features. Some previous trials have produced parts in less than 8 hours, however they suffered from porosity (poor density) and high surface roughness.

In summary, there have been many trials completed by TWI to determine a set of features that will be used for manufacturing the parts. Higher laser power enables the machine to produce parts much quicker, up to 3mm/s. However density reduces with an increase in speed

as there is not enough time for the laser beam to penetrate the powder and melt it. Powder size and composition is also important to the build process. Bulk batch powder was bought for the trials and was between 15-45 Microns, where over 98% of the batch by weight had a micron layer thickness less than 45 and 0.5% less than 15. Smaller grain size powder could be used to produced better parts; whereby better parts could be parts with reduced surface roughness or higher density parts, however there is a substantial cost increase as a result, which was not thought worthwhile for these tests.

There have been a number of trials (sample pieces) produced prior to the manufacture of the X-Stream components, to review the effects of various parameters on product density, which was considered the most important feature for a successful build. The features monitored, were, the point distance and exposure time, laser power was originally kept constant. Figure 4.16 shows a series of test blocks that were trialled, varying the exposure time and point distance, Figure 4.17 shows the results of whether the build itself was successful.

Figure 4.16 Manufactured test blocks

As can be seen a number of the blocks failed to form at all, which was as a direct result of insufficient energy transferred to the powder; as a direct result of poor exposure time, to fully melt the powder and form the part. A green tick indicates that the part successfully built, with the number indicating how many blocks were built (the tests aimed for two samples at each point distance and exposure time), yellow shows a partly successful build and red X meant that no blocks were successfully completed. Further, the wall thickness of the parts were measured and compared for certain samples, showing that the most successful features occurred when the point distance was at its lowest value and exposure time was at either 100 or 150 micro seconds.

			Exposure (micro seconds)					
			A	B	C	D	E	F
			50	100	150	200	250	300
Pd (micro meters)	1	30	0	2	2	1	1	1
	2	64	0	2	2	1	1	1
	3	98	0	2	2	2	1	1
	4	132	0	2	2	2	2	1
	5	166	0	0	2	0	0	1
	6	200	0	0	0	0	0	1

Wall thickness (mm)			Exposure (micro seconds)					
			A	B	C	D	E	F
			50	100	150	200	250	300
Pd (micro meters)	1	30		0.34	0.38			
	2	64		0.28	0.31			
	3	98		0.29	0.3	0.26		
	4	132		0.26	0.29	0.24	0.27	
	5	166			0.23	0.24	0.28	
	6	200				0.29	0.26	

Figure 4.17 Results of manufactured test blocks

4.4 Parts Produced

In total four parts have been successfully manufactured for testing from varied designs and process parameters. One of these parts was produced previously, which was an original design SLM trim (called original SLM trim test in Table 4.1)

This part also included an inner and outer sleeve to assist the build process, which was removed by turning. These features used a slightly reduced laser power of 100W and a reduced exposure time of 200 Micro seconds. This trim had undergone flow testing using the process as detailed in Chapter 3; the results can be seen in Table 2.1 [31] and again in section 4.2, whereby the part produced an overall Cv_{Trim} of 26.6. This part has already been flow and numerically tested in a previous study by Asim [31], and hence is not considered for either testing in the present study. However, the method of manufacture/process parameters, which was not reported by Asim, is being reviewed in the present study because of its importance to the main aims of this study. The other 3 parts produced were;

- Version 5.0
- Version 5.2
- Original Design XLO8-040 – New process

Table 4.1 shows the complete final process parameters used during the manufacture of the 4 successful samples (complete with an image of each for reference). Designs 5.0 and 5.2 used a different machine with an improved optical train for their manufacture; however most of the

process parameters were very similar to those used on the Renishaw machine, which was unavailable for use with these builds.

The original design trim with new process conditions was manufactured on a completely different machine with very different process parameters. These parameters were defined by the manufacturer to reduce the potential for deformation of the part and to ensure, not just a fully dense part, but a part matching closest to the required geometry. This manufactured part shown in Figure 4.18, also used the principle of Osakada and Shiomi, whereby the scan speed was increased, which resulted in a reduction in laser power during the process to prevent deformation as a result of temperature gradients causing overly high stress levels in the material.

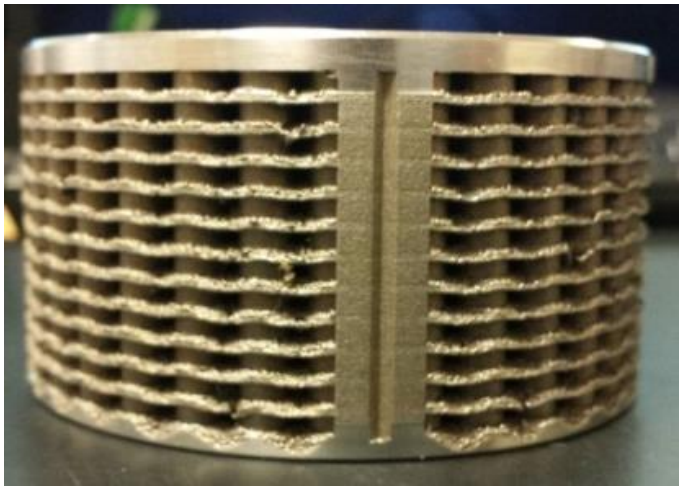

Figure 4.18 XLO8-040 New process Conditions

As can be seen from the results of build time, the new process parameters used resulted in a significant increase in production time over the other three parts produced, 35 hours compared to 16 and 14 for the other three builds. All three parts showed high values for density, with the part produced using the M1 laser the densest, possibly as a result of the much smaller layer thickness value. This low value for layer thickness is a principle reason why the build rate was much slower compared to the other builds as nearly double the number of layers were required. The hatch distance was also much smaller for the new process parameters, meaning that many more lines of spots/features were being applied, this would have also meant that the part produced would be denser.

Unfortunately surface roughness parameters have not been measured for all of these parts, as the trim shown in figure 4.18 (the original design with new conditions) was a one off production sample which could not be destroyed as was required for further testing. The quality of parts could not be immediately determined, as the part cannot be disassembled or undergo internal geometry inspection without destroying the part. However as discussed previously (see figure 4.10), various deformities were evident with version 5.0, whereby the part was not concentric and had slipped during manufacturing. The other two parts i.e. v5.2

and original design XLO8-040-new process, produced a much better overall structure as can be seen in figure 4.18, and for V5.2 in figure 4.15. Due to the structure of these parts been sufficient, they could then undergo final machining and be flow tested in accordance with Chapter 3, whereas the part produced to design V5.0 was not selected for flow testing. The valve used was the same valve design used by Asim [31] in previous comparative tests between SLM and EDM and as such all other internal parts (Seat, Cage and Plug) were the same. This ensures that the effect of the seat and the body on the overall Cv can be assumed constant and will provide a better comparison for the results.

4.5 Recorded Test Data

The 100mm valve (As per the datasheet shown in Chapter 3) was installed in the flow loop at the university to undergo capacity testing to determine the valve flow co-efficient (Cv), testing would be performed in accordance with IEC 60534-2-3 and results would be recorded in accordance with this standard. The results from the capacity testing using the flow loop have been collated and included as Appendix 3 of this study. The results at each percentage opening were taken at a variety of pump speeds, which was controlled by a variable speed drive invertor.

Units for the recorded data are as follows;

Q – Volumetric Flow Rate – m^3/hr
P – Inlet Pressure – Bar(g)
ΔP – Differential Pressure - Bar
T_1 – Fluid Temperature (Measured downstream of the valve) – Degrees C

Each flow rate value was recorded over a 20 second time interval as the flow meter value fluctuated regularly. This enabled an average for flow rate to be calculated. All three results were recorded automatically by a data logging device. The value of T_1 is recorded so that more accurate values of density can be interpolated for water from steam tables. Typical flow tests in accordance with the international standard IEC 60534-4 also use this for the calculation of F_L (pressure recovery for the valve), however this has not been calculated for this test, as flow was not choked within the test setup.

Table 4.1 Complete details of process parameters used, including image of each model below

	Original SLM Trim Test	Original Design - New Process	Version 5.0	Version 5.2
Density	99.80%	99.90%	99.60%	99.80%
Layer Thickness	50 Microns	30 Microns	50 Microns	50 Microns
Feature Size	200 Microns	180 Microns	40 Microns	40 Microns
Laser Spot Size	100 Microns	90 Microns	20 Microns	20 Microns
Hatch Distance	0.013mm	80 Microns	0.01mm	0.01mm
Point Distance	50 Microns	30 Microns	50 Microns	50 Microns
Laser Power	120W	200W & 90W*	80W	120W
Exposure Time	220 Micro Seconds	150 Micro Seconds	200 Micro Seconds	200 Micro Seconds
Overall Production Time	16 Hours	35 Hours	16 Hours	14 Hours
Machine Used	Renishaw ALM 250	M1 Concept Laser 200W	Realizer SLM 100	Realizer SLM 100


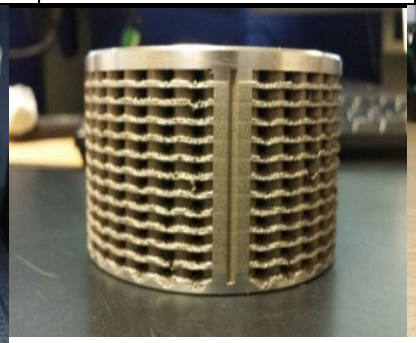
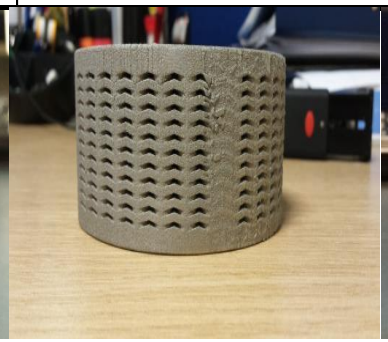


4.5.1 Flow Loop Set-Up

The flow loop was set up in accordance with details laid out in Chapter 3.1. The valve was operated by a 100ins^2 diaphragm actuator which was fed with a 4bar(g) air supply. The actuator was fitted with an air filter regulator to regulate air pressure to the valve positioner. The positioner, a Siemens PS2, controls the actuator via a 4-20mA signal, usually from a plant controlling system. For the purposes of this test program the 4-20mA signal was provided via a small handheld device, (figure 4.19). This device connects directly to the positioner and can send mA signals with 0.01mA accuracy. As the actuator was setup in the air failed closed position (Its inherent safety function) an increasing signal tends to open the valve. In this case a simple signal of 8mA moves the valve to 25% open, 12mA to 50% open and the full signal of 20mA fully opens the valve.

Figure 4.19 4-20mA controlling device

4.6 Analysis of Recorded Test Data

The results obtained can now be collated, converted to standard units (defined by the international standards) and tabulated to calculate the values of Cv (For the valve), Cv_{Trim} and K_{Trim}, using the equations 3.1 - 3.6 in Chapter 3. Factors F_p and F_R are both set at one for the purpose of Cv calculation. This is because the valve has not been installed with attached fittings. The pipe is a 100mm PN16 pipe and the valve bore matches this. F_R the correction for Reynolds number is as stated during chapter 3, not applicable as flow rates and fluid viscosity are not low enough for the flow to be laminar through the valve.

The units of measure have been changed, for the purpose of this table, into standard SI units. The column N_1 is the conversion unit provided in IEC 60534-2-1 for the use of metric units when

determining Cv. As discussed above, ρ/ρ_o is the ratio of density of the fluid against the standard for water at 60ºF (15.5ºC). Table 4.2 contains the results for the original design X-Stream, manufactured using the optimised process parameters and table 4.3 shows the results for the new design XLO8-040 Version 5.2. Body and seat Cv's for both valves are the same and are based on the areas as shown in table 3.1. The K factor used for the body was 24 (Determined previously via empirical testing) and the seat K factor is 38. Both body and Seat K factors are unaffected by changes in valve opening position so will remain constant throughout the test.

Table 4.2 Full Cv and K for XLO8-040 Original design with new process parameters

Valve Opening Position (%)	**Variable Drive Speed (%)**	**Q (m^3/hr)**	**ΔP (kPa)**	**Cv_{Total}**	**Cv_{Body}**	**Cv_{Seat}**	**Cv_{Trim}**	**K_{Trim}**
100	75	38.4	287	26.2	301.6	65	28.7	45.5
	38	19.3	73	26.0	301.6	65	28.5	45.3
	10	6.0	7	26.0	301.6	65	28.5	45.3
75	75	30.2	288	20.6	301.6	65	21.8	46.0
	38	14.9	73	20.2	301.6	65	21.3	45.0
	10	4.7	7	20.6	301.6	65	21.8	46.2
50	75	20.7	291	14.0	301.6	65	14.4	45.6
	38	10.5	75	14.0	301.6	65	14.4	45.6
	10	3.2	7	14.1	301.6	65	14.5	46.0
25	75	12.0	296	8.1	301.6	65	8.1	51.6
	38	6.0	73	8.1	301.6	65	8.1	51.7
	10	1.8	7	7.9	301.6	65	8.0	50.8

Table 4. 3 Full Cv and K Calculations for V5.2 new design

Valve Opening Position (%)	**Variable Drive Speed (%)**	**Q (m^3/hr)**	**ΔP (kPa)**	**Cv_{Total}**	**Cv_{Body}**	**Cv_{Seat}**	**Cv_{Trim}**	**K_{Trim}**
100	75	34.5	287	23.5	301.6	65	25.3	48.3
	38	17.4	73	23.5	301.6	65	25.3	48.2
	10	5.2	6.7	23.4	301.6	65	25.1	47.9
75	75	25.8	278	17.8	301.6	65	18.6	47.2
	38	13.2	72	18	301.6	65	18.7	47.6

	10	4	6.7	17.9	301.6	65	18.7	47.5
50	75	17.9	286	12.2	301.6	65	12.5	47.5
	38	8.8	70	12.1	301.6	65	12.4	47.1
	10	2.7	6.4	12.1	301.6	65	12.4	47.1
25	75	10.2	293	6.9	301.6	65	6.9	52.6
	38	4.7	67	6.7	301.6	65	6.7	51.1
	10	1.2	4.5	6.6	301.6	65	6.6	50.5

Analysing the results presented in Table 4.2, Figure 4.20 depicts the variations in Cv_{Trim} at various valve opening positions for the three flow conditions on which the tests were performed. It can be seen that as the valve opening position increases, Cv_{Trim} increases. The increase in Cv_{Trim} with regards to the valve opening position is almost fully linear. Furthermore, it can also be seen in the Figure that for various flow conditions, Cv_{Trim} is nearly constant at a specific valve opening position. Hence, Cv_{Trim} is a function of valve opening position, but is independent of flow conditions.

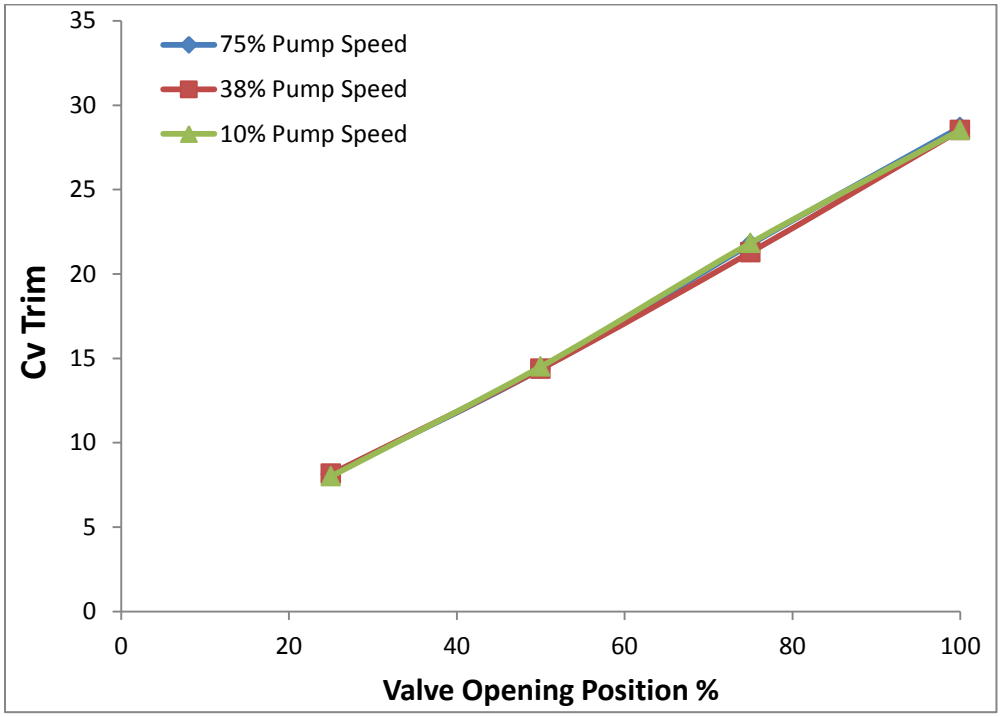

Figure 4.20 Cv_{Trim} against valve opening position for Original Design XLO8-040 with new process parameters

The interesting part of the results is the K factor values that have been calculated from the effective area of the disc stack. As shown in Table 4.2, the values for K have remained very similar to the original design that included the shroud on the outer diameter (as discussed in

section 4.2). The original design, manufactured using the original method, resulted in a Cv_{Trim} value of 26.6, and when considering that this part was made up of 44 flow paths (11 discs, 4 paths per disc), it is clear that this is less than the 48 paths used for this part 912 discs, 4 paths per disc). As such the almost linear increase in value for Cv_{Trim} would suggest that the value of Cv_{Trim} would increase by a factor of 48/44 (approximately 1.09). This would result in a predicted Cv_{Trim} value of 29.02, for a matching sized trim. Therefore, the improvement for a set of optimised process parameters has had a negligible effect on the performance characteristics of the trim, where purely Cv_{Trim} and Trim K Factor have been concerned.

Values for K are not constant and actually show a minimum value at 100% of valve travel. This however can be attributed to the annular clearance between the plug and the trim. As the valve moves more open the K factor is reducing, this is because the effect of annular flow (Flow up the annular clearance between the plug and stack) is reduced when the plug is providing least resistance to fluid flow. No effect of annular area and thus annular Cv have been considered to modify values for K as due to the nature of the trim quality, exact values may not be achievable and as such only estimates for annular area could be predicted. Figure 4.21, again shows the variations in Cv_{Trim} at various valve openings, this time for version 5.2 trim (results displayed in table 4.3). Similar to the results for the optimised process on the original trim, the trend is showing an almost fully linear increase of Cv_{Trim} with respect to VOP and that again this effect is constant independent of process conditions.

Analysis of the K Factor values for this trim, have shown a slight increase compared to the original design (with original process parameters) an increase of 5% and 6.15% compared to with optimised process parameters. However as mentioned in section 4.3, this design is actually not of the full stack height due to an error with the way that end plates of the stack were extruded. As such there is a reduction in flow paths to 40 for this trim design; which had been taken into account for the formulation of values for K.

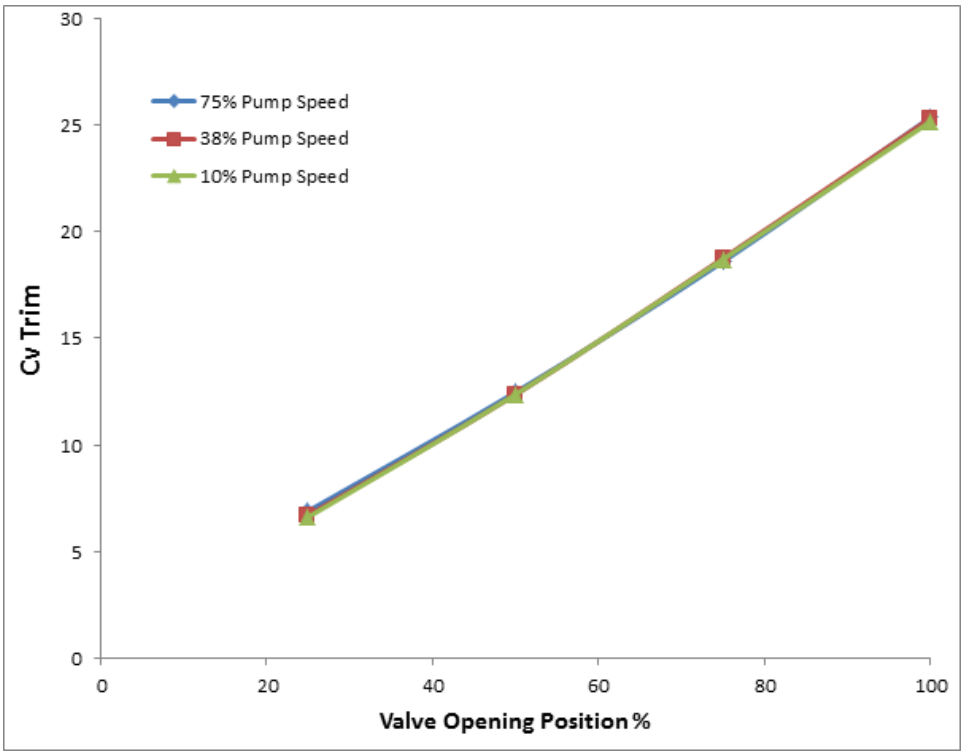

Figure 4.21 Cv_{Trim} against valve opening position for V5.2

This reduction in overall flow area now explains the reduction in values of Cv_{Trim} which are 13.4% lower than that for the other trim tested (results of table 4.3) and 5.14% lower than the original design using the original process parameters. The reduction in area means that Version 5.2 has 40 flow paths compared to 48 for the other trim tested and 44 for the original tested trim. A reduction of 20% and 10% in flow areas respectively has been observed. As the trend is showing an almost fully linear increase in Cv_{Trim} against VOP, for the basis of analysis, comparable results have been estimated assuming a full 48 flow path trim, by applying an increase in value for flow rate at 75% pump speed, all other factors (pressure drop, temperature etc.) have been assumed to be the same as originally recorded; results are shown in table 4.4

Table 4.4 Amended Flow Rate values for Version 5.2

Valve Opening Position (%)	**Variable Drive Speed (%)**	**Q (m^3/hr)**	**ΔP (kPa)**	**Cv_{Total}**	**Cv_{Body}**	**Cv_{Seat}**	**Cv_{Trim}**	**K_{Trim}**
100	75	41.40	287.00	28.30	301.60	65.00	31.50	50.10

Assuming a linear increase in flow rate (to 41.4m^3/hr), for a stack comprised of 48 paths, now results in an overall valve Cv of 28.3, corresponding to a Cv_{Trim} value of 31.5 and a revised K

value of 50.1. Thus for a comparable number of flow paths (or comparable effective area of the trim) the new design trim, using existing process parameters, results in an increase in like for like Cv_{Trim} value of 18.42% against the original test values and an increase of 9.7% compared to the same design when optimising the process of manufacture alone.

4.7 Summary

Selective Layer Melting (SLM) has been used in this chapter to produce two different X-Stream trim models. Although the surface roughness of the models seems to have increased significantly by using this manufacturing method, the cost of the manufacturing has reduced substantially. These trim models have been flow tested and the results presented in this chapter. Flow tests clearly show the variations in the global performance parameters (such as Cv) between the trim models considered for testing, however a local flow field analysis is not possible using experimental methods. Hence, illustrative Computational Fluid Dynamics (CFD) based investigations on the flow structures within these trim models has been carried out in the next chapter. Furthermore, the effect of the manufacturing method on the performance characteristics of the trims, in terms of average roughness height and surface uniformity, has been discussed in detail in the next chapter.

CHAPTER # 5
NUMERICAL ANALYSIS OF THE MANUFACTURED TRIMS

This chapter looks at the second research aim of completing numerical testing of new designs using different manufacturing methods. The testing focuses on the changes to the performance characteristics for trims with hydro-dynamically smooth surfaces against trims with applied uniform surface roughness and also non uniform roughness. Contours of static pressure and velocity are reviewed to ascertain the effects of geometric features on the performance of the trims.

5.1 Introduction

As mentioned in chapter 4, five designs have been created and the reasoning for various features has been discussed. It was intended that all five designs were to undergo both experimental and numerical testing, however as discussed in chapter 4, it has only been possible to manufacture three trims in total and have successfully tested two of them.

Different manufacturing processes generate different surface patterns on the trim models. Hence, the surface roughness height and surface uniformity needs to be considered in the present study for accurate prediction of the performance characteristics of the trims. Asim [13] reported that EDM manufacturing process generally prints an average surface roughness height of around 100μm on the trim surfaces, whereas SLM manufacturing method prints an average surface roughness height of around 1000μm. Hence, the trim models generated using different manufacturing methods leave different roughness characteristics on the trim surfaces. In order to compare the performance characteristics of the trim models manufactured using both the aforementioned manufacturing methods, average surface roughness heights of 100μm and 1000μm have been generated on the trim models. These trim models have then been numerically tested, and the results compared against each other in order to quantify the effectiveness of each manufacturing method. Similar approach has been used to quantify the effects of surface uniformity, where a value of 0.5 ensures a uniformly textured surface, and a value of 1 ensures an irregularly textured surface have been analysed for the effect on liquid flow within the trim, when various surface roughness parameters are applied to the trims.

The five trims that have been analysed are;

- XLO8-040 SLM V4.1
- XLO8-040 SLM V4.2
- XLO8-040 SLM V5.0
- XLO8-040 SLM V5.1
- XLO8-040 SLM V5.2

The chapter has been split into five main sections to suitably structure the analysis on each trim design for each variable. Starting with an analysis on all five trim designs using hydraulically smooth walls, analysing the effect on capacity for the varied geometry, before moving onto vary surface roughness (Epsilon) and then vary the uniformity of the roughness. Each section will begin by reviewing the velocity and static pressure contours, showing variation on these parameters for each varied feature of roughness and uniformity. This qualitative analysis will analyse the effect of geometry changes on the potential areas (within the trim) that could suffer from high resistance, cavitation and erosion.

Mass flow rate and thus Cv_{Trim} have been predicted using CFD for each of these scenarios at three different pressure conditions of 25, 50 and 100Bars of differential pressure. It is vital to test the X-Streams at higher pressures; because in real world applications, these trims are used in severe service applications/conditions, and hence their rigorous high pressure testing is extremely important to establish whether their capacity remains the same at higher pressure or not and whether it remains the same when the surface roughness parameters are varied. Section 5.2 will show these contours for all five trim designs. The design showing the most optimal results, will then be analysed further for the variance of surface roughness and uniformity.

5.2 Validation of Numerical Results

One of the most important steps while conducting numerical studies is the benchmarking of the results. This means that some of the results obtained from the numerical simulations are compared against experimental findings to confidently authorise that the numerical model represents the physical model of the real world. Hence, all the geometric, flow and solver-related parameters/variables become important in benchmarking studies.

For the present study, the numerical model has been validated against the experimental findings for the performance characteristics (Cv and k) of the trim version 5.2. This version of the trim has been chosen for validation purposes because it is the only trim model that has been tested both experimentally and numerically. Table 5.1 presents the operating conditions and the results for the validation purposes. It can be seen that the CFD results are in close agreement with the experimental results, with an average variation of less than 10%. It can thus be concluded that the numerical model considered in the present study does represent the physical model of a severe service control valve with an X-Stream trim installed within it.

Table 5.1 Validation of the numerical results

	Units	**Value**
Valve Opening Position	(%)	100
ΔP across the valve	(bar)	2.87
Q (Exp.)	(m^3/hr)	34.5
Q (CFD)	(m^3/hr)	37.3
Diff. in Q w.r.t. Exp.	(%)	8.12
C_{vTrim} (Exp.)	(-)	25.3
C_{vTrim} (CFD)	(-)	27.2
Diff. in C_{vTrim} w.r.t. Exp.	(%)	7.51
k_{Trim} (Exp.)	(-)	48.3
k_{Trim} (CFD)	(-)	51.8
Diff. in k_{Trim} w.r.t. Exp.	(%)	7.25

5.3 Analysis of Velocity and Pressure Contours for Smooth Walls

The five designs that have been created, have sufficiently different geometry from the original design XLO8-040, that the impact of these design changes must be reviewed for each trim. The performance characteristics of the trim, specifically the qualitative values of velocity and static pressure must be analysed to understand how these design changes will affect the basic, but required, function of the X-Stream. Each design of trim will be analysed to identify potential areas for high resistance that could affect the values of Cv_{Trim} and K_{Trim} but also be areas with high potential for erosion and cavitation. The aim of analysis in this format is to identify key geometrical features that could be causing these reductions, to better understand the effects of geometry on Cv.

5.3.1 Version 4.1

In order to analyse the flow structure at a micro level within trim 4.1, pressure and velocity variations have been shown in Figures 5.1 and 5.2. The variations in the flow variables have been represented in the form of static pressure and velocity magnitude contours, where the units of static pressure are psi and that of velocity magnitude are m/sec.

Figure 5.1 depicts the variations in the static pressure of water for a differential pressure of 100bar and at a valve opening position of 100%. Both, full and zoomed in views of the trim have been shown in figure 5.1 As all the trims used for incompressible flow analysis are flow over trims, the flow in Figure 5.1(a) and 5.1(b) is inwards. It can be seen in Figure 5.1 that the inlet section has high pressure compared to the outlet section. It can be further seen in Figure 5.1 that pressure drops within the trim, and from one stage to another. As water passes between two cylinders, due to an area reduction the pressure drops. As water exits a row and enters another one, due to increase in area available for the flow, pressure increases again, this is called pressure recovery and is categorised by the control valve industry as F_L.

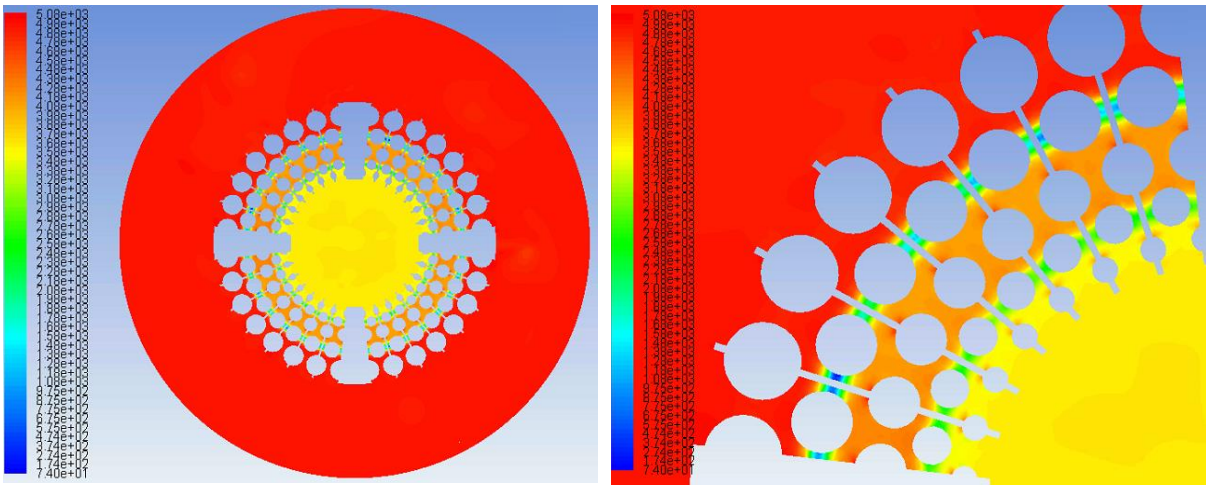

Figure 5.1 Variations in Static Pressure (Hydrodynamically Smooth Walls)

Typically the recovery of pressure between stages of pressure reduction is of great importance to the control valve manufacturer, however it is evident from figure 5.1 that there are areas of very low static pressure on the second row of columns, such that the pressure drops to a minimum of just 74psi, which represents a local pressure reduction from the inlet of the trim of about 5000psi, followed by a pressure recovery at the entrance to the third row of columns of 4400psi. This value of pressure recovery is extremely high. Although not visible on this angle view, the areas of these low static pressures are located in the area between the discs, shown again by the red circles in Figure 5.2

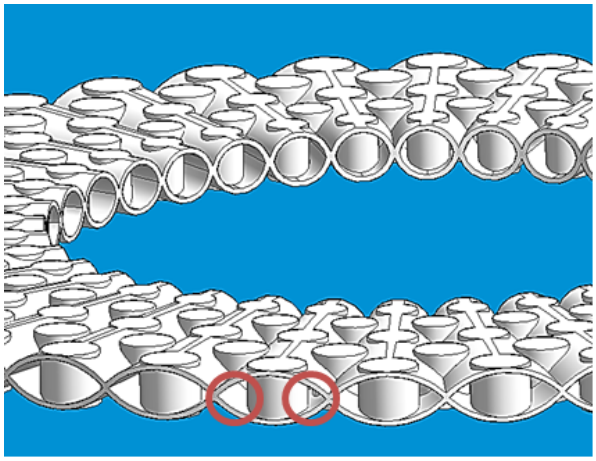

Figure 5.2 Areas of Re-Circulation

It is at these points that the area is at its lowest with a minimum gap feature of just 0.25mm. Of further interest to this analysis of static pressure contours is the apparent non-linearity of the pressure drop across the trim. Each of the flow paths around the columns are geometrically identical, however the minimum static pressure is not uniform across the second row of columns shown on the right hand view of figure 5.1. Figure 5.3 depicts the variations in the flow velocity

within Version 4.1 trim stack at 100% valve opening position. It can be seen in Figure 5.2 that flow velocity is significantly higher in the discharge section of the trim as compared to the inlet section. Furthermore, in Figure 5.2, it can be seen that the flow velocity increases between the cylinders of a row, where the area available for the flow to take place is reduced, hence forming jet effects. As water exits a row and enters another one, due to area increase, velocity reduces to satisfy continuity.

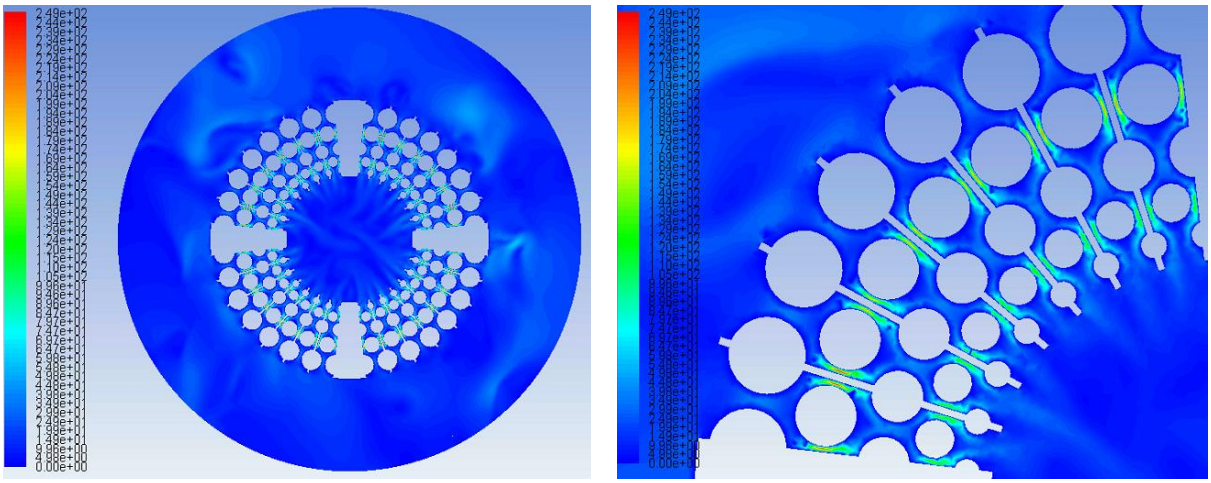

Figure 5.3 Variations in Velocity (Hydrodynamically Smooth Walls)

Likewise with figure 5.1, there are areas of peak velocity at the area between the columns on row 2 and also on the fourth row of columns. To satisfy continuity the velocity has increased with the reduction in pressure at this point, with peak values approaching 249m/s. This increase in velocity at these points will significantly increase the potential for erosion within these areas, as well as a significant potential for the onset of cavitation, whereby the static pressure of the fluid could drop below the vapour pressure of the fluid in some instances. Interestingly there are little areas of re-circulating flow shown behind the columns, which appeared more evident in the early research by Morton. However this could be as a result of further development on column spacing to reduce this potential. Figure 5.3 does show areas of lower velocity around the back of the columns on the second and fourth rows which would indicate a lower static pressure, although that feature is not easily visible in figure 5.1.

The non-uniformity of static pressure shown in Figure 5.1 does not seem as evident on the velocity contours shown in figure 5.3. There is the peak in velocity at the same point on the second row of columns but appears to show a more uniform profile than that of static pressure.

5.3.2 Version 4.2

In order to analyse the flow structure at a micro level within trim 4.2, pressure and velocity variations have been shown in Figures 5.4 and 5.5. The variations in the flow variables have been represented in the form of static pressure and velocity magnitude contours, where the units of static pressure are psi and that of velocity magnitude are m/sec.

Figure 5.4 depicts the variations in the static pressure of water for a differential pressure of 100bar and at a valve opening position of 100%. Both, full and zoomed in views of the trim have been shown in figure 5.4 As all the trims used for incompressible flow analysis are flow over trims, the flow in Figure 5.4(a) and 5.4(b) is inwards. It can be seen in Figure 5.4 that the inlet section has high pressure compared to the outlet section. It can be further seen in Figure 5.4 that pressure drops within the trim, and from one stage to another. As with V4.1, water passes between two cylinders, due to an area reduction the pressure drops.

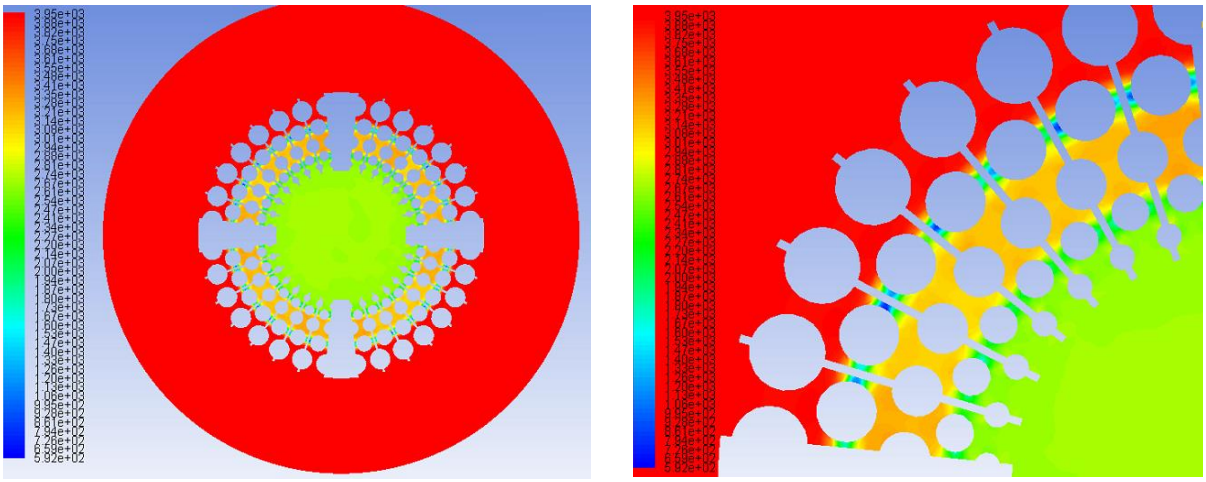

Figure 5.4 Variations in Static Pressure (Hydrodynamically Smooth Walls)

Similarly with V4.1, there are areas of relatively low static pressure between the columns on the second and fourth rows of columns. The second row minimum static pressure is just 592psi; although this is a significant improvement on the like for like section of V4.1 this still means that the pressure recovery at this point is almost 2500psi following the reduction between the columns and prior to the next stage of pressure reduction turning around the third row. As with V4.1 this low pressure region occurs as fluid flows through the disc. The subsequent pressure recovery following the pressure recovery on the fourth row of columns is to a similar level, which is indicative of the similar small area region at this point. Although as the area is increasing to reduce the velocity of the fluid the pressure drop in this region is lower and as such so is the pressure recovery. This, as it would with V4.1, will increase the potential for cavitation somewhat at this area, which is not shown on this model as the outlet pressure from the trim is

considerably higher than vapour pressure from the fluid, which would be approximately 0.4psi for the temperatures used.

Although these process conditions would not result in cavitation of the valve it is evident that the pressure recovery could lead to potential for cavitation to occur in these regions when dealing with applications where the outlet pressure is much closer to the vapour pressure, which are typically applications requiring the use of Severe service trim designs like X-Stream. As with V4.1, there is non-uniformity to the static pressure across the second row of columns, resulting in the large pressure recovery areas slightly off the centre of the disc. Figure 5.5 depicts the variations in the flow velocity within Version 4.2 trim stack at 100% valve opening position. It can be seen in Figure 5.5 that flow velocity is significantly higher in the discharge section of the trim as compared to the inlet section. Furthermore, in Figure 5.5, it can be seen that the flow velocity increases between the cylinders of a row, where the area available for the flow to take place is reduced, hence forming jet effects.

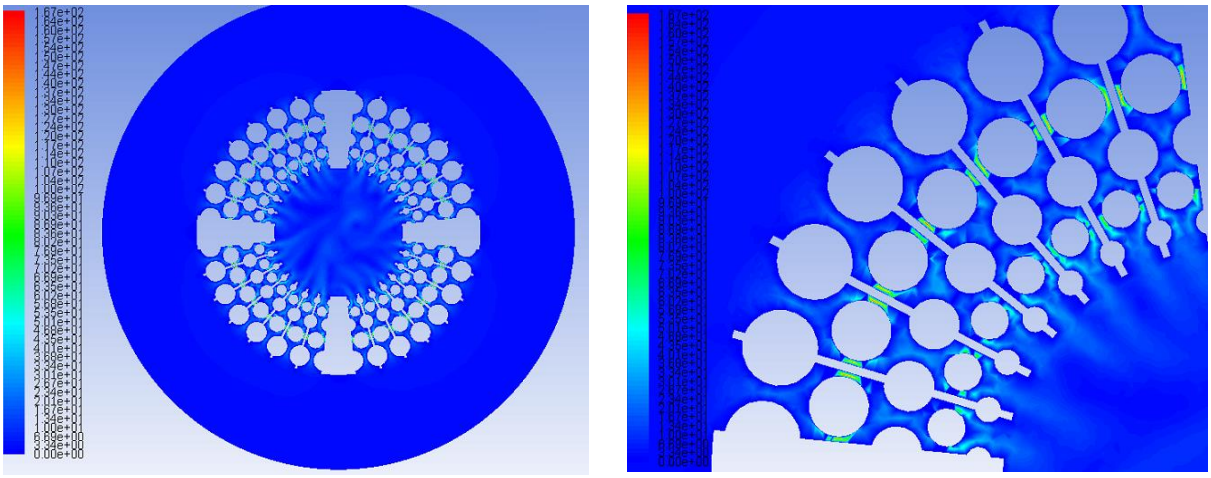

Figure 5.5 Velocity Variations (Hydrodynamically Smooth Walls)

Likewise with figure 5.3, there are areas of peak velocity at the area between the columns on row 2 and also on the fourth row of columns. To satisfy continuity the velocity has increased with the reduction in pressure at this point, with peak values approaching 170m/s. This increase in velocity at these points will significantly increase the potential for erosion within these areas, as well as a significant potential for the onset of cavitation, whereby the static pressure of the fluid could drop below the vapour pressure of the fluid in some instances. As with V4.1 there are few areas of re-circulating flow behind the columns for V4.2 Figure 5.5 does show areas of lower velocity around the side of the columns on the second and fourth rows which would indicate a lower static pressure, although that feature is not easily visible in figure 5.5

It would appear that there is significantly lower maximum velocity for V4.2 when compared to V4.1 indicating an improvement with the removal of the ridge section from V4.1. However there

does appear to be an area on the fourth row where the velocity is at a minimum between the columns in the middle section of the trim (Shown slightly better, on the right hand view of figure 5.5). Velocity does not appear to be uniform across this section of the stack, which does seem to fit with the non-uniformity of the contours of static pressure and the apparent non uniformity of V4.1. Generally the trim seems to perform better for velocity and pressure control over V4.1, but is not providing sufficient control compared to the original design. Again the features possible with SLM, applied to V4.2 design as discussed in chapter 4, have only reduced the performance characteristics of the standard X-Stream trim.

5.3.3 Version 5.0

In order to analyse the flow structure at a micro level within trim 5.1, pressure and velocity variations have been shown in Figures 5.6 and 5.7. The variations in the flow variables have been represented in the form of static pressure and velocity magnitude contours, where the units of static pressure are psi and that of velocity magnitude are m/sec.

Figure 5.6 depicts the variations in the static pressure of water for a differential pressure of 100bar and at a valve opening position of 100%. Both, full and zoomed in views of the trim have been shown in figure 5.6 As all the trims used for incompressible flow analysis are flow over trims, the flow in Figure 5.6(a) and 5.6b) is inwards. It can be seen in Figure 5.6 that the inlet section has high pressure compared to the outlet section. It can be further seen in Figure 5.6 that pressure drops within the trim, and from one stage to another. As with V4.1, water passes between two cylinders, due to an area reduction the pressure drops. As water exits a row and enters another one, due to increase in area available for the flow, pressure increases again, this is called pressure recovery and is categorised by the control valve industry as F_L.

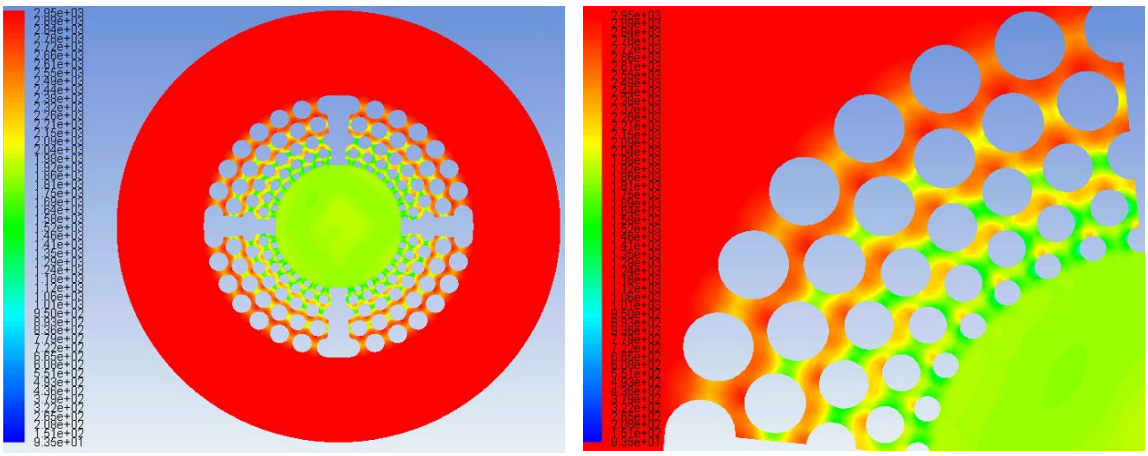

Figure 5.6 –Variations in Static Pressure (Hydrodynamically Smooth Walls)

Similarly with V4.1 and V4.2, there are areas of relatively low static pressure between the columns on the second and fourth rows of columns. The second row minimum static pressure is approximately the same as the outlet pressure of the trim, although this is a significant improvement on the like for like section of V4.1 and V4.2 this still means that the pressure recovery at this point is almost 1000psi following the reduction between the columns and prior to the next stage of pressure reduction turning around the third row.

Unlike with V4.1 and V4.2, this trim design does not have the flow flowing through the disc, but rather reverts to flowing across the top of the disc, much in the same manner as the original design. As such this minimum static pressure area has occurred in the same area as previous CFD analysis has shown for the original design trim, however with much higher values for pressure recovery than would be expected with this design. This, as it would with V4.1, will increase the potential for cavitation somewhat at this area, which is not shown on this model as the outlet pressure from the trim is considerably higher than vapour pressure from the fluid, which would be approximately 0.4psi for the temperatures used. As with V4.2, these process conditions would not result in cavitation of the valve, it is evident that the pressure recovery could lead to potential for cavitation to occur in these regions when dealing with applications where the outlet pressure is much closer to the vapour pressure, which are typically applications requiring the use of Severe service trim designs like X-Stream.

The static pressure looks much more uniform than had been the case with the previous two designs, with no areas of “peaks” i.e. low areas of static pressure occurring a s single point with the trim. Distribution of pressure drop looks linear across each row of columns, which is expected for sections of identical area and geometry. Figure 5.7 depicts the variations in the flow velocity within Version 5.0 trim stack at 100% valve opening position. It can be seen in Figure 5.5 that flow velocity is significantly higher in the discharge section of the trim as compared to the inlet section. Furthermore, in Figure 5.4, it can be seen that the flow velocity increases between the cylinders of a row, where the area available for the flow to take place is reduced, and hence forming jet effects. As water exits a row and enters another one, due to area increase, velocity reduces to satisfy continuity.

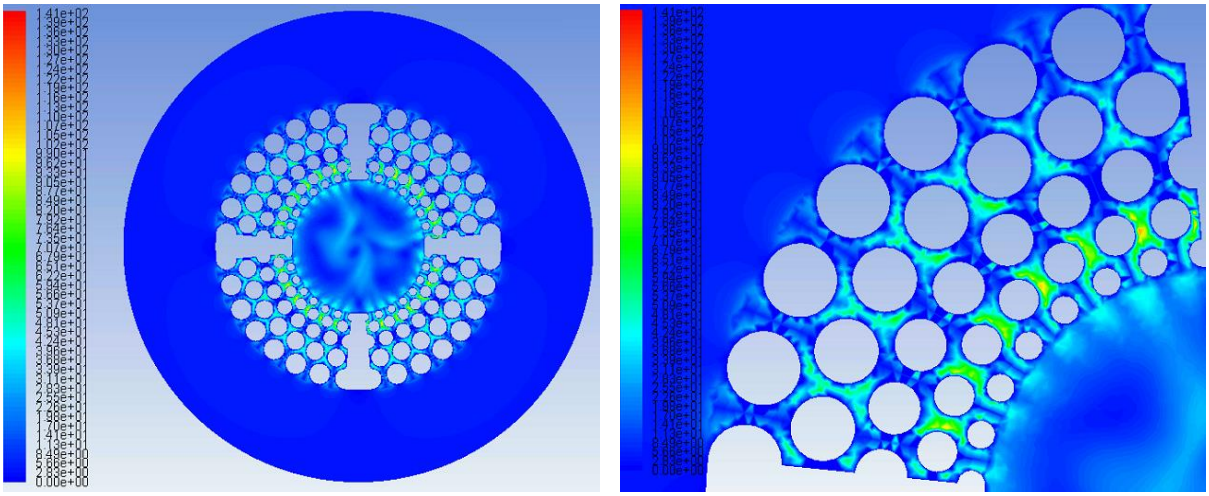

Figure 5.7 Velocity Variations for Hydrodynamically Smooth Walls

Likewise with figure 5.3, there are areas of peak velocity at the area between the columns on row 2 and also on the fourth row of columns. To satisfy continuity the velocity has increased with the reduction in pressure at this point, with peak values approaching 140m/s. This increase in velocity at these points will significantly increase the potential for erosion within these areas, as well as a significant potential for the onset of cavitation, whereby the static pressure of the fluid could drop below the vapour pressure of the fluid in some instances.

It would appear that there is significantly lower maximum velocity for V5.0 when compared to V4.1 and V4.2 indicating an improvement for the change back to the original flow profile of "on top of the surface of the disc". However there does appear to be areas on the fourth row where the velocity peaks significantly. This could be caused by an issue in the angle of the disc (the bottom of the flow path) in this area, which increases from the outlet of the disc inwards due to the naturally reduced area, to allow for the expansion of the fluid. This area is causing a sharper point in the areas between the columns which has increased the flow rate locally. Velocity does appear to be almost uniform across this section of the stack though, which does satisfy this theory, as the static pressure is also uniform at these points also.

Version 5.0 performs significantly better at control of velocity and static pressure than with the previous two designs; however the peak velocities on the fourth row could be an area of concern because this will increase the local erosion potential at an area where the column diameters are reduced and there is less metal for resistance to erosion. The design is also not the optimal from a manufacturing point of view. The trim was unsuccessfully manufactured; the straight edges and reasonably shallow angles do not provide the best attributes for manufacturing using SLM and do not appear to have provided improvements to the performance of the standard X-Stream trim.

5.3.4 Version 5.1

In order to analyse the flow structure at a micro level within trim 5.1, pressure and velocity variations have been shown in Figures 5.8 and 5.10. The variations in the flow variables have been represented in the form of static pressure and velocity magnitude contours, where the units of static pressure are psi and that of velocity magnitude are m/sec.

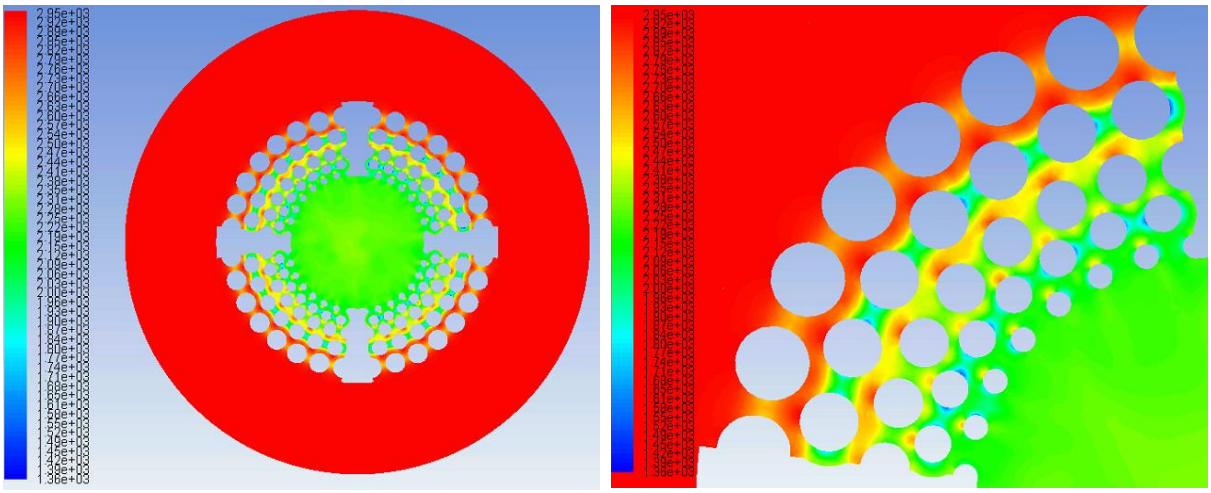

Figure 5.8 Variations in Static Pressure (Hydrodynamically Smooth Walls)

Figure 5.8 depicts the variations in the static pressure of water for a differential pressure of 100bar and at a valve opening position of 100%. Both, full and zoomed in views of the trim have been shown in figure 5.8. As all the trims used for incompressible flow analysis are flow over trims, the flow in Figure 5.8(a) and 5.8b) is inwards.

It can be seen in Figure 5.8 that the inlet section has high pressure compared to the outlet section. It can be further seen in Figure 5.8 that pressure drops within the trim, and from one stage to another. As with V4.1, water passes between two cylinders, due to an area reduction the pressure drops. As water exits a row and enters another one, due to increase in area available for the flow, pressure increases again, this is called pressure recovery and is categorised by the control valve industry as F_L.

Similarly with the previous 3 designs, there are areas of relatively low static pressure between the columns on the second, but with V5.1 this is not the case on the fourth row of columns. The second row minimum static pressure is approximately the same as the outlet pressure of the trim, although this is a significant improvement on the like for like section of V4.1 and V4.2 this still means that the pressure recovery at this point is almost 1000psi following the reduction between the columns and prior to the next stage of pressure reduction turning around the third row.

Version 5.1 does have an area in line with the centre of each column where the area is at a minimum, this appears to have an impact on the static pressure in this region, where the discs join as circled in Figure 5.9. This, as it would with V4.1, will increase the potential for cavitation somewhat at this area, which is not shown on this model as the outlet pressure from the trim is considerably higher than vapour pressure from the fluid, which would be approximately 0.4psi for the temperatures used.

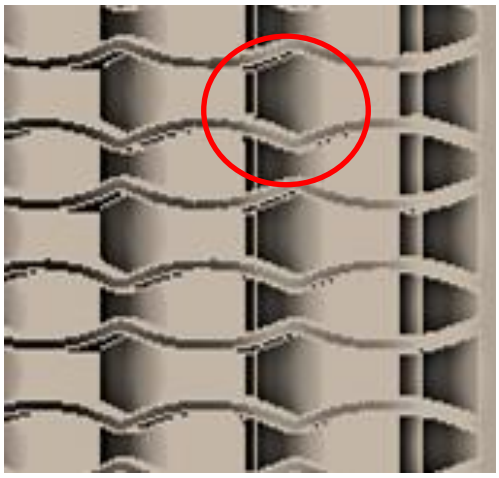

Figure 5.9 Close up of Section for V5.1

As with the other designs, these process conditions would not result in cavitation of the valve, it is evident that the pressure recovery could lead to potential for cavitation to occur in these regions when dealing with applications where the outlet pressure is much closer to the vapour pressure, which are typically applications requiring the use of severe service trim designs like X-Stream. The static pressure again shows uniformity to a much more obvious extent than with V4.1 and V4.2 looks much more uniform than had been the case with the previous two designs, with no areas of "peaks" i.e. low areas of static pressure occurring a s single point with the trim. Distribution of pressure drop looks linear across each row of columns, which is expected for sections of identical area and geometry.

Figure 5.10 depicts the variations in the flow velocity within Version 5.0 trim stack at 100% valve opening position. It can be seen in Figure 5.10 that flow velocity is significantly higher in the discharge section of the trim as compared to the inlet section. Furthermore, in Figure 5.10, it can be seen that the flow velocity increases between the cylinders of a row, where the area available for the flow to take place is reduced, and hence forming jet effects. As water exits a row and enters another one, due to area increase, velocity reduces to satisfy continuity. Likewise with figure 5.3, there are areas of peak velocity at the area between the columns on row 2 and also on the fourth row of columns. To satisfy continuity the velocity has increased with the reduction in pressure at this point, with peak values approaching 130m/s. This increase in velocity at these points will significantly increase the potential for erosion within these areas, as

well as a significant potential for the onset of cavitation, whereby the static pressure of the fluid could drop below the vapour pressure of the fluid in some instances.

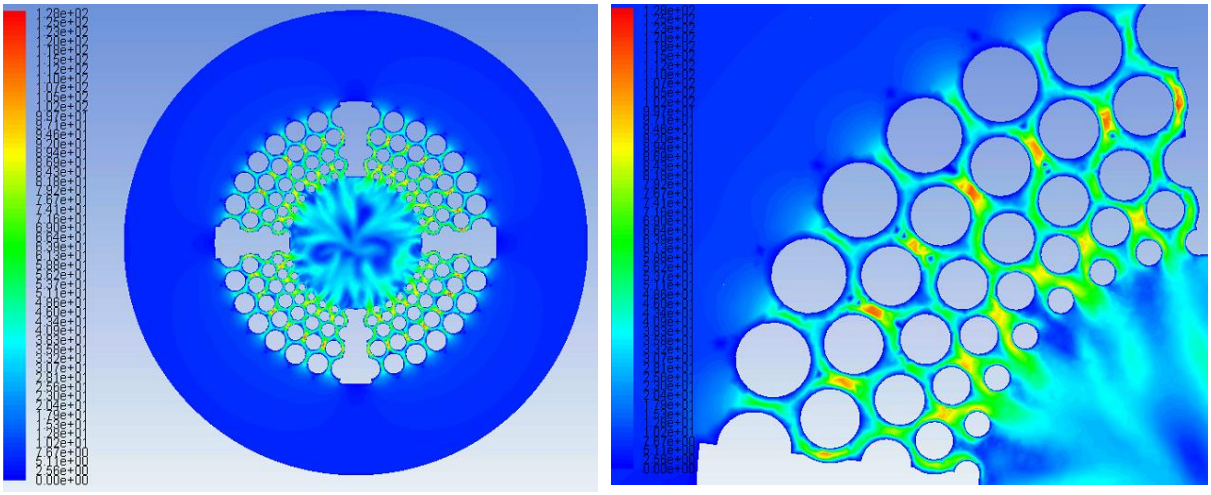

Figure 5.10 Velocity Variations for Hydrodynamically Smooth Walls

It would appear that there is significantly lower maximum velocity for V5.1 when compared to V4.1, V4.2 and V5.0. However there does appear to be areas on the second and fourth rows where the velocity peaks significantly. Again as shown in Figure 5.9, this could be caused as a result of the geometry effect of reducing the area at the circled section. Version 5.1 performs significantly better at control of velocity and static pressure than with the previous 3 designs; however this design is still being out performed in terms of control of velocity by the original design, although it may be possible that reduction in resistance may display an increase in Cv_{Trim} and K_{Trim}, when compared to the original design XLO8-040. The design features discussed in chapter 4 for this trim, with a opposing disc shape construction do benefit the SLM process, but have left minimum gaps between the opposing discs as shown in figure 5.9, removal of these features, may have less effect on the ability to manufacture using SLM but may improve the performance characteristics further.

5.3.5 Version 5.2

The last design, V5.2, has undergone the same micro analysis of the flow structure, where pressure and velocity contours are shown in Figures 5.11 and 5.12. The variations in the flow variables have been represented in the form of static pressure and velocity magnitude contours, where the units of static pressure are psi and that of velocity magnitude are m/sec.

Figure 5.11 depicts the variations in the static pressure of water when using the same boundary conditions as used for V5.1 and at a valve opening position of 100%. Both, full and zoomed in views of the trim have been shown in figure 5.11. As all the trims used for incompressible flow

analysis are flow over trims, the flow in Figure 5.11(a) and 5.11b) is inwards. It can be seen in Figure 5.11 that the inlet section has high pressure compared to the outlet section. It can be further seen in Figure 5.11 that pressure drops within the trim, and from one stage to another. As with V4.1, water passes between two cylinders, due to an area reduction the pressure drops.

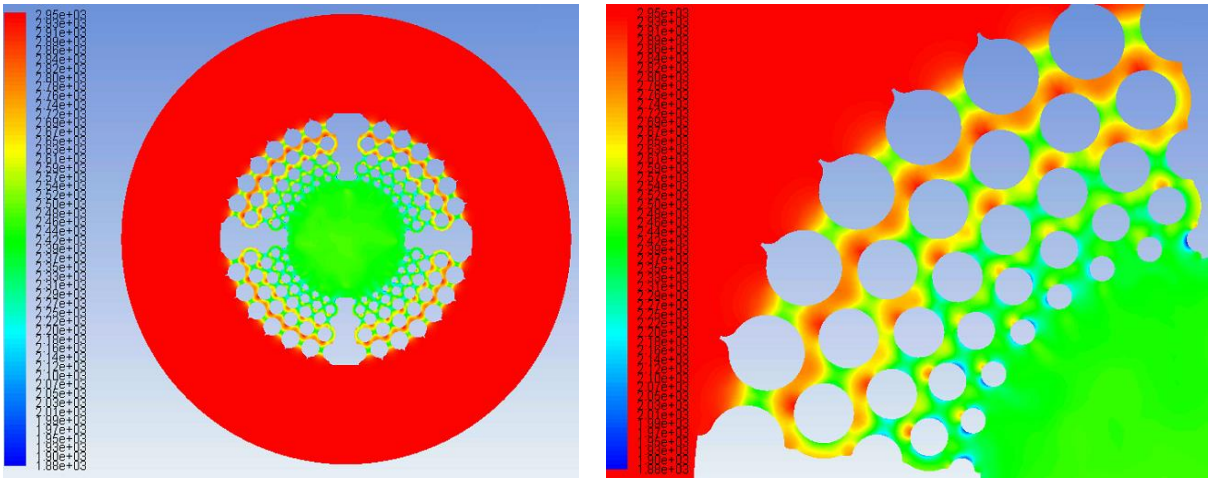

Figure 5.11 Variations in Static Pressure (Hydrodynamically Smooth Walls)

Similarly with the previous 4 designs, there are areas of relatively low static pressure between the columns on the second row, but with V5.2 all the rows are showing a reduction in static pressure between each row of columns, in the same manner as the results for a flow profile through the original disc design. The second row minimum static pressure is approximately the same as it is at the outlet of the trim, although with V5.2 the minimum static pressure at this stage is around 2500psi, meaning that the pressure recovery to the next row is much lower (Approximately 150psi) following the reduction between the columns and prior to the next stage of pressure reduction turning around the third row.

This distribution of pressure is not just uniform in each row, but also across each feature of each row, such that each row of columns has displayed an area of relatively low static pressure at the centre of each column, rather than having each row with differing effects on static pressure. This means that the trim is performing now in much the same manner as the original X-Stream was designed for. Unlike the other designs, the minimum static pressure is controlled to a much better extent, meaning that the potential for cavitation to occur has reduced significantly when compared to the previous 4 designs. There are no sharp features with V5.2 or points on the trim where the area is reducing between walls other than in the controlling regions between the columns, meaning that the columns are causing the restriction to flow rate rather than the top or bottom surfaces of each disc.

Figure 5.12 depicts the variations in the flow velocity within Version 5.2 trim stack at 100% valve opening position. It can be seen in Figure 5.12 that flow velocity is significantly higher in the discharge section of the trim as compared to the inlet section. Furthermore, in Figure 5.12, it can be seen that the flow velocity increases between the cylinders of a row, where the area available for the flow to take place is reduced, hence forming jet effects. As water exits a row and enters another one, due to area increase, velocity reduces to satisfy continuity. Likewise with figure 5.3, there are areas of peak velocity at the area between the columns on row 2 and also on the fourth row of columns; however as with the contours of static pressure, V5.2 also shows the velocity peaking at the gap between columns on each row of columns rather than these two rows.

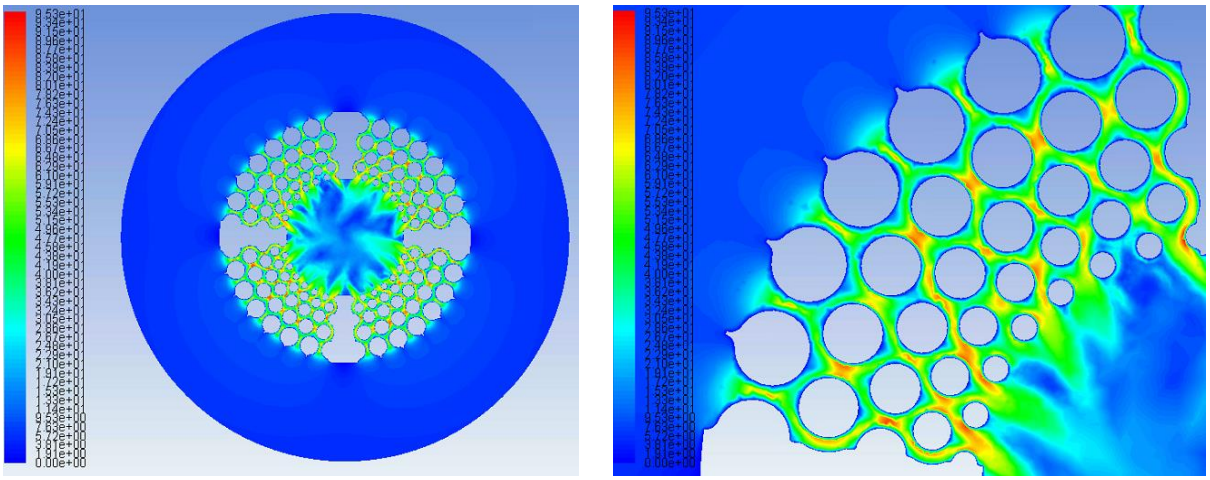

Figure 5.12 Velocity Variations for Hydrodynamically Smooth Walls

The peak velocity within the trim, has actually occurred on the fifth row (outlet row) in the corners bordering the edges of each flow path, with this velocity peak being approximately 94m/s. Peaks between other rows are slightly lower and occur at the areas of minimum static pressure between the columns, around 75-80m/s. As with the other designs the increase in velocity at these points can increase the potential for erosion, however the significant reduction over the previous four designs, means that this potential has also significantly reduced, knowing that the kinetic energy of the fluid reduced with a square relationship of velocity.

Version 5.2 performs significantly better at control of velocity and static pressure than with the previous four designs and has met the same performance criteria of the standard X-Stream design. The removal of small area sections (sharp sections or joining areas) has had a significant effect on the performance characteristics of the trim, providing the most optimal control of velocity and pressure, whilst also meeting the structural/design requirements for manufacture using SLM as discussed during chapter 4.

5.4 Performance Characteristics of X-Stream trims with Hydrodynamically Smooth Walls

Now that a qualitative analysis of pressure and velocity has been completed for each of the five designs, CFD has been used to predict the mass flow rate through each individual trim design at three defined differential pressures. Solver settings maintain hydraulically smooth walls to show principally the effect of the designed geometry for each trim on Cv_{Trim}, Cv_{Total} and K_{Trim}.

As can be seen there is a significant increase in the predicted mass flow rates when the differential pressure increases, but that there is also an increasing trend from the earliest designs to the latest design of V5.2. Mass flow rate remains relatively constant from the geometrically changes between versions 4.1 and 4.2, this however is expected as the change in geometry between these two designs was minimal, especially when compared with geometrically changes with V5.0, 5.1 and 5.2.

Table 5.2 Mass Flow Rate – Hydrodynamically Smooth Walls

ΔP (bar)	Model	m (Kg/sec)
25	4.1	18.56
	4.2	18.45
	5.0	30.91
	5.1	44.45
	5.2	45.99
50	4.1	26.63
	4.2	26.39
	5.0	44.00
	5.1	63.53
	5.2	65.58
100	4.1	37.84
	4.2	37.65
	5.0	62.43
	5.1	90.13
	5.2	92.87

Figure 5.13 graphically presents the increase in mass flow rate for the five different designs with an individual trend line for each differential pressure tested, whereby;

- 1 = V4.1
- 2 = V4.2

- 3 = V5.0
- 4 = V5.1
- 5 = V5.2

Now that the values for the mass flow rate have been predicted, the other parameters can be used to formulate a value for the Cv_{Trim}, Cv_{Total} and K_{Trim} which has been shown for each trim design in Table 5.2 – Using the equations 3.1 - 3.6 in Chapter 3.

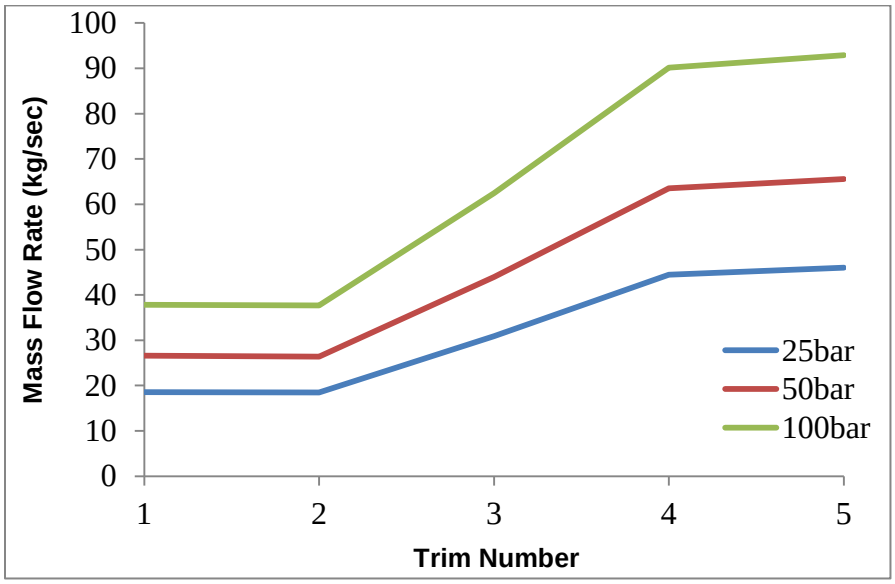

Figure 5.13 Mass Flow Rate through each trim design when considering Hydrodynamically Smooth Walls

Table 5.3 Cv Calculations – Hydrodynamically Smooth Walls

ΔP (bar)	Model	m (Kg/sec)	ΔP (kPa)	$Cv_{(without\ annular)}$	Cv_{Total}	Cv_{Trim}	K_{Trim}
25	4.1	18.56	2499	15.45	15.02	15.46	24.54
	4.2	18.45	2499	15.36	14.93	15.36	24.38
	5	30.91	2499	25.73	25.3	27.58	47.75
	5.1	44.45	2499	37	36.57	44.71	85.16
	5.2	45.99	2499	38.29	37.86	47.12	89.74
50	4.1	26.63	4999	15.68	15.25	15.7	24.93
	4.2	26.39	4999	15.53	15.1	15.55	24.68
	5	44	4999	25.9	25.47	27.8	48.13
	5.1	63.53	4999	37.4	36.97	45.44	86.54
	5.2	65.58	4999	38.6	38.17	47.74	90.92

100	4.1	37.84	9997	15.75	15.32	15.79	25.06
	4.2	37.65	9997	15.67	15.24	15.7	24.92
	5	62.43	9997	25.99	25.56	27.91	48.33
	5.1	90.13	9997	37.52	37.09	45.66	86.96
	5.2	92.87	9997	38.66	38.23	47.84	91.11

The values of the constants F_P, F_R, N_1, specific gravity, Cv_{Body} and Cv_{Seat} remain the same as in experimental test results discussed in Chapter 4, and hence have not been included here, although they have been used to calculate Cv_{Trim}. Moreover, it can be seen in table 5.2 that there is an additional factor of Cv (without annular) included. The reason to include this factor is for better accuracy of the results. It accounts for the Cv value of the annular region between the stack's inner walls and the plug that alters the valve opening position. In experimental tests, this factor is automatically adjusted because of physical testing of the X-Stream trims. However, within CFD environment, this factor needs to be calculated separately and subtracted from the calculated Cv to give Cv_{Total} value. This is because the annular region has not been modelled within CFD, because its size is too small which gives rise to solver instabilities, and also results in highly skewed mesh elements which adversely affects the accuracy of the results. For BV500 control valve, annular clearance Cv can be calculated as:

$$Cv_{\text{Annular Clearance}} = \frac{35\pi}{4} \left(Dmax_{Stack}{}^2 - Dmax_{Plug}{}^2\right) \qquad (5.1)$$

where $Dmax_{Stack}$ and $Dmax_{Plug}$ are the maximum diameters of the stack and the plug. These maximum diameters can be obtained from the drawings of the stack and the plug, in which the tolerances are mentioned. For the valve used in the present study, this factor has been calculated to be equal to 0.43. Hence, 0.43 has been subtracted from the calculated Cv, in order to obtain Cv_{Total} values. The calculated results for Cv_{Trim} and K_{Trim} are also shown in Figures 5.14 and 5.15 respectively, for ease of comparison with the same number designation as for trim design as used in Figure 5.13. It can be seen from the table of results that the these values are reasonably constant for each trim design across the three differential pressures measured, satisfying the derivation of Bernoulli for Cv within control valves. It is also clear that there is a significant increase in Cv_{Trim} and K_{Trim} from the original concept designs of 4.1 and 4.2 to the latest design of 5.2

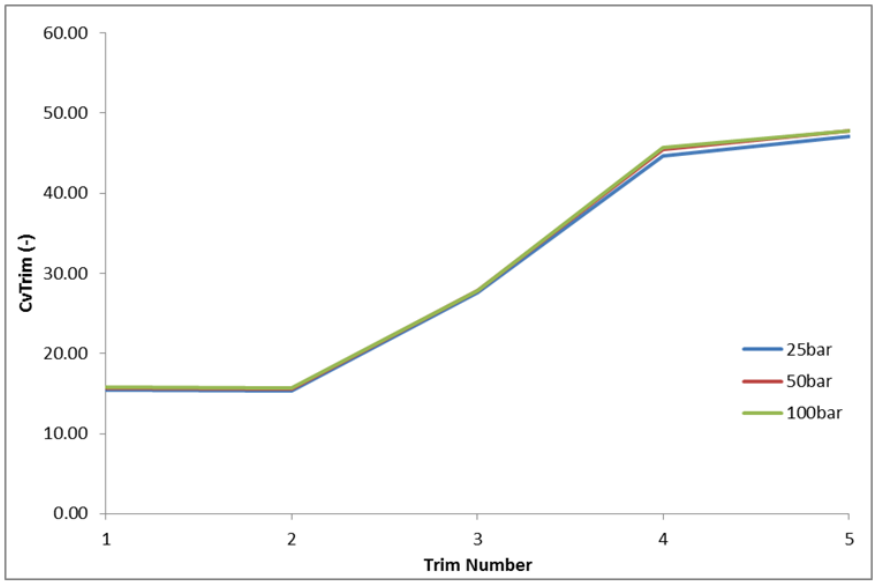

Figure 5.14 Summary of values for Cv_{Trim} for each design for Smooth Walls

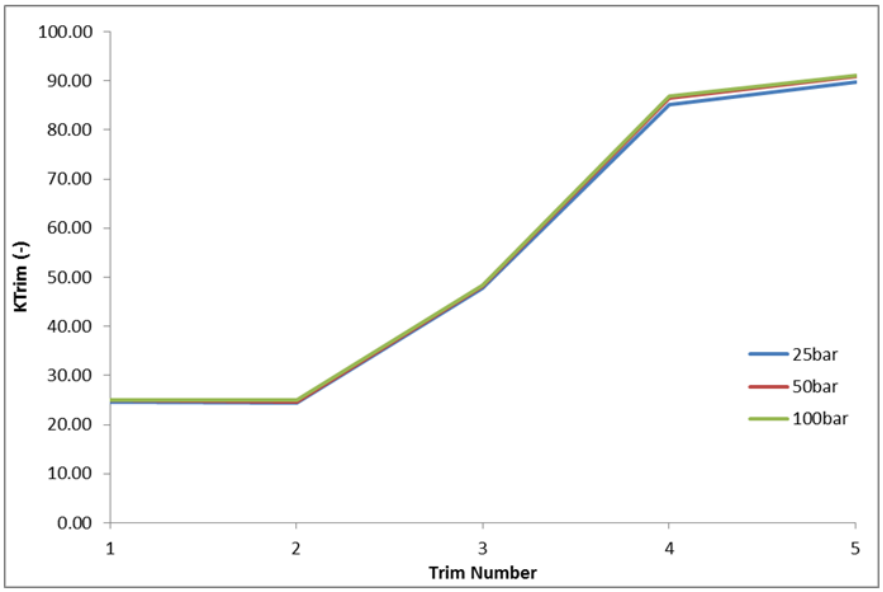

Figure 5.15 Summary of values for K_{Trim} for each design for Smooth Walls

There is a slight reduction in both K_{Trim} and Cv_{Trim} for from Version 4.2 to V4.1, however this is not as surprising as these two trims had only minor geometrical differences to each other. Results for K_{Trim} and Cv_{Trim} are much lower than the standard original design for X-Stream that has been tested previously with smooth walls, by Asim [31]. Their initial testing gave values for Cv_{Trim} and K_{Trim} of approximately 35 and between 62 and 70 respectively. This indicates that the resistance within trims 4.1 and 4.2 is significantly higher than with the original design and that this resistance is purely related to the geometrical changes that have been applied to improve the ability to manufacture the trim using SLM Version 5.0 however has a significant increase in

these values compares to V4.1 and V4.2. The design of the trim is much closer to the original design with the angled flow path representing a similar flow regime across the surface of the disc to that of the original XLO8-040. However the Cv for V5.0 is still lower than the original design was achieving during flow testing of the EDM sample when using smooth walls, so it can be assumed that the geometry changes for SLM have again reduced the performance.

The difference between Version 5 and original is just 21% for a like for like differential pressure for both Cv_{Trim} and K_{Trim}, whereV4.1 differed by almost 56%. Version 5.1 provides a significant improvement on values for Cv_{Trim} and K_{Trim}, increasing to 45 and 86 respectively, an increase from the original design of 27%, with 5.2 showing a further improvement to almost 36% on the original design X-Stream. These two design alterations for SLM have led to improvements compared to the manufactured EDM samples of XLO8-040.

5.5 Effect of Surface Roughness Height on the Performance Characteristics of X-Stream trims

Following the analysis for Cv and other performance characteristics on the five trims designs, it is now vital to see how these trims perform when an average surface roughness is applied to each trim using CFD due to the manufacturing constraints discussed in section 5.1. Two values of surface roughness were applied to each trim, these values were selected following earlier analysis by Asim [31] on the surfaces of a number of SLM samples and EDM samples, these values were 100 and 1000 Microns. CFD has now been used to initially predict the mass flow rate through each individual trim design at the same three defined differential pressures used when working with the smooth wall trims. Solver settings selected firstly 100 microns and then 1000microns to compare the effects of Cv_{Trim}, Cv_{Total} and K_{Trim} against the hydraulically smooth walls.

5.5.1 Roughness of 100 Microns

Figures 5.16 and 5.17 show the micro analysis of the flow structure, for pressure and velocity contours of V5.2 as with previous micro flow analysis the variations in the flow variables have been represented in the form of static pressure and velocity magnitude, where the units of static pressure are psi and that of velocity magnitude are m/sec. It is clear at this stage in the research, that V5.2 is the only trim design that showing suitable results for the both the Cv_{Trim} and also the general performance analysis. The detailed micro analysis performed on the other trim designs has shown that those designs are not suitable at controlling the pressure and velocity through the trim, to an extent, where cavitation and erosion could be a cause for concern depending on the process parameters for which they would be required to work.

Therefore, only V5.2 will undergo the micro analysis of the flow structure for the contours of pressure and velocity, with analysis on the variation of these parameters against the smooth wall contours. Figure 5.16 depicts the variations in the static pressure of water when using the same boundary conditions as used for the smooth wall analysis and at a valve opening position of 100%. Both, full and zoomed in views of the trim have been shown in figure 5.16. As with the analysis on the smooth walled trim, fluid flows from outside to in with this design, reducing pressure as the fluid changes direction and is contracted by flowing around the columns.

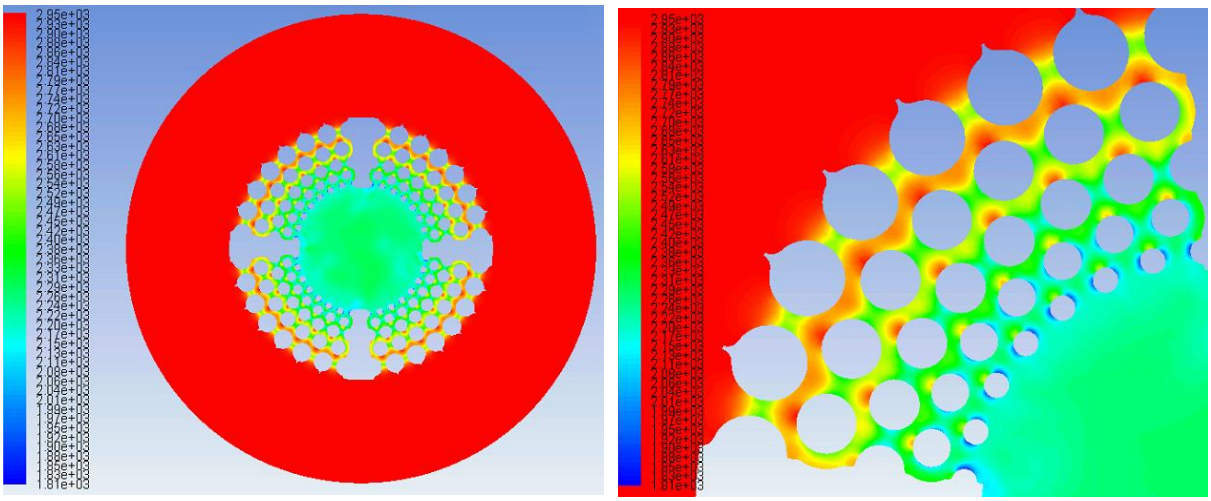

Figure 5.16 Variations in Static Pressure for Uniform Roughness of 100 Microns

As with the smooth walled analysis, there are areas of relatively low static pressure between the columns on the second row, but with V5.2 all the rows are showing a reduction in static pressure between each row of columns, in the same manner as the results for a flow profile through the original disc design and the smooth walled analysis. Static pressure is showing a much better uniform distribution than had been seen on the smoothed wall analysis. There are areas of minimum static pressure on the side walls of each of the columns on the outlet row of the disc, at a minimum value of 1800psi, which in this instance would not be a potential area for cavitation. This is region is not seen to the same extent on the earlier rows due to the presence and spacing of a following row, with row 5 the fluid is free to flow into an open area after this row of columns and promotes the separation of the fluid from the wall of the column in this region.

However it is a relatively low drop at this point, further review of the effect of the valve outlet section, which has not been included in this analysis, may provide a better understanding on the potential issues in this region. A further geometric change to V5.2 to include the addition of an aerofoil shape on the outlet column may prevent separation of the fluid on this outlet row to increase the minimum static pressure at this point. Figure 5.17 depicts the variations in the flow velocity within Version 5.2 trim stack at 100% valve opening position when applying the uniform roughness of 100 microns. The average y^+ in this case is 45.57, which is well within the

wall logarithmic law i.e. 25-200. Hence, the mesh considered in the present study is good enough to accurately resolve the roughness features. It can be seen in Figure 5.17 that flow velocity is significantly higher in the discharge section (behind the fifth row of columns) of the trim as compared to the inlet section. Furthermore, in Figure 5.17, it can be seen that the flow velocity increases between the cylinders of a row, where the area available for the flow to take place is reduced, hence forming jet effects. As water exits a row and enters another one, due to area increase, velocity reduces to satisfy continuity.

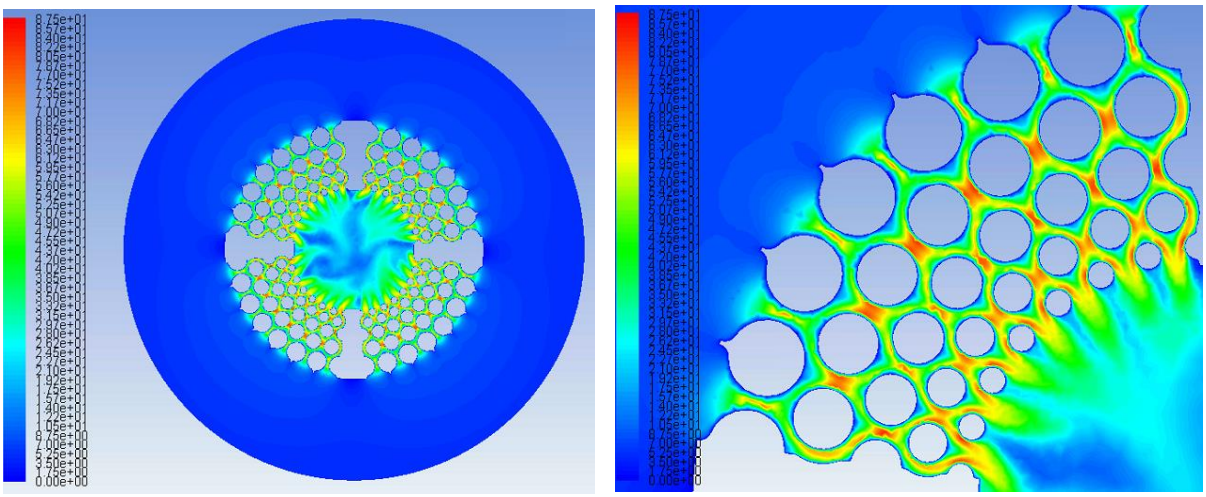

Figure 5.17 Variations in Velocity for Uniform Roughness of 100 Microns

The inclusion of the surface roughness parameter to V5.2 has improved the velocity distribution across the disc and has reduced the overall maximum velocity to 87.5m/s, a reduction of 8% from the smooth wall analysis. Velocity peaks at the area of minimum static pressure, but unlike with the smooth wall analysis, this appears almost completely uniform across the surface of the disc. A uniform surface roughness of 100 microns does not appear to have had any detrimental effect on either static pressure or velocity within V5.2. It is still representing similar or possibly improved characteristics to the original design XLO8-040. Table 5.3 shows the predicted values for mass flow rate through the five different trim designs when a uniform roughness of 100 microns is applied to the trim designs. Mass flow rates have been predicted over three differential pressures of 25, 50 and 100 bar.

Table 5.4 Mass Flow Rate at 100 Microns

ΔP (bar)	**Model**	**ε (μm)**	**Surface Roughness Uniformity (-)**	**m (Kg/sec)**
25	4.1	100	0.5	13.96
	4.2	100	0.5	14.73

	5.0	100	0.5	26.37
	5.1	100	0.5	39.62
	5.2	100	0.5	40.37
50	4.1	100	0.5	19.69
	4.2	100	0.5	20.86
	5.0	100	0.5	37.07
	5.1	100	0.5	56.08
	5.2	100	0.5	57.12
100	4.1	100	0.5	27.96
	4.2	100	0.5	29.58
	5.0	100	0.5	52.54
	5.1	100	0.5	79.47
	5.2	100	0.5	80.85

Now that the values for the mass flow rate have been predicted, the other parameters can be used to formulate a value for the Cv_{Trim}, Cv_{Total} and K_{Trim} which has been shown for the each trim design in Table 5.4 – Using the equations 3.1 - 3.6 in Chapter 3 and in the same manner as done for the smooth wall analysis.

Table 5.5 Cv Calculations for roughness of 100 Microns

ΔP (bar)	**Model**	**m (Kg/sec)**	**ΔP (kPa)**	**$Cv_{(without\ annular)}$**	**Cv_{Total}**	**Cv_{Trim}**	**K_{Trim}**
25	4.1	13.96	2499	11.62	11.19	11.37	18.04
	4.2	14.73	2499	12.26	11.83	12.04	19.11
	5.0	26.37	2499	21.95	21.52	22.87	39.60
	5.1	39.62	2499	32.98	32.55	37.90	72.18
	5.2	40.37	2499	33.61	33.18	38.89	74.08
50	4.1	19.69	4999	11.59	11.16	11.34	17.99
	4.2	20.86	4999	12.28	11.85	12.06	19.14
	5.0	37.07	4999	21.82	21.39	22.72	39.33
	5.1	56.08	4999	33.01	32.58	37.94	72.27
	5.2	57.12	4999	33.62	33.19	38.92	74.13
100	4.1	27.96	9997	11.64	11.21	11.39	18.07
	4.2	29.58	9997	12.31	11.88	12.10	19.20
	5.0	52.54	9997	21.87	21.44	22.77	39.43

	5.1	79.47	9997	33.08	32.65	38.05	72.47
	5.2	80.85	9997	33.65	33.22	38.97	74.22

The values of the constants F_P, F_R, N_1, specific gravity, Cv_{Body} and Cv_{Seat} remain the same as in experimental test results discussed earlier in chapter 4, and hence have not been included here, although they have been used to calculate Cv_{Trim}. Moreover, it can be seen in table 5.4 that there is an additional factor of Cv (without annular) included as explained in section 5.2. The calculated results for Cv_{Trim} and K_{Trim} are also shown in Figures 5.18 and 5.19 respectively, for ease of comparison with the same number designation as for trim design as used in Figure 5.13. It can be seen from the table of results that the these values are reasonably constant for each trim design across the three differential pressures measured, satisfying the derivation of Bernoulli for Cv within control valves.

It is also clear that there is a significant increase in Cv_{Trim} and K_{Trim} from the original concept designs of 4.1 and 4.2 to the latest design of 5.2, but equally that the application of a surface roughness has reduced the overall value of Cv_{Trim} and K_{Trim} for each design. Versions 4.1 and version 4.2 have shown the highest reduction in Cv_{Trim} and K_{Trim} for the five designs. When using smooth walls, there was a slight reduction in Cv_{Trim} and K_{Trim} for V4.2 compared to V4.1, however when the surface roughness has been applied V4.2 now displays higher values for Cv_{Trim} and K_{Trim} compared to V4.1. Trim 4.1 has reduced in values for K_{Trim} by an average of 27% across the three differential pressures, with V4.2 reducing by 22%. It is thought that the variation from the smooth wall calculations is as a result of the applied surface roughness having a greater impact on the removed ridge section of the trim, which has a larger surface area of wall to apply the surface roughness too.

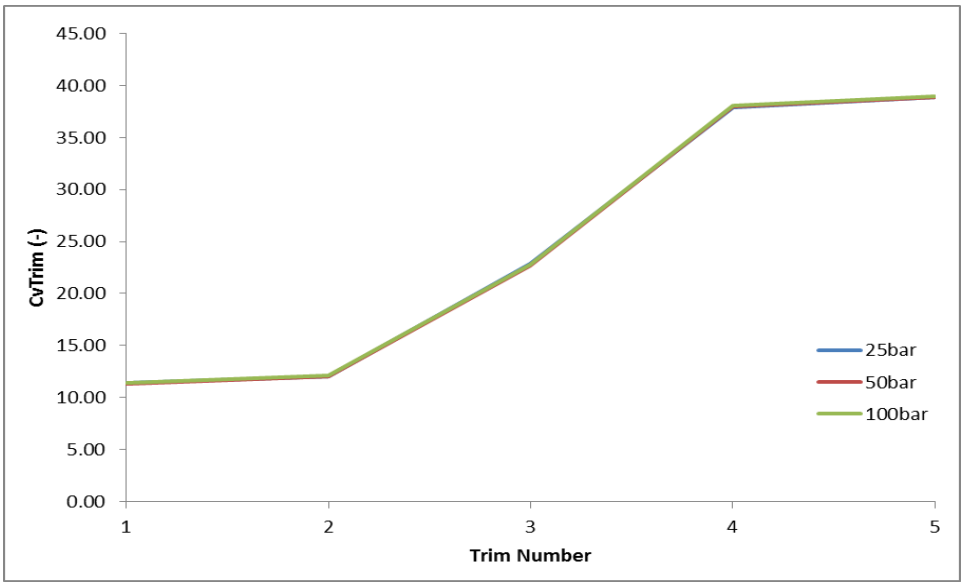

Figure 5.18 Cv Trim Variations, Roughness of 100 Microns

Trend lines for Cv_{Trim} and K_{Trim} remain similar to those shown in Figures 5.14 and 5.15 for smooth walls, with V5.2 showing the highest overall values. As with the smooth wall analysis, changing differential pressure has had no effect on the values for K_{Trim} and Cv_{Trim}. Trim 5.1 has shown the lowest percentage reduction in Cv_{Trim} and K_{Trim}, of 16%, V5.2 and 5.0 have both reduced by 18%. The reduction in Cv_{Trim} and K_{Trim} for all the designs is an expected result as this has followed previous flow testing by Asim [31], it is also understandable that applying a uniform roughness to a surface will increase the resistance to flow against a hydraulically smooth wall equivalent. The results of Cv for V5.2 are higher for a like for like roughness applied to the XLO8-040 trim manufactured using EDM, which is a positive sign that this design is an overall improvement on the original design XLO8-040.

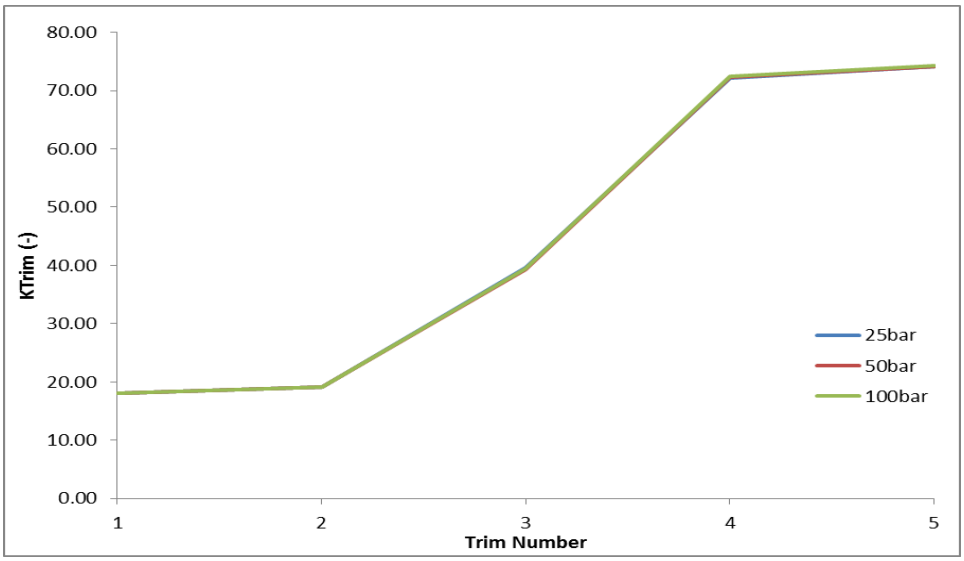

Figure 5.19 K Trim Variations, Roughness of 100 Microns

5.5.2 Roughness of 1000 Microns

As with the review at 100microns, only V5.2 will be analysed at the micro level for the impact on velocity and pressure performance for the increase in surface roughness to 1000microns. Figure 5.20 depicts the variations in the static pressure of water when using the same boundary conditions as used for the smooth wall analysis and a roughness of 100 microns and at a valve opening position of 100%. Both, full and zoomed in views of the trim have been shown in figure 5.20.

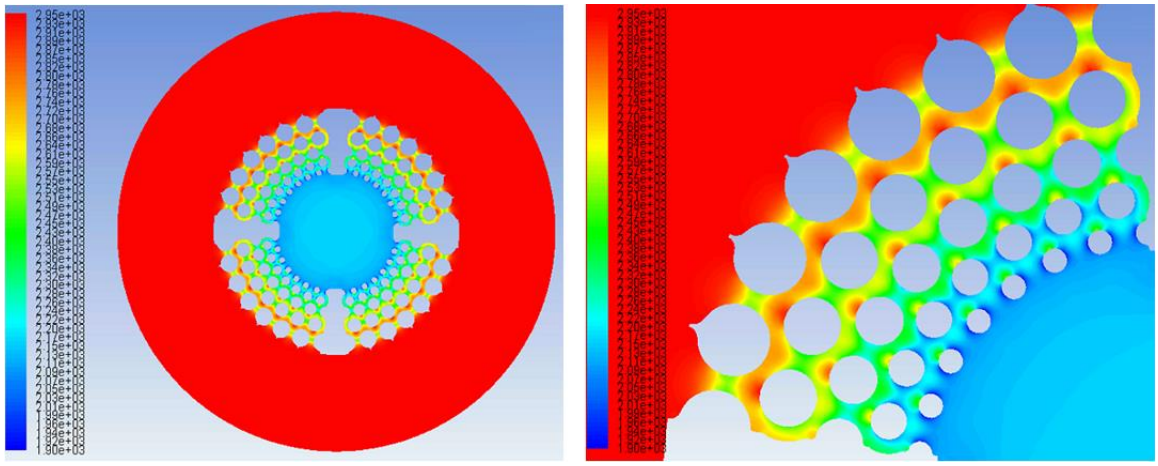

Figure 5.20 Variations in Static Pressure for Uniform roughness of 1000 microns

There is very little difference in the distribution of pressure that can be seen when comparing Figure 5.20 to 5.16. Both pressure contours are almost fully uniform; however there is a slight increase in the minimum value for min static pressure with figure 5.20. This could be as a result of the slight reduction in mass flow rate through the trim, as a result of the increased friction of a rougher surface. There are no areas of specific concern caused by the increase in roughness, the trim is still providing the same level of pressure and velocity control as shown and discussed with the previous analysis.

Figure 5.21 depicts the variations in the flow velocity within Version 5.2 trim stack at 100% valve opening position when applying the uniform roughness of 1000 microns. It can be seen in Figure 5.21 that flow velocity is significantly higher in the discharge section (behind the fifth row of columns) of the trim as compared to the inlet section. Furthermore, in Figure 5.21, it can be seen that the flow velocity increases between the cylinders of a row, where the area available for the flow to take place is reduced, hence forming jet effects. As water exits a row and enters another one, due to area increase, velocity reduces to satisfy continuity.

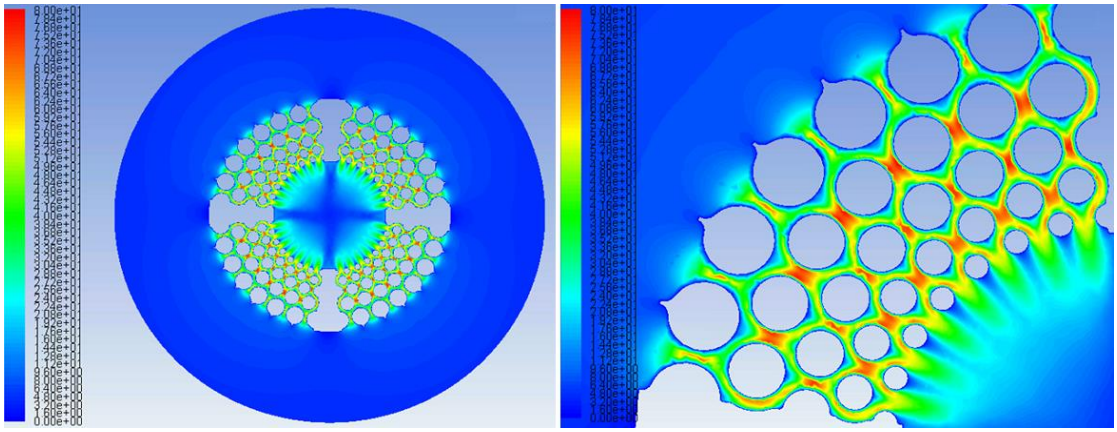

Figure 5.21 Variations in Velocity for Uniform roughness of 1000 microns

There is a slight reduction in the maximum value of velocity shown in Figure 5.21 which is directly related to the reduction in mass flow rate for the higher average surface roughness of 1000 microns. As with the analysis on the contours of static pressure, there is no area of specific note where there is a noticeable change in velocity profile between the two roughness's. Table 5.5 shows the predicted values for mass flow rate through the five different trim designs when a uniform roughness of 1000 microns is applied to the trim designs. Mass flow rates have been predicted over three differential pressures of 25, 50 and 100 bar.

Table 5.6 Mass Flow Rate at roughness of 1000 Microns

ΔP (bar)	**Model**	**ε (μm)**	**Surface Roughness Uniformity (-)**	**m (Kg/sec)**
25	4.1	1000	0.5	14.18
	4.2	1000	0.5	14.95
	5.0	1000	0.5	22.84
	5.1	1000	0.5	36.12
	5.2	1000	0.5	37.25
50	4.1	1000	0.5	19.62
	4.2	1000	0.5	21.20
	5.0	1000	0.5	32.37
	5.1	1000	0.5	51.13
	5.2	1000	0.5	52.71
100	4.1	1000	0.5	28.61
	4.2	1000	0.5	30.00
	5.0	1000	0.5	45.96
	5.1	1000	0.5	72.24
	5.2	1000	0.5	74.49

Now that the values for the mass flow rate have been predicted, the other parameters can be used to formulate a value for the Cv_{Trim}, Cv_{Total} and K_{Trim} which has been shown for the each trim design in Table 5.6 – Using the equations 3.1 - 3.6 in Chapter 3 and in the same manner as done for the smooth wall analysis.

Table 5.7 Cv Calculations, roughness of 1000 Microns

ΔP (bar)	Model	m (Kg/sec)	ΔP (kPa)	$Cv_{(without\ annular)}$	Cv_{Total}	Cv_{Trim}	K_{Trim}
25	4.1	14.18	2499	11.80	11.37	11.56	18.35
	4.2	14.95	2499	12.45	12.02	12.24	19.42
	5.0	22.84	2499	19.01	18.58	19.43	33.65
	5.1	36.12	2499	30.07	29.64	33.50	63.81
	5.2	37.25	2499	31.01	30.58	34.88	66.43
50	4.1	19.62	4999	11.55	11.12	11.29	17.93
	4.2	21.20	4999	12.48	12.05	12.27	19.48
	5.0	32.37	4999	19.05	18.62	19.48	33.73
	5.1	51.13	4999	30.10	29.67	33.54	63.89
	5.2	52.71	4999	31.03	30.60	34.91	66.48
100	4.1	28.61	9997	11.91	11.48	11.67	18.52
	4.2	30.00	9997	12.49	12.06	12.28	19.49
	5.0	45.96	9997	19.13	18.70	19.57	33.88
	5.1	72.24	9997	30.07	29.64	33.50	63.81
	5.2	74.49	9997	31.01	30.58	34.87	66.42

The values of the constants F_P, F_R, N_1, specific gravity, Cv_{Body} and Cv_{Seat} remain the same as in experimental test results discussed earlier in chapter 4, and hence have not been included here, although they have been used to calculate Cv_{Trim}. Moreover, it can be seen in table 5.6 that there is an additional factor of Cv (without annular) included as explained in section 5.2. The calculated results for Cv_{Trim} and K_{Trim} are also shown in Figures 5.22 and 5.23 respectively, for ease of comparison with the same number designation as for trim design as used in Figure 5.13. However it can be seen from the table of results that the these values are reasonably constant for each trim design across the three differential pressures measured, satisfying the derivation of Bernoulli for Cv within control valves. As with the analysis on smooth walls and with a uniform roughness of 100 microns there is a significant increase in Cv_{Trim} and K_{Trim} from the original concept designs of 4.1 and 4.2 to the latest design of 5.2, but equally that the application of a surface roughness of 1000 microns has further reduced the overall value of Cv_{Trim} and K_{Trim}.

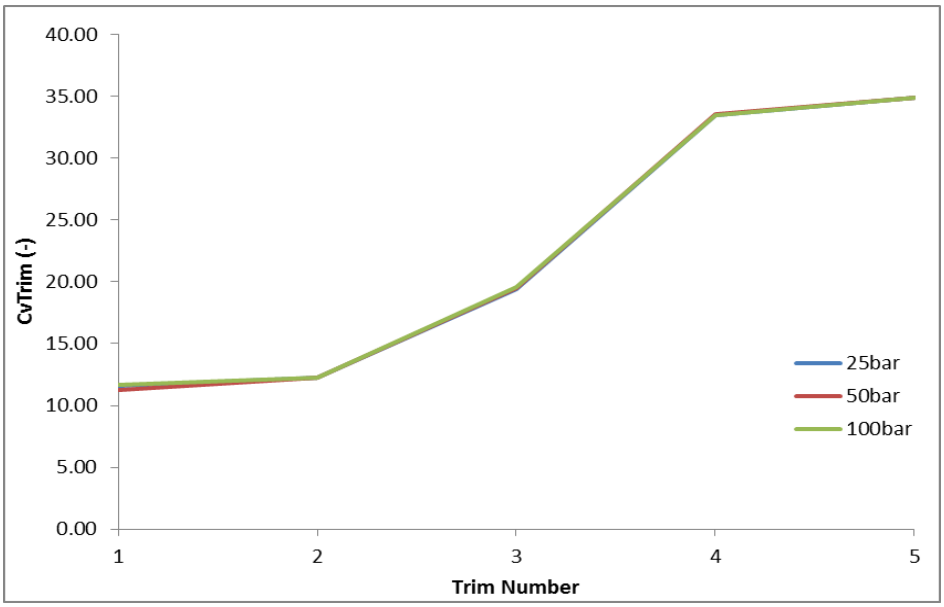

Figure 5.22 Cv Trim, Roughness of 1000 Microns

Versions 4.1 and version 4.2 however have not shown a reduction in Cv_{Trim} and K_{Trim} from the increase in roughness to 1000 microns. When comparing a roughness of 100 microns against smooth walls, both Cv_{Trim} and K_{Trim} for V4.1 and V4.2 reduced by approximately 25%, with a slightly higher reduction for V4.1 than V4.2. However when further increasing the roughness, the Cv_{Trim} and K_{Trim} values have, on average across the three differential pressures, slightly increased; by up to 2%. V5, V5.1 and V5.2 have however all reduced further from the roughness of 100 microns. V5.0 has reduced by a further 14%, V5.1 by a further 12% and V5.2 by 10% from the 100 micron roughness. The effect of increasing the roughness by a further 900 microns has not seen as a significant reduction in the Cv as increasing by 100 microns from the smooth wall surfaces. As with all the previous analysis the three differential pressures are displaying no variation in values for Cv_{Trim} and K_{Trim}.

It was anticipated that the results of increasing the surface roughness would have had a more profound effect on a reduction in Cv_{Trim} and K_{Trim} than is indicated as the minimum gaps assigned during the design phase between certain features on each disc vary between 0.25mm and 1.2mm. A roughness of 1000 microns could effectively reduce the gap between these columns further which, as shown with V5, 5.1 and 5.2, should reduce the mass flow rate through the trim and consequently the value for Cv_{Trim} and K_{Trim}.

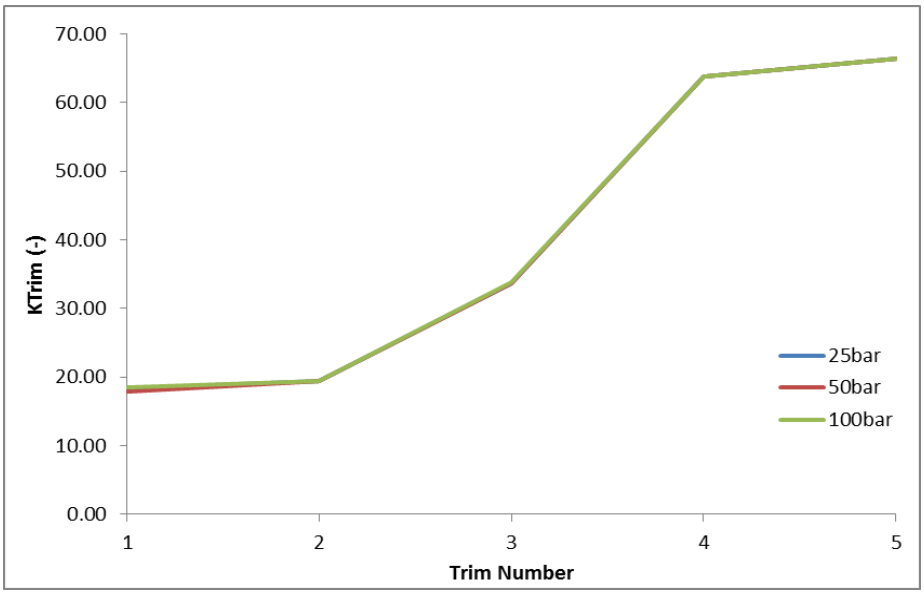

Figure 5.23 K_{Trim}, Roughness of 1000 Microns

It could be considered that the areas between the discs highlighted in figure 5.2, which were showing areas of high velocity and low static pressure, may have been causing a higher restriction to flow rate than if they were not there; reducing the overall mass flow rate for a like for like differential pressure. When applying a small surface roughness, i.e less than the gap between the columns, this has caused a further restriction, however when increasing the roughness to a size greater than this minimum feature then the restriction in this area has been reduced, resulting in a higher mass flow rate through the trim for the same differential pressure analysis. Values for Cv_{Trim} and K_{Trim} are still higher for V5.2 when using a uniform roughness of 1000microns than had been achieved with the original design X-Stream in flow testing. V5.1 is only marginally lower than the original design X-Stream; however the smooth wall analysis on this trim design showed potential areas for erosion and cavitation, the effect of applying surface roughness, it is thought, would not have the effect of removing these issues.
Were SLM able to apply uniformity to the surface roughness, which can be aided by the design improvements as detailed in chapter 4, the performance characteristics of V5.2 are still on par / slightly better than the original XLO8-040.

5.6 Effect of Uniformity of Surface roughness on Cv

Analysis of surface roughness effects on Cv in section 5.3 maintained a full uniform distribution of the surface roughness, however it is clear from samples and measurement of the roughness profile across the SLM discs that this is not necessarily the case. As such this section will review the effect of a fully non uniform roughness, whereby the average surface roughness is kept as

either 100 or 1000 microns, but the peaks and troughs of the surface are the most un-uniform to still provide this same value of average surface roughness.

CFD has now been used to initially predict the mass flow rate through each individual trim design at the same three defined differential pressures used when working with the smooth wall trims. Solver settings selected firstly 100 microns with a roughness constant of 1 and then 1000microns with a roughness constant of one, to compare the effects of Cv_{Trim}, Cv_{Total} and K_{Trim} against the a trim with the same average surface roughness, but that had a fully uniform surface.

5.6.1 Review at 100 Microns, Roughness Constant 1

As with the review at 100microns uniform roughness, only V5.2 will be analysed at the micro level for the impact on velocity and pressure performance for the change to a non-uniform surface roughness. As with the review for uniform roughness, only V5.2 will be analysed at the micro level for the impact on velocity and pressure performance application of non-uniform roughness of 100microns. Figure 5.24 depicts the variations in the static pressure of water when using the same boundary conditions as used for a uniform roughness of 100 microns and at a valve opening position of 100%. Both, full and zoomed in views of the trim have been shown in figure 5.24.

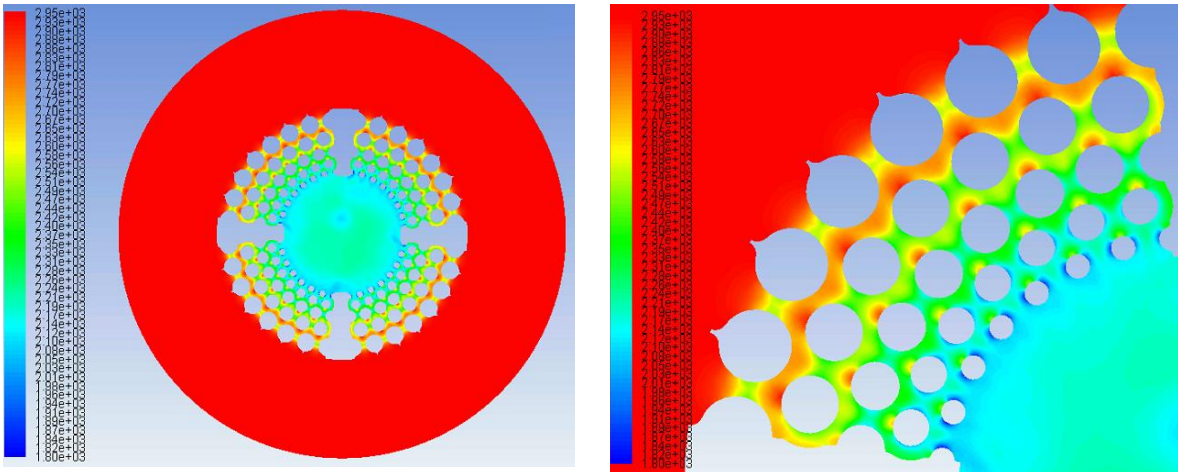

Figure 5.24 Variations in Static Pressure for Non-uniform roughness of 100 microns

There is very little visible difference in the distribution of pressure when comparing Figure 5.24 to 5.16. Both pressure contours are almost fully uniform, the minimum static pressure on the fourth and fifth row of columns has kept a similar value, however is now distributed over a slighter larger area than before becoming easier to see. In general the observations on how this contour plot might affect performance of the trim are as described in section 5.2.5 for the smooth wall analysis of V5.2.

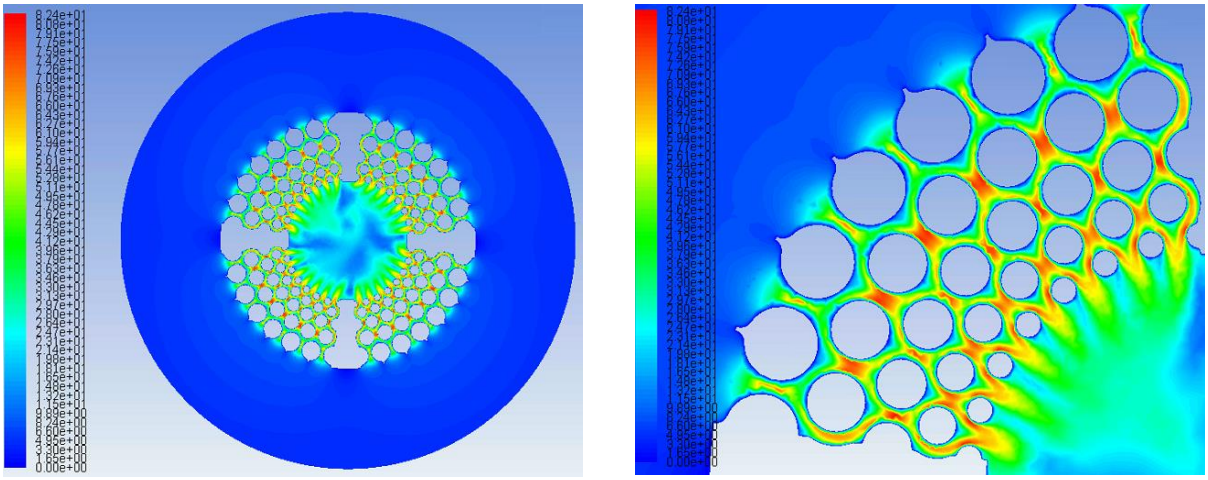

Figure 5.25 Variations in Velocity for Non- uniform roughness of 100 microns

Figure 5.25 depicts the variations in the flow velocity within Version 5.2 trim stack at 100% valve opening position when applying the non-uniform roughness of 100 microns. It can be seen in Figure 5.25 that flow velocity is significantly higher in the discharge section (behind the fifth row of columns) of the trim as compared to the inlet section. Furthermore, in Figure 5.25, it can be seen that the flow velocity increases between the cylinders of a row, where the area available for the flow to take place is reduced, hence forming jet effects. As water exits a row and enters another one, due to area increase, velocity reduces to satisfy continuity. The overall maximum velocity has reduced by approximately 5m/s for the non-uniform roughness of 100 microns applied to V5.2 when compared to the uniform roughness. This decrease in velocity should result in a reduction in mass flow rate and thus Cv between these two tests. The application of non-uniformity appears to have had no significant visual effect on either the pressure or velocity contours for V5.2 Table 5.7 shows the predicted values for mass flow rate through the five different trim designs when a uniform roughness of 100 microns is applied to the trim designs. Mass flow rates have been predicted over three differential pressures of 25, 50 and 100 bar.

Table 5.8 Mass Flow Rate at 100 Microns – Roughness Constant of 1

ΔP (bar)	**Model**	**ε (μm)**	**Surface Roughness Uniformity (-)**	**m (Kg/sec)**
25	4.1	100	1	11.63
	4.2	100	1	12.67
	5.0	100	1	24.14
	5.1	100	1	37.03
	5.2	100	1	37.64
50	4.1	100	1	16.48

	4.2	100	1	17.92
	5.0	100	1	34.18
	5.1	100	1	52.41
	5.2	100	1	53.25
100	4.1	100	1	23.35
	4.2	100	1	25.36
	5.0	100	1	48.39
	5.1	100	1	74.15
	5.2	100	1	75.19

Now that the values for the mass flow rate have been predicted, the other parameters can be used to formulate a value for the Cv_{Trim}, Cv_{Total} and K_{Trim} which has been shown for the each trim design in Table 5.8 – Using the equations 3.1 - 3.6 in Chapter 3 and in the same manner as done for the smooth wall analysis.

Table 5.9 Cv Calculations 100 Microns – Roughness Constant of 1

ΔP (bar)	**Model**	**m (Kg/sec)**	**ΔP (kPa)**	**$Cv_{(without\ annular)}$**	**Cv_{Total}**	**Cv_{Trim}**	**K_{Trim}**
25	4.1	11.63	2499	9.68	9.25	9.35	14.84
	4.2	12.67	2499	10.55	10.12	10.25	16.27
	5.0	24.14	2499	20.10	19.67	20.68	35.81
	5.1	37.03	2499	30.83	30.40	34.61	65.92
	5.2	37.64	2499	31.33	30.90	35.36	67.35
50	4.1	16.48	4999	9.70	9.27	9.37	14.87
	4.2	17.92	4999	10.55	10.12	10.25	16.27
	5.0	34.18	4999	20.12	19.69	20.71	35.86
	5.1	52.41	4999	30.85	30.42	34.64	65.99
	5.2	53.25	4999	31.35	30.92	35.38	67.39
100	4.1	23.35	9997	9.72	9.29	9.39	14.90
	4.2	25.36	9997	10.56	10.13	10.26	16.28
	5.0	48.39	9997	20.14	19.71	20.73	35.90
	5.1	74.15	9997	30.86	30.43	34.66	66.02
	5.2	75.19	9997	31.30	30.87	35.31	67.25

The values of the constants F_P, F_R, N_1, specific gravity, Cv_{Body} and Cv_{Seat} remain the same as in experimental test results discussed earlier in chapter 4, and hence have not been included here,

although they have been used to calculate Cv_{Trim}. Moreover, it can be seen in table 5.8 that there is an additional factor of Cv (without annular) included as explained in section 5.2. The calculated results for Cv_{Trim} and K_{Trim} are also shown in Figure 5.26 and 5.27 respectively, for ease of comparison with the same number designation as for trim design as used in Figure 5.13. However it can be seen from the table of results that the these values are reasonably constant for each trim design across the three differential pressures measured, satisfying the derivation of Bernoulli for Cv within control valves. As with the analysis on smooth walls and with a uniform roughness of 100 microns there is a significant increase in Cv_{Trim} and K_{Trim} from the original concept designs of 4.1 and 4.2 to the latest design of 5.2, but equally that the application of a surface roughness of 1000 microns has further reduced the overall value of Cv_{Trim} and K_{Trim}.

There is a further reduction in Cv_{Trim} and K_{Trim} for all five designs with the application of a non-uniform surface. The percentage reduction is lower than the initial reduction for the application of a uniform roughness; however this further reduction is proof that the uniformity of the surface is a major factor on the performance characteristics of the trim. As with analysis for the uniform roughness V4.1 and V4.2 have shown the highest reduction in Cv_{Trim} as a result of the change to a consent of 1; applying a non-uniform surface, dropping by 18 and 15% respectively. The geometrical issues with the flow through the disc and the minimum feature gap of 0.25 again are the main distinguishing factors between these designs and the V5.0, 5.1 and 5.2 designs therefore it is logical to assume that the inclusion of this feature is the main reason for the significant difference in Cv_{Trim} and K_{Trim} between the designs. All of three of the V5 designs have shown a further reduction in Cv_{Trim} of an equal value of 9%, indicating that the preference for "flow on top" of the disc and maximising feature size is more prevalent factor on the performance characteristics.

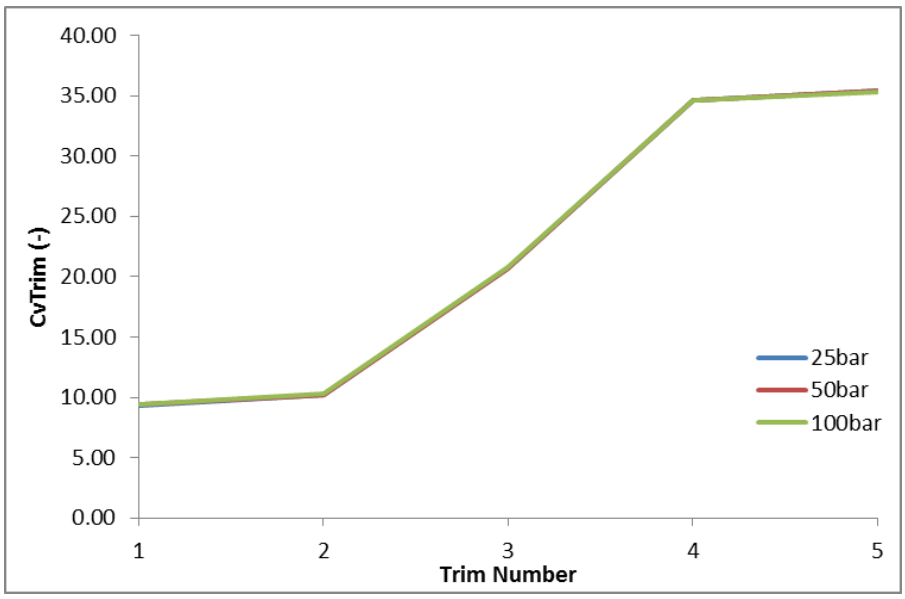

Figure 5.26 Cv Trim Roughness of 100 Microns – Roughness Constant of 1

As can be seen from Figures 5.26 and 5.27, the trends showing the values of Cv_{Trim} and K_{Trim} for the three differential pressures are so close together that the only 25 bar is visible. The application of non-uniform roughness, which from previous testing by Asim [31] appears to be more prevalent with SLM, has led to the results been similar to the EDM method of manufacture when using the roughness parameters of EDM trims.

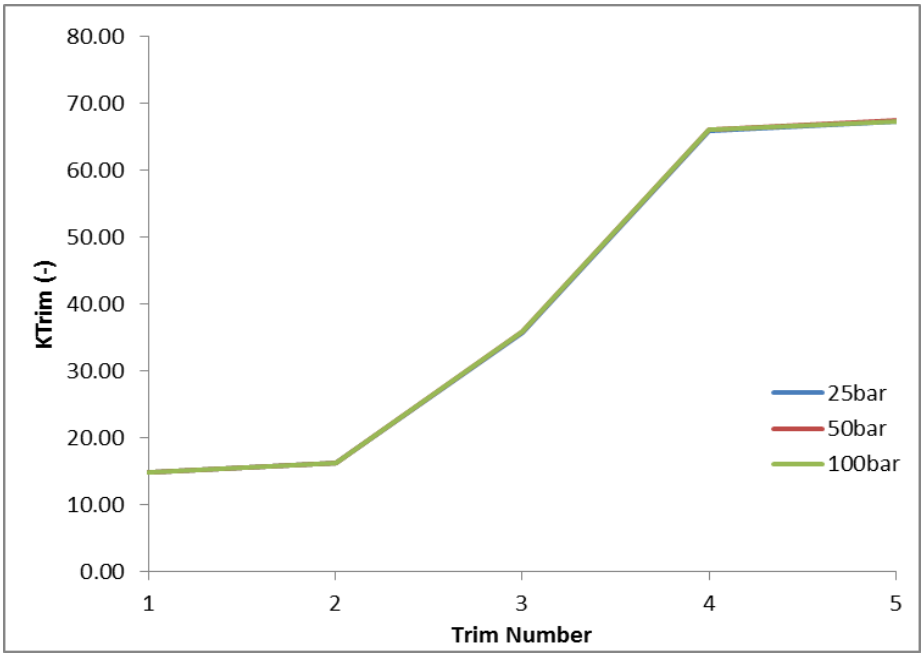

Figure 5.27 K_{Trim} Roughness of 100 Microns – Roughness Constant of 1

5.6.2 Review at 1000 Microns, Roughness Constant 1

As with the review at 100microns (section 5.5.1), only V5.2 will be analysed at the micro level for the impact on velocity and pressure performance for the increase in surface roughness to 1000microns. Figure 5.28 depicts the variations in the static pressure of water when using the same boundary conditions as used for a uniform roughness of 1000 microns and at a valve opening position of 100%. Both, full and zoomed in views of the trim have been shown in figure 5.28. There isn't much to differentiate the distribution of pressure when comparing Figure 5.28 to 5.16. Both pressure contours are almost fully uniform, the minimum static pressure on the fourth and fifth row of columns has kept a similar value but is slightly lower than the uniform roughness. It is anticipated that this further reduction of minimum static pressure would indicate in an increase in resistance at these points and as such we might expect that the resultant effect of Cv_{Trim} and K_{Trim} would be a reduction, compared to the uniform roughness.

Figure 5.29 depicts the variations in the flow velocity within Version 5.2 trim stack at 100% valve opening position when applying the non-uniform roughness of 1000 microns. It can be

seen in Figure 5.29 that flow velocity is significantly higher in the discharge section (behind the fifth row of columns) of the trim as compared to the inlet section. Furthermore, in Figure 5.29, it can be seen that the flow velocity increases between the cylinders of a row, where the area available for the flow to take place is reduced, hence forming jet effects. As water exits a row and enters another one, due to area increase, velocity reduces to satisfy continuity.

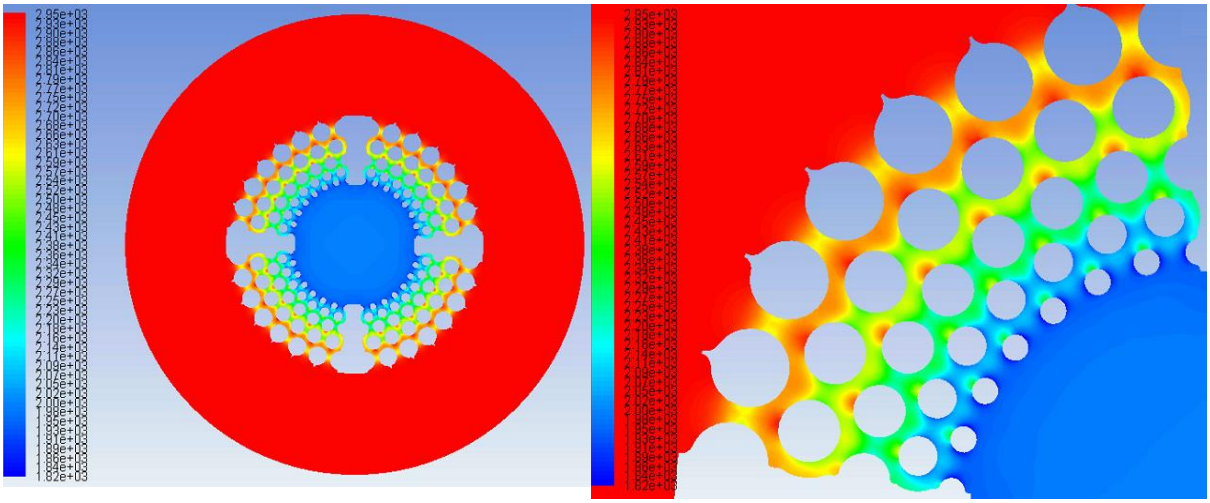

Figure 5.28 Variations in Static Pressure for Non-uniform roughness of 1000 microns

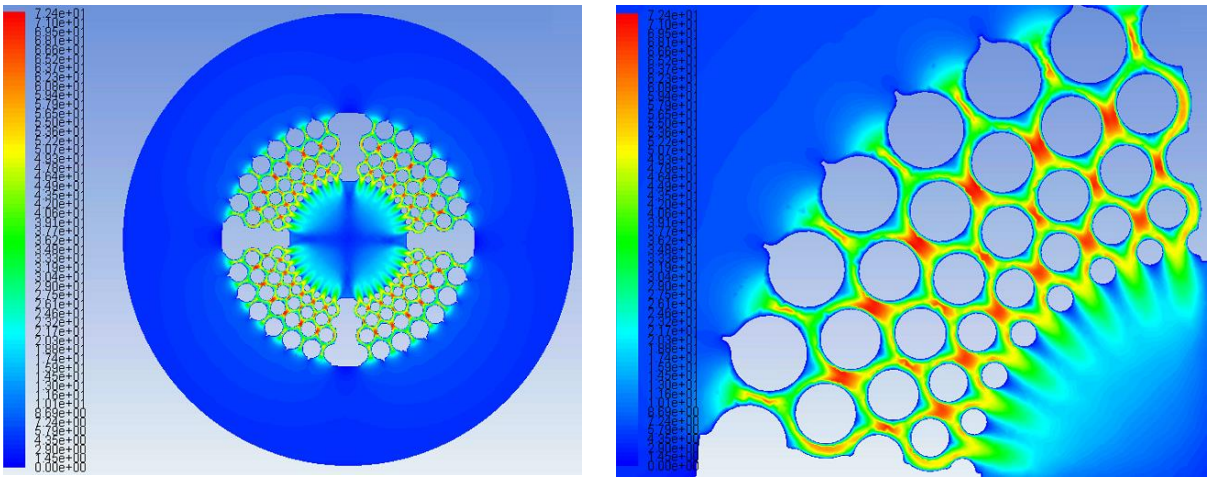

Figure 5.28 Variations in Velocity for Non- uniform roughness of 1000 microns

The overall maximum velocity has reduced by approximately 7m/s for the non-uniform roughness of 1000 microns applied to V5.2 when compared to the uniform roughness. This decrease in velocity should result in a reduction in mass flow rate and thus Cv between these two tests. The application of non-uniformity appears to have had no significant visual effect on either the pressure or velocity contours for V5.2. Table 5.9 shows the predicted values for mass flow rate through the five different trim designs when a uniform roughness of 1000 microns is applied

to the trim designs. Mass flow rates have been predicted over three differential pressures of 25, 50 and 100 bar.

Table 5.10 Mass Flow Rate at 1000 Microns – Roughness Constant of 1

ΔP (bar)	Model	ε (μm)	Const.	m (Kg/sec)
25	4.1	1000	1	11.09
	4.2	1000	1	12.07
	5.0	1000	1	18.80
	5.1	1000	1	30.93
	5.2	1000	1	31.87
50	4.1	1000	1	15.39
	4.2	1000	1	17.09
	5.0	1000	1	26.66
	5.1	1000	1	43.76
	5.2	1000	1	45.08
100	4.1	1000	1	22.40
	4.2	1000	1	24.25
	5.0	1000	1	37.83
	5.1	1000	1	62.00
	5.2	1000	1	63.91

Now that the values for the mass flow rate have been predicted, the other parameters can be used to formulate a value for the Cv_{Trim}, Cv_{Total} and K_{Trim} which has been shown for the each trim design in Table 5.10 – Using the equations 3.1 - 3.6 in Chapter 3 and in the same manner as done for the smooth wall analysis.

Table 5.11 Cv Calculations 1000 Microns – Roughness Constant of 1

ΔP (bar)	Model	m (Kg/sec)	ΔP (kPa)	$Cv_{(without\ annular)}$	Cv_{Total}	Cv_{Trim}	K_{Trim}
25	4.1	11.09	2499	9.23	8.80	8.89	14.11
	4.2	12.07	2499	10.05	9.62	9.73	15.44
	5.0	18.80	2499	15.65	15.22	15.68	27.14
	5.1	30.93	2499	25.75	25.32	27.60	52.57
	5.2	31.87	2499	26.53	26.10	28.62	54.52
50	4.1	15.39	4999	9.06	8.63	8.71	13.82

	4.2	17.09	4999	10.06	9.63	9.74	15.46
	5.0	26.66	4999	15.69	15.26	15.72	27.22
	5.1	43.76	4999	25.76	25.33	27.62	52.60
	5.2	45.08	4999	26.54	26.11	28.63	54.53
100	4.1	22.40	9997	9.32	8.89	8.98	14.26
	4.2	24.25	9997	10.09	9.66	9.78	15.52
	5.0	37.83	9997	15.75	15.32	15.78	27.33
	5.1	62.00	9997	25.81	25.38	27.68	52.72
	5.2	63.91	9997	26.60	26.17	28.72	54.70

The values of the constants F_P, F_R, N_1, specific gravity, Cv_{Body} and Cv_{Seat} remain the same as in experimental test results discussed earlier in chapter 4, and hence have not been included here, although they have been used to calculate Cv_{Trim}. Moreover, it can be seen in table 5.8 that there is an additional factor of Cv (without annular) included as explained in section 5.2. The calculated results for Cv_{Trim} and K_{Trim} are also shown in Figures 5.30 and 5.31 respectively, for ease of comparison with the same number designation as for trim design as used in Figure 5.13. However it can be seen from the table of results that the these values are reasonably constant for each trim design across the three differential pressures measured, satisfying the derivation of Bernoulli for Cv within control valves.

As with the analysis on smooth walls and with a uniform roughness of 1000 microns there is a significant increase in Cv_{Trim} and K_{Trim} from the original concept designs of 4.1 and 4.2 to the latest design of 5.2, but equally that the application of a non-uniform surface roughness of 1000 microns has further reduced the overall value of Cv_{Trim} and K_{Trim} when compared specifically to a uniform surface roughness of the same average height. As with the analysis on a roughness of 100 microns (uniformity and non-uniformity) there is a further reduction in Cv_{Trim} and K_{Trim} for all five designs with the application of a non-uniform surface. When comparing these values against the uniform roughness of 1000 microns, there is the highest reduction for V4.1 of 23%. V4.2 has further reduced; a 21% reduction, whereas V5.0, 5.1 and 5.2 have all reduced by approximately 18-19%.

The application of non-uniform roughness for 1000 microns has had a greater impact on the reduction of Cv_{Trim} than it had with the 100 microns. The reduction is almost double that of the 100 micron analysis in section 5.4.1. It is evident that the potentially higher peaks and lower troughs in the surface are now having a more profound effect on the differing geometries, with potentially these minimum gaps now becoming more of a resistance to flow rate through the trim.

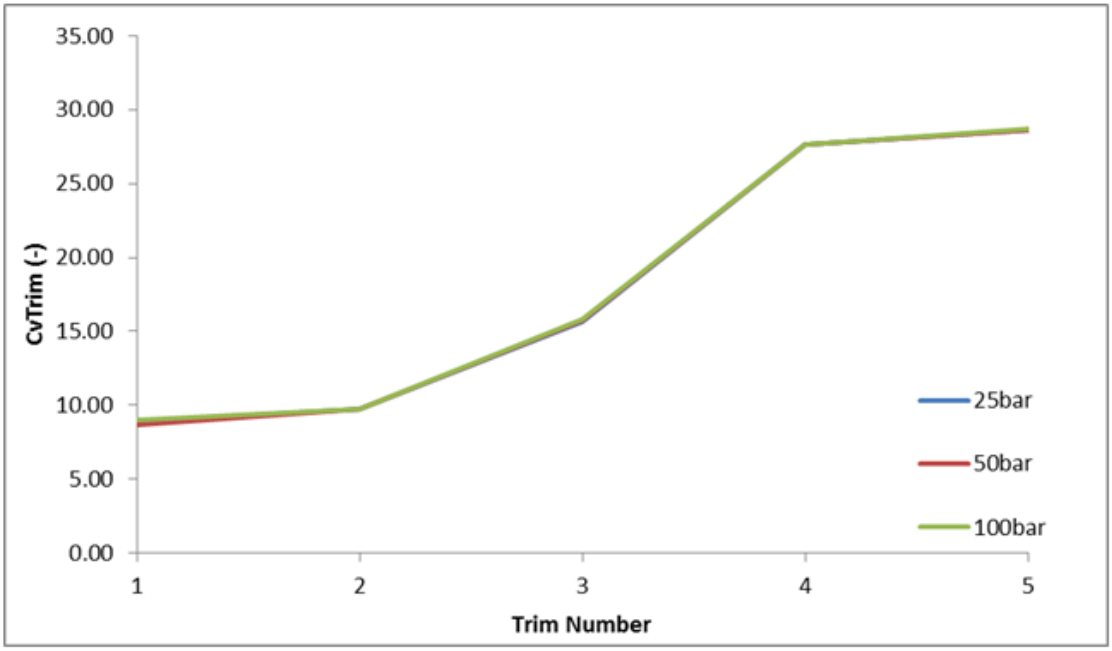

Figure 5.30 Cv_{Trim} at Roughness of 1000 Microns – Roughness Constant of 1

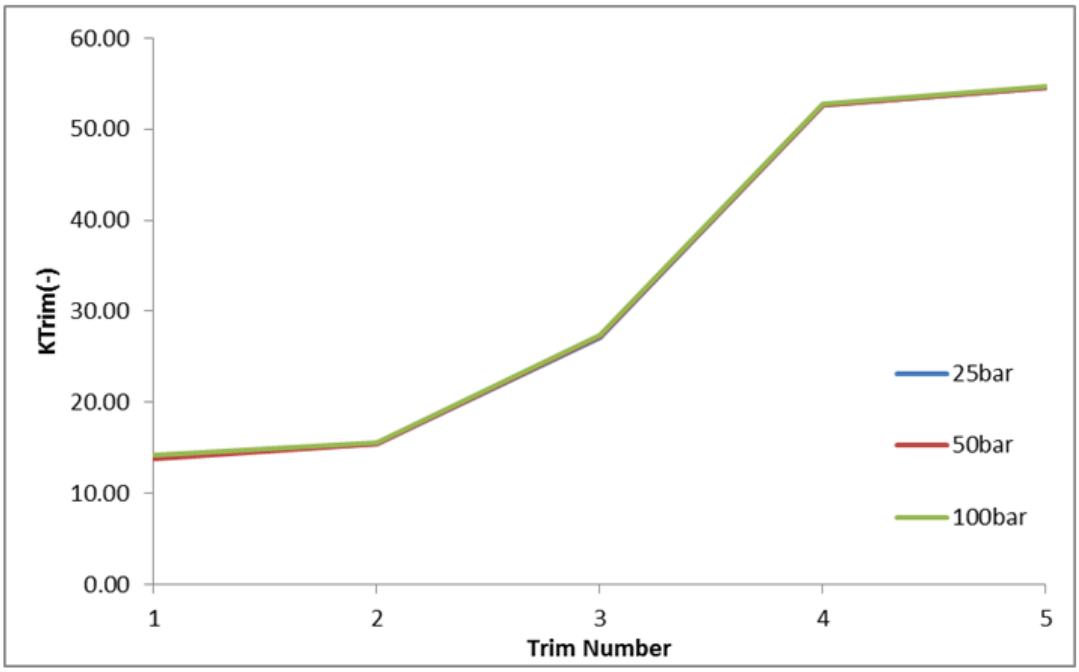

Figure 5.31 K_{Trim} at Roughness of 1000 Microns – Roughness Constant of 1

Figure 5.30 and 5.31 showing the variation of K_{Trim} and Cv_{Trim} for the five trim designs, again follows the same increase from the earliest versions of 4.1 and 4.2 to the latest version of 5.2.

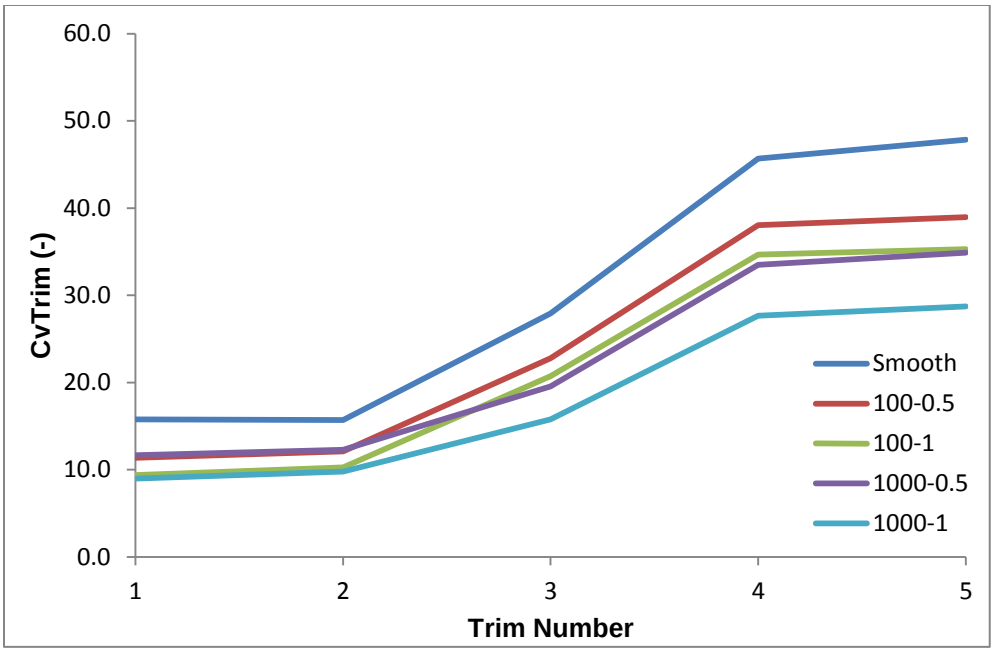

Figure 5.32 Effect of roughness parameters on Cv_{Trim} for all the trims

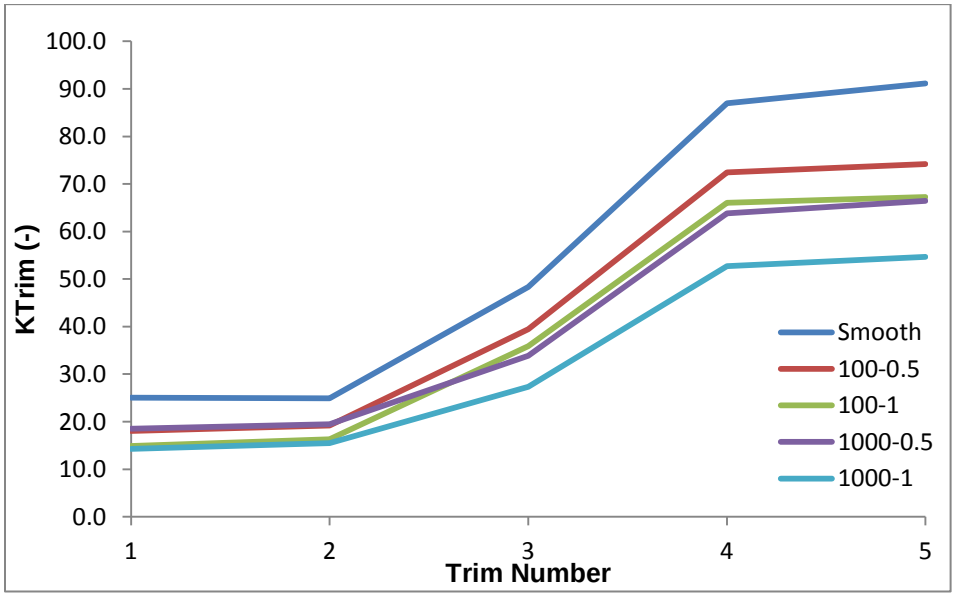

Figure 5.33 Effect of roughness parameters on K_{Trim} for all the trims

Figures 5.32 and 5.33 have been added at the end of this section to show a complete comparison of the five trim designs, developed in chapter 4, for all of the roughness conditions applied during numerical testing. These figures clearly show the trends as described during this chapter and it can be seen graphically that the improvement in flow conditions from V5.1 to V5.2 are less prevalent when applying the non-uniform roughness of 1000 microns to both models.

5.7 Summary

All five trim designs have now been analysed for their performance, specifically for the values of Cv_{Trim}, K_{Trim} and the potential for cavitation and erosion. This analysis includes the effects of surface roughness at 100 and 1000 microns, specifically comparing against a smooth surface and also an analysis when the roughness of the trims was fully non-uniform. It can be confirmed at this stage that the effect of differential pressure has had no impact on the values for Cv_{Trim} and K_{Trim} and as such it can be confirmed that pressure drop has not affected the changing results from a change of surface roughness or surface uniformity. Interestingly there is little difference between the results for a non-uniform roughness of 100 microns and a uniform roughness of 1000 microns, which is indicating that at this point increasing the surface roughness is less effective at reducing the capacity of the trim than the uniformity. Application of surface roughness to the trims has seen a general reduction in the value of Cv_{Trim} and K_{Trim} and the qualitative analysis of velocity and pressure has identified areas in the trim that are having a larger impact on performance characteristics. Specifically sections with small gaps between columns or the inclusion of ridged surfaces (added for manufacturing purposes) can be seen to be affected to a larger extent.

CHAPTER # 6
CONCLUSIONS

From the results obtained in the previous chapters, detailed conclusions have been drawn in this chapter. The major aims of the study are reviewed and concluded and finally, the works carried out in this study are evaluated and requirements for future work are defined.

6.1 Summary of Conclusions

The research completed has enabled a number of conclusions to be made about the suitability of the five designs and their performances compared to the original design of XLO8-040. The use of SLM is considered by the valve industry as an economically more viable method of manufacture for the X-Stream product; however their earlier work had produced samples which did not meet the application/performance needs of the product. Due to relative infancy of SLM technologies for the manufacture of production components there is limited research available, however there is little to none available in specific areas of the manufacture of complex geometry parts by SLM for use in control valves or even fluid flow applications.

It had been clear that the SLM method of manufacture was a cost effective method of manufacturing the X-Stream, however the geometric imperfections and large reduction in the performance characteristics, meant that research needed to be conducted to review the effect of surface roughness on fluid flow and also to analyse the process against design, when using SLM. From a comprehensive review of the published literature, a number of limitations have been found out which are concerned with the aforementioned points. A summary of the primary aims and conclusions on the objectives (detailed in Chapter 2) of the thesis is provided in the following sections of this chapter.

6.2 Research Aims and Achievements

The main aims of the thesis defined from an extensive literature review in this area are as follows:

Research Aim #1

This was the development of an appropriate method of manufacture for the X-Stream trim, with the specific aim of improving the previously used SLM method, such that this method would provide the required product performance characteristics that had been previously achieved using the EDM method of manufacture. The thesis reviewed both methods of manufacture with a detailed literature review on SLM to review areas of further research to improve the manufacturability of components and improve the performance characteristics as a result. The thesis has concluded that modifications to geometry of the part, specifically considering an SLM manufacture method, results in improved performance characteristics over a part manufactured using optimised process parameters.

The research has shown a potential improvement when optimising the design of almost 20% on Cv_{Trim} for the valve, with an improved value of K_{Trim} as well. The results of the thesis also give a

clear indication on the effects of the surface roughness on the fluid flow, showing clearly that the increase in surface roughness reduces the mass flow rate of fluid through the trim, reducing Cv_{Trim} and K_{Trim}. It has also been shown that this numerical analysis is conducive to the experimental analysis.

6.3 Thesis Conclusions

A comprehensive study has been carried out to support the existing literature regarding the improvement to the manufacturability of parts using SLM by various methods and to provide novel additions to the current understanding by directly comparing these methods. The major conclusions of the research objectives (discussed in more detail in Chapter 2) are summarised as follows;

Research Objective # 1: To perform a critical analysis on the manufacturability of X-Stream by altering the process or the design

Conclusion # 1: From the investigations regarding the comparison of process improvement of an existing part, against design modifications of the part to suit a standard process, it can be concluded that a design optimisation has shown a greater improvement in the final shape of the trim as compared to previous attempts at manufacturing the XLO8-040. Process improvement also significantly improved the overall final shape of the product and resulted in reduced finishing machining operations against previous attempts. However the process optimisation resulted in a large increase in process time, which would lead to a large increase in cost (when paying for parts via machine usage). Design optimisation represented a reduction in processing time of 18 hours against the process optimisation, which for the purpose of this study, could result in a like for like reduction in cost of almost 50%. Version 5.2 (the design improvement) displayed the best overall shape and required the least finishing operations to prepare the trim for installation into the test valve.

Research Objective # 2: To review the performance characteristics of a part manufactured with process improvements against a part with design optimisation.

Conclusion # 2: This objective was reviewed by empirical testing of a modified design against a part manufactured by a modified process. Results showed that the modifications to process improved the performance (Cv_{Trim}) of the part by 8%, whereas potentially this increased to 20% for the design modifications. The results are of great importance for future work with SLM, as design optimisation for process changes are not usually considered and this may save time for manufacturing engineers and design engineers reviewing this process for their parts. It has also made the process attractive to the control valves industry as the overall reduction in Cv_{Trim}

against a like for like EDM part is now below 20% and combined with the cost saving potential mentioned in conclusion #1, this makes SLM a possibility for certain applications.

Research Objective # 3: To perform numerical analysis on the effects of surface roughness on multiple designs of X-Stream, reviewing specific geometrical differences.

Conclusion # 3: Using CFD to predict mass flow rates within each design modification, the values of Cv_{Trim}, Cv_{Total} and K_{Trim} were determined. The variation in these values between the five designs analysed was impressive. What were perceived as minor geometrical changes to assist In the manufacturability of the part, resulted (for V4.1 and 4.2) in significant reductions in Cv_{Trim} and K_{Trim} against earlier testing on EDM parts. Far greater than had been seen with earlier attempts at manufacture the standard XLO8-040 using SLM. The analysis of smooth wall trims using CFD also showed a reduction for these trims, which could be directly related to the features with minimal areas causing peak fluid velocities and very high pressure drops. Standard approach to design improvements with SLM involves the addition of lattice support structures, which to an extent were employed with V4.1 and V4.2. This method of design optimisation is not ideal, as it created minimum gaps of around 0.25mm between flow channels, significantly reducing the Cv.

The designs with more hydrodynamically smooth channels (V5.1 and V5.2) resulted in increases in Cv_{Trim} and K_{Trim}, for both smooth wall and rough surfaces when compared to earlier tests on the original design XLO8-040. These designs removed any unsupported flat areas of the original design and replaced them with cylindrical/curved supporting surfaces. V5.2, based on a numerical analysis alone, produced higher predicted values for Cv_{Trim} and K_{Trim} than had been achieved for any smooth or none smooth wall analysis previously and was the, from a design perspective, the simplest modification. The understanding on the effects of geometrical changes are of great importance for the designers of the X-Stream product and also for any designer / manufacturing engineers reviewing the potential design changes to suit an SLM method of manufacture.

Research Objective # 4: To review the effect of surface uniformity on Cv via numerical analysis.

Conclusion # 4: It was possible, within the CFD environment, to apply both fully uniform and non-uniform roughness to the walls of the parts. SLM parts had, through previous analysis (discussed in chapter 2), produced parts with a very non-linear uniformity. These parts had also showed very high variations in peaks and valleys, which would potentially represent high resistance to fluid flow. Tests were conducted to review this effect from a numerical perspective on the five designed parts. Results showed that the application of a non-uniform surface further reduced the values of Cv_{Trim} and K_{Trim} for the parts, but they also showed that this application of

a non-uniform surface roughness had a greater impact on the reduction of Cv_{Trim} and K_{Trim} than the increase of surface roughness by 10 times.

Versions 4.1 and 4.2 actually increased Cv_{Trim} and K_{Trim} when the surface roughness was increased from 100 microns to 1000 microns on a uniform finish, however when these roughness's were non-uniform the values of Cv_{Trim} and K_{Trim} reduced as expected. Version 5.2, reduced in Cv_{Trim} by 23% with the application of a uniform roughness of 100 microns and an additional 10% reduction for a non-uniform surface. However the 1000 micron roughness resulted in a 37% reduction, which increased to 67% for a non-uniform roughness. This concludes that surface uniformity has a higher impact on Cv_{Trim} than average surface roughness alone.

Research Objective # 5: To review other performance characteristics on each of the design modifications proposed.

Conclusion # 5: This objective was achieved by analysis of the velocity and pressure contours of each design, when varying the pressure on a smooth wall only trim design. The results pinpointed areas of each design that could increase the potential for cavitation to occur as a result of points of minimum static pressure and high pressure recovery, whilst also identifying areas of high velocity that could cause premature erosion of trim. Results showed that again the design modification that uses a typical lattice like structural enhancement's, not only resulted in lower values of Cv_{Trim}, but that these features would increase failure potential by means of cavitation and erosion. Minimum gap size and increase in area is the inherent principle of the X-Stream design. The designs that reduced these gaps and thus areas, V4.1, 4.2, 5.0 and V5.1 all displayed areas of concern for cavitation and erosion, whereas V5.2 was the only trim that displayed matching or potentially improved performance characteristics over the original design XLO8-040. The understanding on the effects of geometrical changes are of great importance for the designers of the X-Stream product and also for any designer / manufacturing engineers reviewing the potential design changes to suit an SLM method of manufacture.

6.4 Thesis Contributions

The main contribution of this research study is the linkage between the manufacturing process and the performance characteristics of severe service control valve's trims, through numerical investigations. No such study has been carried out previously in the published literatures. Hence, this study helps in understanding the effects of the manufacturing methods, and their constraints, on the performance of X-Stream trims. Similar type of studies can be conducted on other kinds of trims as well.

6.5 Recommendations for Future Work

Although the research conducted has provided great insight into the potential for SLM and provided a new approach for the X-Stream trim for use with this manufacturing process, there are still areas that have not been looked at by this study and further areas that could be researched following the analysis of this study.

Recommendation # 1

This study has only concentrated on an analysis of improving the manufacturability of the X-Stream trim by comparing process improvement against design improvement. There has been no review to see the effect of combining these features and reviewing the effects on manufacturability, surface features and likewise performance characteristics. This had not been included in the study because cost to manufacture is a major contributing factor for the potential application of SLM. However process optimisation may not necessarily increase the build rate to the same extent when using a specially designed part.

Recommendation # 2

The study reviewed the effect of average surface roughness on the fluid flow through the trim and also looked at the uniformity of the surface. However there is a much larger field of surface metrology reviewing further aspects like the number of valleys against peaks on fluid flow. Aspects like core roughness are deemed by surface metrologists to be more important than average surface roughness's, whether they be in 2D or 3D. Further research in this area could be conducted to see the variation for these parts when using either further optimised processes or finishing techniques (as described in Chapter 2) to improve the surface structure.

Recommendation # 3

The study provided a relatively simple review on the performance characteristics of the X-Steam from a velocity and pressure point of view. However no actual cavitation prediction was performed as this feature was not enabled within ANSYS. Pressure drops were deliberately selected to prevent cavitation in the valve so that this feature would not impact on the results of mass flow rate, Cv_{Trim} or K_{Trim}. Further study would be more relevant to real applications as the effect on these features for a cavitating fluid is not known.

REFERENCES

[1] BS EN 60534-2-1:2011, Industrial Process Control Valves – Part 2.1 Flow Capacity – Sizing Equations for fluid flow under installed conditions

[2] Bernoulli, D et al. (1738) "Hydrodynamica"

[3] ISA-RP75.23 (1995), "Considerations for Evaluating Control Valve Cavitation"

[4] Kiesbauer, J. Vnucec. D, Roth, M. Stoffel, B. (2006) "Predicting Cavitation damage in Control Valves", Special print from Hydrocarbon processing March 2006

[5] Kent Introl (1993) "Technical Sizing and Selection Manual", TS.02

[6] Weir Valves (2011) "Technical Sizing Manual", TB-C0-R0

[7] Miller, H.L. (1993) "Recommended specifications for severe service control valves", Technical literature published by CCI Rancho Santa Margarita, California 92688

[8] Miller, H.L. Stratton, L.R (1997) "Fluid Kinetic Energy, as a selection criterion for control valves", Published in the August 1997 edition of Valve World.

[9] Miller, H.L. (2007) "Control Valve Trim Fluid Exit Kinetic Energy and Velocity", Technical literature published by CCI Rancho Santa Margarita, California 92688

[10] The American Petroleum Institute Recommended Practice 14E (fifth edition) (2013), Offshore Production Platform Piping Systems

[11] ISA Handbook of Control Valves (1998) "Practical Guides for measurement and Control" ISBN 1-55617-565-5

[12] Burns, M. (1993), "Automated Fabrication: Improving Productivity in Manufacturing", PTR Prentice-Hall Inc.

[13] Tsopanos, S. (2008) "Micro Heat Exchanges by selective laser melting". EThOS Persistent ID: uk.bl.ethos.507633

[14] The Welding Institue (TWI), http://www.twi-global.com/

[15] TWI (2008), "Additive Layer Manufacturing", An article submitted to association of industrial laser users.

[16] Article from High performance composites (2008) "Focus on design: the promise of rapid manufacturing"

[17] The Additive Fabrication Spy (2009) "Rapid Prototyping, 3D Printing and Rapid Manufacturing", an online article http://www.additive3d.com/

[18] Jobi, M. Vansteenkiste, G. (2009) "Topography and optical properties of polished laser melted Maraging Steel, Cobalt Chromium and Inconel 718", FP6- STREP RC2 project

[19] Yadroitsev, I. Bertrand, PH. Laget, B. Smurov, I (2007) "Application of laser assisted technologies for fabrication of functionally graded coatings and objects for the International Thermonuclear Experimental Reactor components", Article for the journal of nuclear materials 263 (20007) pp: 189-196

[20] Osakada, K. Shiomi, M. (2006) "Flexible manufacturing of metallic products by selective laser melting of powder", an article for the international journal of machine tools and manufacture issue 46 pp: 1188-1193

[21] Rossi, S. Deflorian, F. Venturini, F. (2003) "Improvement of surface finishing and corrosion resistance of prototypes produced by direct metal laser sintering", Journal of Materials Processing Technology 148 (2004) pp: 301–309

[22] ASME B46.1 (2009), "Surface Texture (Surface Roughness, Waviness and Lay)".

[23] Yadroitsev, I. Thivillon, L. Bertrand, B. Smurov, I (2007) "Strategy of manufacturing components with designed internal structure by selective laser melting of metallic powder", In the Proceedings of Applied Surface Science 254 (2007) pp:980–983

[24] Morton, KM. (2003) "Optimisation of a high energy loss control valve trim using computational and experimental techniques", A thesis submitted to the university of Manchester

[25] Zukauskas, A. (1998), "Fluid dynamics and flow induced vibration in tube banks", published by Hemisphere

[26] Munson, B.R. Young, D.F. Okiishi, T.H. (1994), "Fundamentals of fluid mechanics (2nd edition)", published by Wiley

[27] Zukauskas, A. Ulinskas, R. (1998), "Banks or plain and finned tubes", Heat exchanger design handbook, Parts 1 and 2: heat exchanger theory/fluid mechanics and heat transfer, section 2.2.4, published by Begell House

[28] Green, J. Mishra, R. Charlton, M. Owen, R. (2012), "Local Analysis of Flow Conditions within a Geometrically Complex Control Valve Trim using CFD", Journal of Physics: Conference Series 364 (2012) 012075

[29] Young Joon An, Byeong Jin Kim and Byeong Rog Shin (2008) "Numerical analysis of 3-D flow through LNG marine control valves for their advanced design", Journal of Mechanical Science and Technology 22 (2008) 1998~2005

[30] Taylor, J.B. Carrano, A.L. Kadlikar, S.G. (2006), "Characterization of the effect of surface roughness and texture on fluid flow—past, present, and future", International Journal of Thermal Sciences 45 (2006) pp:962–968

[31] Asim, T. Mishra, R. Charlton, M. (2013), "Capacity testing of X-Stream valves for single component, single phase flows", a KTP report.

APPENDIX 1 – Results of Talysurf CCI on surface parameters of EDM and previous SLM tests

	Original Design XLO8-040 - EDM Method of Manufacture			Original Design XLO8-040 - SLM Method of Manufacture	
TEST NUMBER	1	2	3	4	5
DATASIZE:	X=1095, Y=831	X=1095, Y=831	X=1095, Y=831	X=1095, Y=831	X=1095, Y=831
MISSING DATA PERCENTAGE:	0.00%(0Pt)	0.00%(0Pt)	0.00%(0Pt)	0.00%(0Pt)	0.00%(0Pt)
DATATYPE:	Texture	Primary	Primary	Primary	Primary
DATAPROCESSING:	Levelling	Levelling	Levelling	Levelling	Levelling
CUTOFF LENGTH:	X=None,Y=None	X=None,Y=None	X=None,Y=None	X=None,Y=None	X=None,Y=None
AMPLITUDE PARAMETERS					
Sq(um)	16.28	10.164	15.17	40.43	54.457
Ssk	3.402	2.309	1.96	1.375	0.438
Sku	19.689	12.332	8.326	6.479	2.763
Sp(um)	135.574	88.346	94.727	264.724	222.04
Sv(um)	46.591	51.634	51.402	105.845	137.099
Sz(um)	182.165	139.981	146.13	370.569	359.139
SPACING PARAMETERS					
Sds(1/mm^2)	682.885	744.965	765.012	631.798	742.379
Str	0.653	0.167	0.301	0.163	0.198
Sal(mm)	0.111	0.113	0.175	0.092	0.119
HYBRID PARAMETERS					
Sdq	2.015	1.253	1.714	2.576	2.877
Ssc(1/um)	1.322	0.622	1.205	1.016	1.277
Sdr(%)	119.993	45.159	81.938	201.513	256.654
CURVES PARAMETERS					
Vmp(um^3/mm^2)	7.57E+05	1.17E+06	1.71E+06	3.56E+06	2.66E+06
Vmc(um^3/mm^2)	2.75E+06	6.58E+06	9.88E+06	3.00E+07	5.28E+07
Vvc(um^3/mm^2)	5.18E+06	1.13E+07	1.90E+07	5.23E+07	7.33E+07
Vvv(um^3/mm^2)	2.22E+05	5.54E+05	6.34E+05	2.71E+06	3.49E+06
SK FAMILY					
Spk(um)	38.558	20.828	31.276	71.78	56.018
Sk(um)	21.873	17.853	24.048	80.022	154.171
Svk(um)	5.579	5.003	5.688	19.535	19.18
Smr1(%)	16.2	15.9	20.3	17	10.7
Smr2(%)	94	93.9	95.9	92.9	97.1
OTHER PARAMETERS					
Std(deg)	0	0	0	45	63
S5z(um)	170.062	120.067	134.074	357.095	345.583
Sa(um)	9.867	6.982	10.869	30.191	45.287

APPENDIX 2 – Flow Loop Operating Manual

Flow Loop Operating Manual

1. Fill 2/3 of the tank with water by opening the tap.

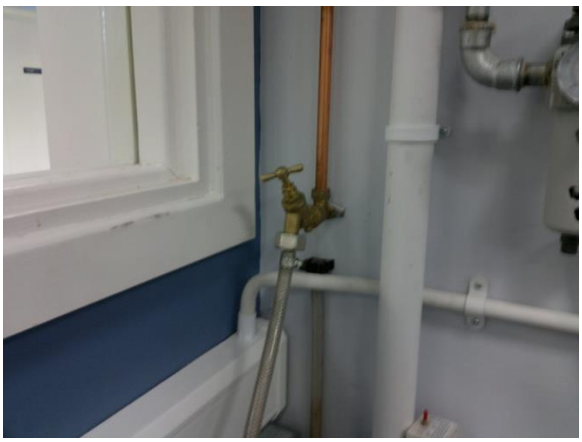

2. Close the vertical line (left) and open the line to the valve (right) by adjusting the valves.

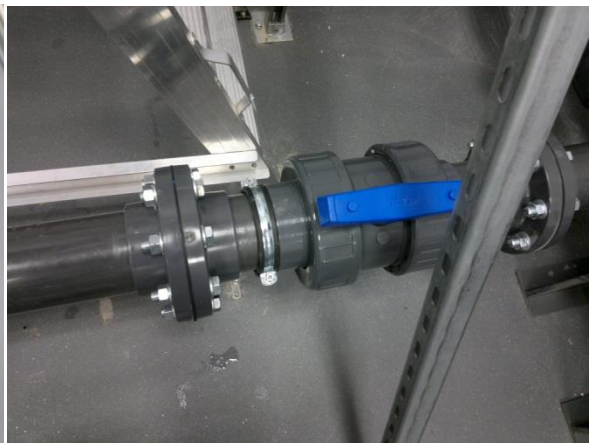

3. Connect the power cable to the pressure transducer where red wire is connected to terminal 1, green to terminal 2 and both black and white to terminal 3.

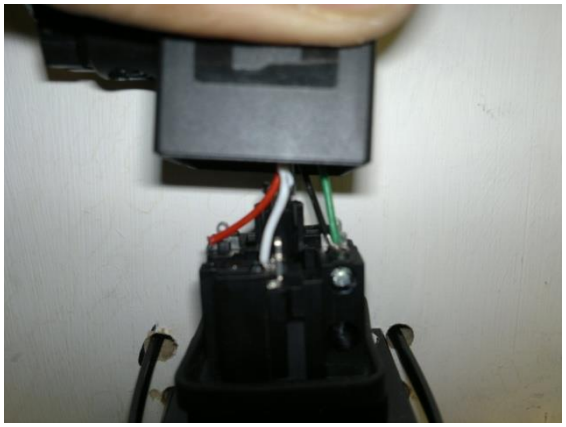

4. Connect the water pipes from the pressure transducer to the pressure tapping on either ends of the valve.

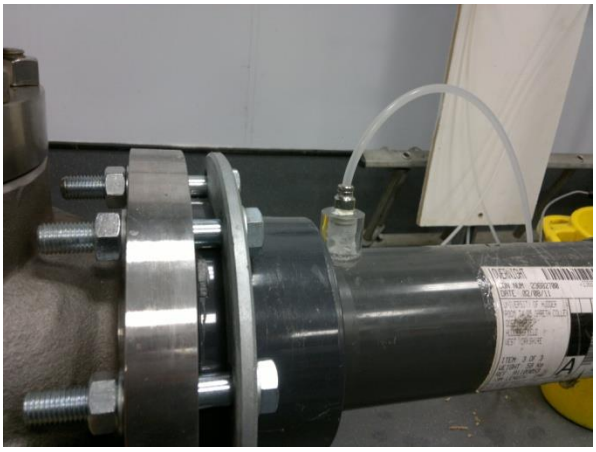

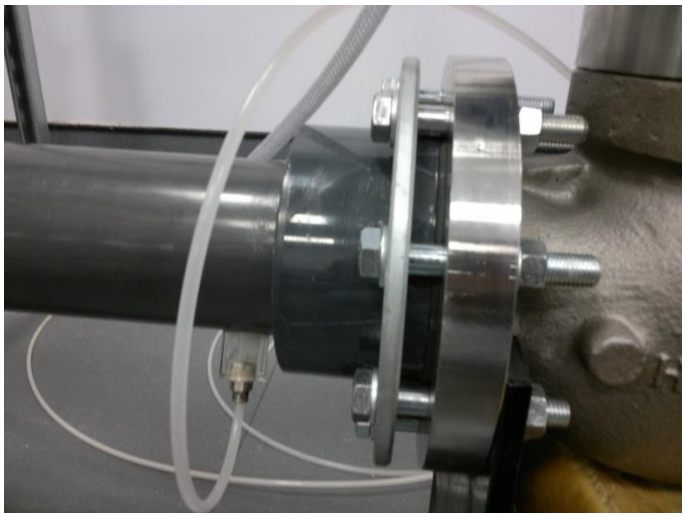

5. Connect the actuator of the valve to the air supply. Set the air supply pressure to 4 bars and double check it on the gauge mounted on the actuator. If the reading on the actuator is not matching with that of the air supply, manually match it using the screw on the top of the gauging unit. Note that the maximum air pressure that can be set for the operation of the valve is 6 bars. Furthermore, the pipe to the air supply can be disconnected by pulling back on the screw attached to the connecting unit.


6. Attach the power cable of the actuator to the calibrator such that blue wire is connected to black terminal and brown wire to the red terminal.


7. The other end of the cable, connected to the pressure transducer in step # 3, is connected to the multimeter and the power supply. The red and black wires are connected to the +ive and –ive output terminals of the power supply. The white and green wires are connected to the VΩ and COM ports of the multimeter via blue and black connecting cables as shown in the figure below.

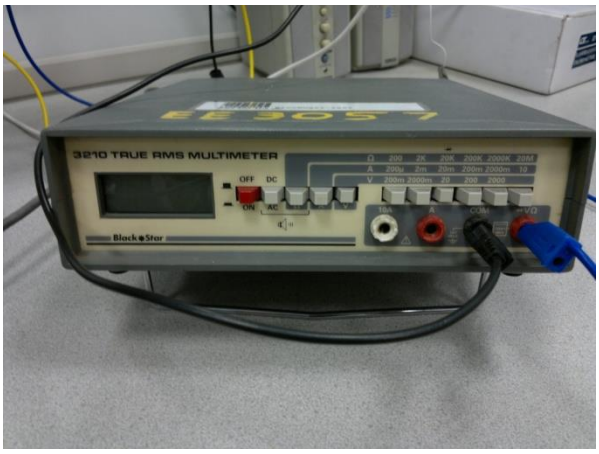

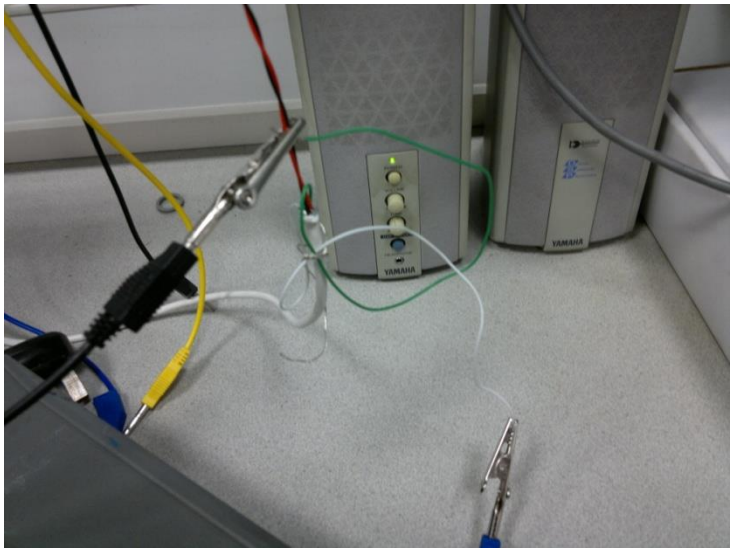

8. Turn on the switch on the pump's control unit. The monitor on the front panel will display the welcome screen. Click Next and the operator screen will be displayed.

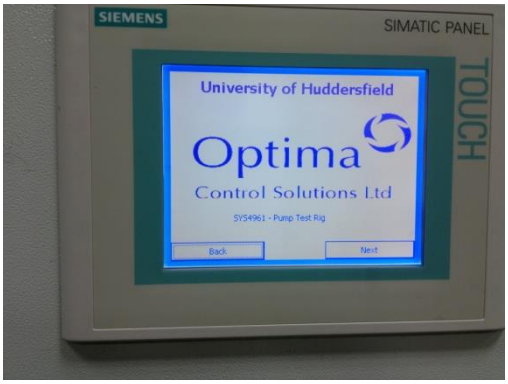

9. Set the Flow Meter Setpoint to 1500 ltrs/min as 1600 ltrs/min is the upper limit. Step numbers can be specified to run multiple tests continuously with various impeller speed settings. Time for each step can also be specified and the Elapsed Time monitor displays the

status of that particular run. To run the same test again, it is still required to input all the settings again, although they have previously been specified and are displayed on the screen. In the example shown below, a test is run for 5 mins at 99% of the maximum impeller speed. Note that the first step is to click on the Set-Up button.

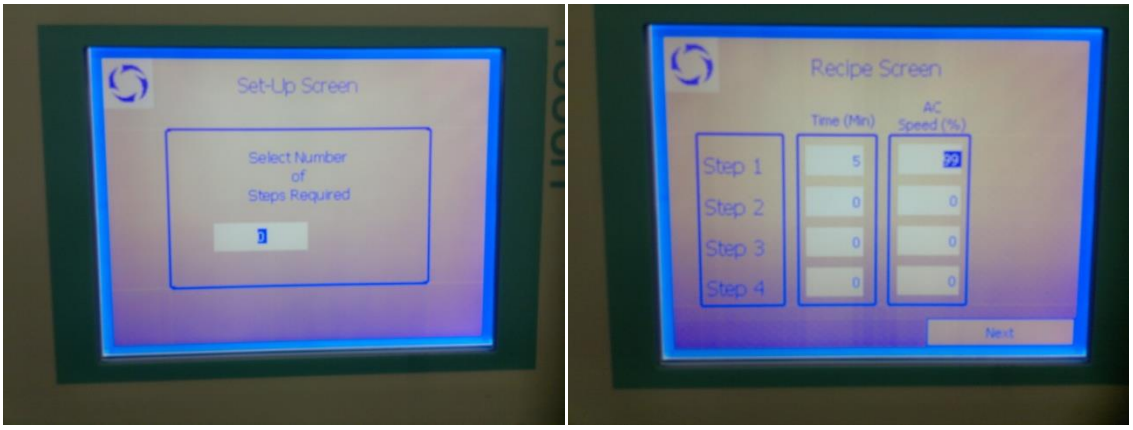

10. After specifying the input settings, the test can be started by clicking the Start button on the monitor. Note that before specifying the input settings (step # 8), the Start button was disabled.

11. The opening of the valve can be controlled by the calibrator. The general settings of the calibrator are to turn the upper most knob (horizontal) far right and the right knob (vertical) to far down positions. There are four black buttons on the calibrator. The upper left button switches the mode of the calibrator from mA to % opening. Note that the range of operation is 4 mA to 20 mA, where 4 mA refers to fully closed and 20 mA refers to fully open valve. The right hand side buttons increases (upper button) and decreases (lower button) the value of the mA on the calibrator. The lower left button is for pre-settings the points into the calibrator for ease of operation. In the figure below, the valve is set to fully closed, i.e. 4.00 mA.

12. On the rear of the actuator there is a window which shows the exact % age by which the valve is actually open. This value should be used in calculations if required. Note that the one currently installed has a zero error of +ive 1.2 % and hence its range is from 1.2 % to 101.2 %. There are a couple of pressure gauges on the right of this monitor which automatically adjusts when the valve is opened or closed.

13. For Cv calculations, the flow rate and the pressure drop across the valve are required. The flow rate can be measured through the digital stand-alone flow meter. The second source of the flow rate measurement is the monitor on the control panel itself but it is not very accurate (the difference is clear in figures below) and hence the digital stand-alone flow meter is recommended. The third source of the flow rate measurement is the analog flow meter installed within the fluid line but it is difficult to read its value accurately because it rotates quite rapidly while operation.

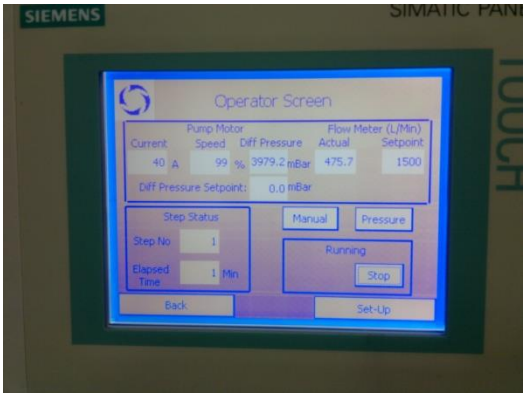

14. The pressure drop across the valve is measured through the multimeter. First of all, both the multimeter and the power supply needs to be turned on using the switches on the individual devices. The scale on the multimeter, for the pressure drop measurement is such that 10.00 V refers to 6 bars of pressure drop.

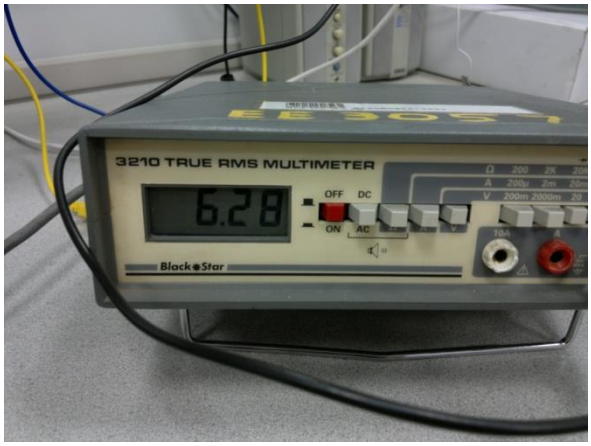

15. After performing the test/s, shutdown/stop/disconnect the pump's control unit, power supply, multimeter and the calibrator. Close the air supply to the actuator. Close the fluid line to the valve. Drain the water tank completely using the valve. Note that by fully opening this valve will flood the flow loop area. Hence, open the valve by 50%. In the figure below, the valve is in fully closed position.

APPENDIX 2 – Flow Loop Operating Manual

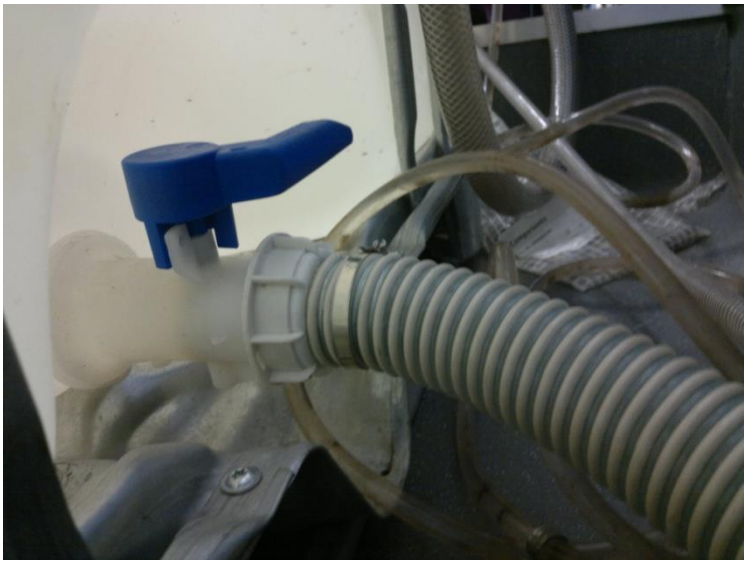

APPENDIX 3 – Flow Loop Results

Original Design Trim – Optimised Process Parameters

Table 1 – Recorded Test Data @ 100% Valve opening

	Test 1:	**Test 2:**	**Test 3:**
Pump Speed =	75%	38%	10%
P =	3.22	1.06	0.39
ΔP =	2.87	0.73	0.07
T_1 =	18.96	19.43	19.52
	Q (MAX)	Q (≈50%)	Q (≈10%)
1	37.51	18.94	5.88
2	37.90	18.74	6.01
3	37.51	18.64	5.81
4	37.21	18.82	5.72
5	36.82	19.34	5.98
6	38.56	20.02	5.85
7	39.71	19.68	5.97
8	39.86	19.39	6.12
9	39.24	19.50	6.07
10	39.31	19.41	6.14
Average =	38.36	19.25	5.96

Table 2 – Recorded Test Data @ 75% Valve Opening

	Test 1:	**Test 2:**	**Test 3:**
Pump Speed =	75%	38%	10%
P =	3.25	1.07	0.39
ΔP =	2.88	0.73	0.07
T_1 =	20.14	20.38	20.55
	Q (MAX)	Q (≈50%)	Q (≈10%)
1	30.20	15.00	4.70
2	31.29	15.03	4.66
3	30.49	14.91	4.77
4	30.18	15.06	4.73
5	29.86	14.66	4.71
6	29.88	14.86	4.65
7	30.30	14.97	4.79
8	30.09	14.90	4.81
9	30.08	14.94	4.76
10	30.04	15.01	4.73

APPENDIX 3 – Flow Loop Results

Average =	30.24	14.93	4.73

Table 3 - Recorded Test Data @ 50% Valve Opening

	Test 1:	**Test 2:**	**Test 3:**
Pump Speed =	75%	38%	10%
P =	3.34	1.07	0.39
ΔP =	2.91	0.75	0.07
T_1 =	20.57	20.85	22.93
	Q (MAX)	Q (≈50%)	Q (≈10%)
1	20.97	10.48	3.24
2	20.72	10.51	3.28
3	20.82	10.71	3.27
4	20.47	10.49	3.22
5	20.51	10.51	3.18
6	20.87	10.44	3.24
7	20.77	10.60	3.32
8	20.74	10.42	3.29
9	20.75	10.38	3.22
10	20.39	10.51	3.15
Average =	20.70	10.51	3.24

Table 4 - Recorded Test Data @ 25% Valve opening

	Test 1:	**Test 2:**	**Test 3:**
Pump Speed =	75%	38%	10%
P =	3.33	1.06	0.77
ΔP =	2.96	0.73	0.07
T_1 =	20.90	21.35	21.40
	Q (MAX)	Q (≈50%)	Q (≈10%)
1	11.70	6.36	1.97
2	12.14	5.66	1.88
3	11.92	5.91	1.72
4	11.96	5.84	1.83
5	12.00	6.09	1.92
6	12.66	5.66	1.76
7	12.62	6.14	1.84

8	11.78	6.12	1.83
9	11.74	5.97	1.70
10	11.56	6.08	1.72
Average =	12.01	5.98	1.82

New Design Trim V5.2 – Standard Process Parameters

Table 5 – Recorded Test Data @ 100% Valve opening

Pump Speed =	**Test 1:** 75%	**Test 2:** 38%	**Test 3:** 10%
P =	3.30	1.08	0.39
ΔP =	2.87	0.73	0.07
T_1 =	23.46	23.70	23.74
	Q (MAX)	Q (≈50%)	Q (≈10%)
1	34.31	17.41	5.23
2	34.75	17.19	5.27
3	34.31	17.07	5.15
4	33.97	17.28	5.28
5	35.12	17.53	5.23
6	34.36	17.50	5.23
7	34.53	17.12	5.33
8	34.70	17.92	5.16
9	35.13	16.92	5.22
10	34.08	17.94	5.30
Average =	34.53	17.39	5.24

Table 6 – Recorded Test Data @ 75% Valve Opening

Pump Speed =	**Test 1:** 75%	**Test 2:** 38%	**Test 3:** 10%
P =	3.31	1.08	0.39
ΔP =	2.78	0.72	0.07
T_1 =	23.46	23.48	23.53
	Q (MAX)	Q (≈50%)	Q (≈10%)
1	25.69	13.29	3.98
2	26.98	13.32	3.93

3	26.03	13.18	4.06
4	25.66	13.36	4.01
5	25.28	12.89	3.99
6	25.31	13.12	3.92
7	25.81	13.25	4.09
8	25.56	13.17	4.11
9	25.55	13.22	4.05
10	25.50	13.30	4.01
Average =	25.74	13.21	4.02

Table 7 – Recorded Test Data @ 50% Valve Opening

	Test 1:	**Test 2:**	**Test 3:**
Pump Speed =	75%	38%	10%
P =	3.31	1.05	0.39
ΔP =	2.86	0.70	0.06
T_1 =	21.57	20.65	22.91
	Q (MAX)	Q (≈50%)	Q (≈10%)
1	18.24	8.76	2.66
2	17.94	8.79	2.71
3	18.06	9.03	2.70
4	17.64	8.77	2.63
5	17.69	8.79	2.58
6	18.12	8.71	2.66
7	18.00	8.90	2.75
8	17.96	8.69	2.71
9	17.98	8.64	2.63
10	17.55	8.79	2.55
Average =	17.92	8.79	2.66

Table 8 – Recorded Test Data @ 25% Valve Opening

	Test 1:	**Test 2:**	**Test 3:**
Pump Speed =	75%	38%	10%
P =	3.35	1.08	0.77
ΔP =	2.93	0.67	0.05
T_1 =	20.75	21.45	21.60
	Q (MAX)	Q (≈50%)	Q (≈10%)

APPENDIX 3 – Flow Loop Results

1	9.83	5.17	1.39
2	10.33	4.34	1.28
3	10.08	4.64	1.09
4	10.12	4.56	1.22
5	10.17	4.85	1.33
6	10.92	4.34	1.14
7	10.86	4.91	1.23
8	9.92	4.89	1.22
9	9.88	4.71	1.07
10	9.67	4.84	1.09
Average =	10.18	4.73	1.21